Maximum Likelihood Identification of some Loops of the Halden Boiling Water Reactor

Olsson, Gustaf

1972

Document Version:
Publisher's PDF, also known as Version of record

MAXIMUM LIKELIHOOD IDENTIFICATION OF SOME LOOPS OF THE HALDEN BOILING WATER REACTOR

GUSTAF OLSSON

REPORT 7207 (B) MARCH 1972
LUND INSTITUTE OF TECHNOLOGY
DIVISION OF AUTOMATIC CONTROL

MAXIMUM LIKELIHOOD IDENTIFICATION OF SOME LOOPS OF THE HALDEN BOILING WATER REACTOR

GUSTAF OLSSON

ABSTRACT

The dynamics of some loops of the Halden Boiling Water Reactor have been identified with the Maximum Likelihood method. The experiments were performed by the OECD Halden reactor project group as a part of the current research program. Rod reactivity, subcooling flow and steam flow demand have been used as inputs, while the two most important outputs are nuclear power and primary pressure.

The model order has never exceeded four. The achieved models are compared partly between different experiments, partly with a state model, developed in Halden. The choice of input signal is shown to be crucial as the reactor time constants cover a broad range.

TABLE OF CONTENTS.

ACKNOWLEDGEMENT

The author is indebted to many persons for different kinds of contributions to the work.

The experiments have been carried out at the OECD Halden Reactor Project, and the permission to have experiments done and to use data is gratefully acknowledged.

Special thanks to Mr Rainer Grumbach, Section Leader for Physics and Control Development in Halden, for his advice and interest during every stage of the work.

Many thanks also to Mr Kazuo Sato, Halden, for stimulating discussions.

Professor Karl-Johan Åström has contributed with constructive criticism and fruitful ideas. Dr Ivar Gustavsson has written the Maximum Likelihood Identification program package, which has been used extensively in the work. Throughout the work he has also spent much time and interest to discuss problems, connected with the identifications.

Mr Leif Klöver has carried out a large amount of computer calculations. He has contributed considerably to the work.

In order to compare models the author has been permitted to use some material from a master thesis, by L. Klöver and L.E. Olsson.

Mrs Gudrun Christensson typed the manuscript and Mr Bengt Lander drew the figures.

1. INTRODUCTION AND PURPOSE OF THE WORK

The Maximum Likelihood method has been used in this work in order to identify the dynamics of some loops of the Halden Boiling Water reactor. Dynamical experiments have been performed on the reactor in the years 1968 and 1969. These experiments are parts of a large program on computer control of the plant. It is desirable to find more accurate models and also to test different control strategies and instrumentation equipment.

As the reactor is a power reactor, a great number of temperature and void dependent reactivity feedbacks occur. The dynamics of the plant is space dependent as well as nonlinear. Control laws based on such models ought to be too complex. Therefore identification methods have been used to find out space independent, linear models.

The experiments have been performed as single loop experiments, that is only one control variable at a time has been moved. The experiments have been made with the IBM 1800 on line computer, which has generated the control signals and registered the interesting outputs.

Three different control devices, which are commonly used in normal operations, have been used in the experiments, viz. the control rods, the subcooling flow and the steam flow to consumer. All the registered outputs have not been used in the identifications, but the most interesting have been nuclear power, the primary, secondary and tertiary pressures and finally the neutron flux.

The purpose of the identifications has been to gain more knowledge about the reactor dynamics and the noise characteristics of the plant, and to compare theoretical results with identification models. Some identification method problems have been illuminated by the work also.

The structure of the models has been assumed linear, time invariant and discrete, and a structure, proposed by Åström |26| has been used throughout the work

$$y(t) + a_1 y(t-1) + \ldots + a_n y(t-n) =$$

$$= b_0 u(t) + \ldots + b_n u(t-n) + \lambda\left(e(t) + c_1 e(t-1) + \ldots + c_n e(t-n)\right)$$

where y and u are the output and input signals respectively. The noise is assumed to be discrete, normal distributed, consisting of independent stochastic variables, e(t).

The unknown parameters in this model have been identified by the maximum likelihood method, originally developed by Åström et.al. |26|.

It is essential to include the control equipment in the models, as its dynamic must be included in the control laws.

An essential goal is also to try different control laws, based on different models, on the plant and compare the results.

In order to get minimal variance of the outputs, it is necessary to gain more knowledge about the noise dynamics.

As the reactor time constants are very different it is very difficult to get models, which are accurate in both the fast and the slow models. In the report this problem is discussed. The sampling interval is 2 seconds in all experiments. The results indicate, however, that futher studies of the influence of the sampling interval on model accuracy has to be performed.

The choice of input signal is known to be very important. Two types of inputs, steps and pseudo random binary sequences, have been used in the experiments. It is shown in the paper, that the accuracy of the step response models is very bad. The results of two different random input sequences are also compared.

In order to gain operating experiences with the second fuel charge a great number of dynamical experiments were performed at the Halden reactor until 1964. The results of different kinds of identifications have been collected in a number of reports |1, 5, 6, 7, 22, 25|. Later it has been emphasized to try modern control methods for the reactor. For this purpose a state model of the plant has been developed in several stages |10, 18, 21|. The model is multivariable, linear and time invariant. As it is very difficult to theoretically derive the quantitative values of the parameters, the mo-

del has been built up by means of the analog computer, and the simulations have been compared successively to experiments. In this work the state model has been used to compare different models of the reactor.

In the state model it is assumed, that every state variable is corrupted by independent noise, an assumption which has been shown to be too rough. The plant dynamics, however, has shown a very good agreement to the experimental results and the identifications.

Similar dynamical experiments have also been performed on other reactors. Random signals have been used as inputs. In most cases the reactivity has been disturbed [4, 23] and in some case turbopump speed or flow demand has been used as input. Cross correlations have been calculated and Bode plots have presented the results.

In [13] a comparison has been made of correlation methods and the maximum likelihood method for the Ågesta reactor in Sweden.

In all the mentioned references model comparison problems arise. Bode plots have been used extensively. Frequency domain comparisons may be quite irrelevant for time domain comparisons, as the transform is an infinite operator. Problems of this type are discussed in chapter 6 of this report.

In chapter 2 a short description of the reactor plant and its dynamics is made. The state model, mentioned before, is summarized and some of its characteristics are presented in appendix.

The experiments are presented in chapter 3. Interesting variables are listed and the inputs are accounted for.

The identification results are presented in chapters 4 and 5. The reactivity - nuclear power loop and the reactivity - primary pressure loop have been analysed.

No model has higher order than four, and several of them have order two or three.

The model structure has been complicated to find sometimes. Redundant parameters are common in models of order 3 and more. Sometimes it has been difficult to find the most relevant structure.

In the experimental data drift has occured in some cases. The common way to eliminate the drift in reactor experiments has been high pass filtering |23|. However, low frequences are quite important and they will be complete neglected, so the model will take care only of the fast modes. The static gain has been very badly calculated, a problem which depends on both the drift elimination and the choice of sampling interval.

The numerical difficulties are quite common for the orders of three and more. Sometimes convergence difficulties have occured, somethimes the parameters have not converged towards the right values.

The test of order has been rather involved as there is no single test values, which will determine the order of the system.

In chapter 6 some model comparisons are made. The accuracy of the models and the comparison methods have been discussed in the first part of the chapter. Among other methods simulations have been used to compare different open loop models. Cross comparisons between different inputs and experiments have also been performed, and the state model has been used as a comparison.

Most of the simulations show the bad low frequency behaviour of the models. The major reason is considered to be the short sampling interval, two seconds. The input frequency content is also important, which is discussed in 3.3 and 6.7.

An interesting way of comparison has been comparison by identification. Not only the outputs of the state model and other models have been compared but also the parameters. A parametric discrete model has been identified from data generated by the state model, and the agreement was surprisingly good. The noise representation, however, was shown to be rather inaccurate in the state model.

In chapter 7 some subjects for further study are mentioned. At first longer sampling interval must be tried to get more accurate models. Attention must also be paid on the choice of identification input signals. Redundant parameter elimination in the identification and multimode control of the reactor are finally two interesting subjects for future research.

2. BRIEF DESCRIPTION OF THE REACTOR SYSTEM.

A summary of the plant performance is given in this chapter. The details of the reactor system are described elsewhere |17|. In 2.1 the different parts of the plant are mentioned. In 2.2 the general dynamic behaviour is described, and in 2.3 a theoretical model is presented.

2.1. THE REACTOR SYSTEM.

The OECD Halden Reactor was made critical in 1959. Since then the plant and the reactor system (HBWR) dynamics have been described in a number of reports |1|, |5|, |6|, |7|, |10|, |22|, |25|.

In order to make the text more understandable for the reader we will summarize the most important features of the plant.

The reactor is a heavy water boiling reactor. The core contains 1.5% enriched UO_2 fuel, moderated by heavy water. A fuel element consists of seven stringers of uranium pellets, canned with Zr-2. There are 100 fuel assemblies in the core, and they are arranged in a hexagonal pattern. The length of the fuel elements is 88 cm. The core diameter is 167.2 cm and it is surrounded by a radial reflector, the thickness of which is 51.4 cm. The bottom reflector is 38.3 cm thick.

Heavy water is entering the coolant channels through ports in the bottom section (fig. 2.1). The lower part of the coolant channel is a nonboiling region, and the rest of the channel is a boiling one. A steam-water mixture leaves the channel through perforations at the top. Steam is collected in the space above the water level. The shrouds in the fuel elements will give a defined flow pattern in the reactor. The upstreaming steam-water mixture is separated from the downstreaming water between the elements.

Figure 2.2 is a simplified sketch of the whole plant. The heavy water steam circulates in the primary circuit to the steam transformers A and B, where it is condensed. Light water steam is produced in the secondary circuit.

Heavy water can also be withdrawn from the core tank into a subcooling circuit. The subcooling flow can be controlled by the valve VA770, which is used here as an input variable. Generally stability increases with increasing subcooling.

The light water steam in the secondary circuit produces light water steam in the tertiary circuit by means of the steam generator. The tertiary steam can be distributed to the consumers through the control valve VB 282.

The thermal power is limited to about 25 MW at a maximum operating pressure of about 32 ata. A maximum power of about 2.2 MW can be taken out from the subcooling circuit. The normal operating conditions in the experiments have been 8-11 MW nuclear power, 1.5 MW subcooling and 30 bar vessel pressure.

2.2. GENERAL DYNAMIC BEHAVIOUR OF THE PLANT.

In this section a brief description of the HBWR dynamics is made in order to simplify the physical understanding of the experiments. A detailed review of the dynamics is given elsewhere, e.g. |25|.

The neutron kinetics is described in a conventional manner. In a power reactor there are several reactivity feedback terms, which will make the dynamic behaviour complex. There are feedback effects from the heat flux through fuel, moderator and coolant channels. We have to know the channel dynamics (void and temperature distributions in the coolant channels), which is a function of heat flux from fuel and moderator, vessel pressure, steam and water velocities and coolant inlet temperature. For similar reasons the moderator dynamics is also complicated. It is also difficult to estimate the thermodynamic parameters of the fuel theoretically.

The hydraulics relates the void content with steam and water velocities and includes steam-water two phase mixture effects, such as slip, buoyancy and friction.

There are some important differences between light water and heavy water boiling reactors. In H_2O system almost all the moderator is

boiling. In D_2O system the boiling takes place only in a fraction of the moderator space, because the moderator to fuel ratio is relatively large. Therefore models of light water boiling reactors, which are described in literature, e.g. |8| , differ from the HBWR in basic assumptions.

Primarily we want to examine, how nuclear power and primary pressure depend on the different inputs.

2.3. A LINEAR DYNAMIC MODEL OF THE HBWR.

In Halden several reports have treated the dynamical behaviour of HBWR. In order to get a model suitable for computer control, attempts have been made to fit a linear state model to the plant |18|.

The model has been built up on an analog computer step by step, starting with the tertiary circuit. The structure of the equations was more or less known.

Several simplifications have been made. The complicated hydraulic equations are approximated by linear equations in subcooling, moderator and fuel temperature. Nonlinear effects, such as flashing, are neglected. The same applies to spatial dependence in coolant channels and steam transformers.

The state variables were chosen in order to get as many states as possible directly measurable. Factor analysis has been used |11| in order to reduce the number of states to the most relevant ones. The model has been improved and modified in a couple of times |21|. The object was to make the model satisfy the following requirements:

- give step responses comparable with the experimental responses,
- show instability similar to the observed behaviour of the reactor (because of increased power and decreased subcooling).

All the state variables do not have a physical meaning, but are introduced only to make the model represent the real process more accurately.

The equations are in the form:

$$\frac{dx}{dt} = Ax + Bu + v$$

$$y = Cx + e$$

x is the state, u is the control vector and y is the output. The matrices A, B, and C are found in appendix. The terms v and e correspond to "white" noise.

The system is of order 11 with 3 inputs and 4 outputs. The state vector is:

x_1 = normalized neutron density $\frac{\delta n}{n_o}$

x_2 = " primary pressure $\frac{\delta p_1}{p_1}$

x_3 = " secondary " $\frac{\delta p_2}{p_2}$

x_4 = " tertiary " $\frac{\delta p_3}{p_3}$

x_5 = " delayed neutron density $\frac{\delta c \cdot \beta}{n_o \cdot \ell}$

x_6 = " fuel temperature $\frac{\delta T_F}{T_F^o}$

x_7 = " moderator " $\frac{\delta T_w}{T_w^o}$

x_8 = " subcooling " $\frac{\delta T_{sub}}{T_{sub}^o}$

x_9, x_{10}, x_{11} are artificial.

In the model comparisons later we first compare the deterministic dynamics.

The eigenvalues of two different reactor conditions, called a and b (subcooling 2 MW and 1.1 MW respectively), are shown in appendix.

The system is observable from any of the four outputs. However, it is not completely controllable from only arbitrary input. With only u_1 (VA770) all states are controllable, with only u_2 (VB282) or with only u_3 (rod) the states $x_8(\theta_{sub})$, x_9, x_{10} and x_{11} are not controllable. In the figures 2.3 - 2.6 the step responses of the most interesting state variables are shown.

3. DESCRIPTION OF THE EXPERIMENTS.

3.1. GENERAL EXPERIMENTAL CONDITIONS.

A process computer IBM 1800 is connected to the plant |31|. The advanced instrumentation makes it possible to get a great number of different inputs and also to make measurements in the core. Instruments are placed in several positions and many interesting flows, temperatures and neutron fluxes can be recorded.

Three inputs, viz. control rods, and the two valves VA770 and VB282 (figure 2.2) will be used for the control, so they are interesting from the identification point of view.

As it is important to know the input exactly, the input signal must be carefully defined. As rod position indication we use the computer signal to the rod step motors. The rod position instrumentation is too rough for identification purposes. The amplitude of the rod input is defined in steps, where 1 step ≈ 7.5 pcm. in these experiments.

For the valves we also use the computer signal as input. As it will take about 6 sec. to move a valve through its whole range, it is very meaningful to include the valve and valve motor dynamics in the model. There is no unique relationship between the flow and the valve area, as the flow depends on the operation conditions, mainly the vessel pressure.

The computer can store a maximum of 40 outputs. The most interesting outputs for the identification are:

Primary circuit:	Primary pressure, P13
	Moderator temperature, T2
	Nuclear power, C10
	Subcooling flow, VA770 (input)
	Neutron flux, e.g. ND306
Secondary circuit:	Secondary pressure, P61
Tertiary circuit:	Tertiary pressure, P62
	Steam flow to consumer, VB282 (input)

We are also interested in storing some other variables as a check, e.g.:

Downcomer subcooled flow	F6
Tertiary circuit steam flow	F21
Lower plenum subcooled flow	F89

The steady state values of all interesting variables are stored in the computer before and after the experiments.

All signals cannot be registered simultaneously by the computer. Every variable is read in once during the 2 second sampling interval. However, the variables C10, P13, ND306, and the pulse to the rod step motors are all read within 40 ms. We neglect this time delay. For the other variables, the time delay during the sampling interval is not at all critical.

The variables have been punched on cards by the IBM 1800 computer. The cards have been transferred to magnetic tapes at the CD 3600 computer in Kjeller. From these tapes we have copied the data to tapes for the CD 3600 computer in Uppsala and the Univac 1108 computer in Lund. The identification has been performed on both the CD 3600 terminal in Lund and on the Univac 1108.

3.2. THE INSTRUMENTS.

The pressures in the three circuits are registered as differential pressures with conventional DP cells P13, P61, P62 with a range of ±0.3 bar. The nuclear power is measured with a ionisation chamber C10. The neutron flux is measured with β current detectors (Co 60 and V 51). The Co 60 detectors are very fast, while the V 51 detectors have ≈5.4 min. time constant. The control rod configuration is shown in figure 3.1, and the actual rods are indicated.

3.3. SUMMARY OF THE EXPERIMENTS.

We have used data from three different experiment series in the identifications. Throughout the report the names of the experiments, defined by the Halden group, are used in order to cause no confusion.

The experiment series has been made during the following periods:

EP-706	October, 1968
EP-708	May, 1969
EP-710	November, 1969

The operational conditions, type of inputs and number of registered variables have not been the same in the different experiments.

In all runs the nuclear power control loop is decoupled. For security reasons it was impossible to decouple the vessel pressure control completely. The vessel pressure has been controlled by feeding back the tertiary circuit steam load, which will give a very slow long term regulation, with a time constant of at least one minute. Therefore the primary pressure variation in the time region about a few seconds and less will not be influenced by this control.

All the experiments are listed in table 3.1 and are commented on below. The sampling interval is all the time 2 seconds. All outputs are recorded in physical units, that is:

Nuclear power C10 in MW
Pressures in bar
Neutron flux ND306 in neutrons/cm^2. sec.
Temperatures in ^{o}C.

Experiment EP-706.

Four runs of the experiments are analysed here. Some of the runs with rod input have been discussed previously in a master thesis |19|.

Step response runs with the valves VA770 (subcooling circuit) and VB282 (tertiary circuit) as inputs have been treated.

Interesting outputs are nuclear power C10, vessel pressure P13, secondary (P61) and tertiary pressures (P62).
There were great difficulties to get accurate models from the step response input experiments. Only first order models with bad parameter accuracy were achieved. The main reason for the bad result is because of the input signal. It causes the output to vary significantly only during the initial stage. Especially the nuclear power (C10) is a problem, because the absolute value and not the changes are measured.
Run 10 and 15 are plotted in fig. 3.2 and 3.3.

Experiment EP-708.

There are two types of inputs:

a) The rod has been moved in deterministic cycles, like fig. 3.4. As the rod can be moved only one step each sampling interval, the slope of the input is like a staircase for big amplitudes.

b) The rod has been moved in a random sequence. The rod position is recorded in steps. The interesting outputs are:

   nuclear power C10
   primary pressure P13

As an example, we have plotted one experiment, run 65 (fig. 3.5).

In table 3.1 the runs are summarized.

Experiment EP-710.

Three different runs have been analysed. The input sequence is the same for all three runs, but the reactivity amplitudes are different.

The sequence is a PRBS signal with maximum length 991 sampling intervals. The smallest interval is 2 seconds.

Consequently the spectrum of the signal is from

$$f_{min} = \frac{1}{N \cdot \Delta T} = 0.50 \cdot 10^{-3} \text{ Hz} \quad \text{to}$$

$$f_{max} = \frac{1}{2\Delta T} = 0.25 \text{ Hz}$$

For further discussion of the input we refer to chapter 6.7.

In runs 4 and 5 (see table 3.1) two or three rods (figure 3.1) are moved simultaneously with one step amplitude. In this way the staircase shape of the input, shown in EP-708, is avoided. The three rods have different reactivity equivalence (figure 3.1) and therefore the system gain cannot be exactly the same in the three runs.

The outputs nuclear power (C10), vessel pressure (P13), neutron flux (ND306) are used. The data from the rod - neutron flux (ND 306) loop gave quite inaccurate results. Therefore this loop is not considered here any more. The stationary conditions are shown in table 3.1.

The nuclear power is a bit higher than in the previous experiments. Moreover, the subcooling is not so great. Consequently the core is more unstable.

From the plots of the experiments (figures 3.6 - 3.8) we see that the nuclear power has a drift, because the input has a nonzero mean. The drift is eliminated by taking forward differences of both input and output. This method is used commonly in reactor systems |9| .

In order to examine method to take differences, we tried to identify the model from run 5 partly with differences of the input-output sequence and partly with the nominal sequence. The consequences of taking input-output differences are discussed in chapter 6.

4. IDENTIFICATION OF THE REACTIVITY-NUCLEAR POWER LOOP.

4.1. THE MODEL STRUCTURE AND THE IDENTIFICATION METHOD.

In the identifications a linear model with time-invariant parameters is fitted to the input-output samples from the experiments. It is also assumed, that the disturbances are stationary normal random processes with rational power spectra.

The model is:

$$A^*(q^{-1})y(t) = B^*(q^{-1})u(t) + \lambda C^*(q^{-1})e(t)$$

This model has been used extensively in a number of papers |13| - |16|, |26| - |27|, |29|.

$$\{u(t), y(t) \mid t = 1, \ldots, N\}$$

is the input-output sequence, while

$$\{e(t) \mid t = 1, \ldots, N\}$$

is a sequence of independent normal (0,1) random variables. q denotes the shift operator $qx(t) = x(t+1)$ and $A^*(q^{-1})$, $B^*(q^{-1})$, and $C^*(q^{-1})$ are polynomials.

$$A^*(q^{-1}) = 1 + a_1 q^{-1} + \ldots + a_n q^{-n}$$

$$B^*(q^{-1}) = b_0 + b_1 q^{-1} + \ldots + b_n q^{-n}$$

$$C^*(q^{-1}) = 1 + c_1 q^{-1} + \ldots + c_n q^{-n}$$

The maximum likelihood identification method is described elsewhere |26|.

Throughout this report the program package written by I. Gustavsson |14| has been used for the maximum likelihood identification.

For simplicity we repeat the definition of the loss function V:

$$V = \frac{1}{2} \sum_{t=1}^{N} \varepsilon^2(t)$$

where the residuals $\varepsilon(t)$ for a certain parameter estimation are given by:

$$C^*(q^{-1})\varepsilon(t) = A^*(q^{-1})y(t) - B^*(q^{-1})u(t)$$

The static gain is defined from the final value theorem:

$$\lim_{q=1} |H(q^{-1})| = \left| \frac{B^*(q^{-1})}{A^*(q^{-1})} \right|_{q=1} = \frac{\sum_{i=0}^{n} b_i}{1 + \sum_{i=1}^{n} a_i}$$

The statistical F test |26| is used for test of the model order. This means, that we examine if the loss function decrease is significant, when the number of parameters has increased.

In all runs the coefficient b_0 is shown to be nonzero, which means, that there is one term going directly through the system. This is easily explained by the neutron kinetics, discussed in 2.3. The reactivity affects the power very fast.

The direct term in the sampled model causes one direct term also in the continuous model. This is not true of physical reasons, but is explained by the sampling time, which is long compared to the neutron kinetics.

The proceeding of the identification work is described in detail in order to explain the parameter set in every case. Redundant parameters occur very often. We call a parameter redundant if it differs

from zero less than one standard deviation.

If there is redundancy in the model the parameter estimates are not consistent. However, the input response and the noise distribution of such a model are the same as in the right model.

In several experiments the output has a drift, which has to be removed. This is made by a high-pass prefilter

$$H(q^{-1}) = 1 - q^{-1}$$

of both input and output. Thus, differences are calculated of the data. The consequences of the prefiltering are discussed in chapter 6.

4.2. EXPERIMENT 3, EP-710.

The input-output sequence, consisting of 1007 data, was prefiltered with $1 - q^{-1}$ in order to eliminate the drift.

4.2.1. Accomplishment of the Identification.

The result of the identifications of different model orders are shown in table 4.1.

In the first order model the parameter b_1 was assumed redundant, so it was removed. The uncertainty of the parameters decreased substantially while the loss function did not increase.

The second order model was found without any trouble (table 4.1).

The third order model with all parameters assumed nonzero (case 3 A, table 4.2) contained large variances. The parameters a_2, b_2 and c_3 seemed to be redundant. Less a number of parameters might describe the system accurately enough. At first both a_2 and b_2 were assumed zero. The uncertainties decreased considerably, but the value of the loss function minimum was larger than in models 2 and 3 A. If all the parameters a_2, b_2 and c_3 in 3 A were neglected, the result was even worse.

Then the second order model was used as initial value of a third order model. The number of parameters was increased step by step. If a_3 was added (3B) the result was better than 3A (table 4.2). The loss function decreased and the uncertainties were acceptable. If further parameters were added (3C) the result was worse again. Model 3B was accepted as the third order model.

The complete fourth order model is shown in table 4.1. No parameter seems to be redundant, and the uncertainties are acceptable. The loss function, however, is only slightly less than the third order model loss function.

4.2.2. Test of Order.

The F test (table 4.1) indicates a third order system within 5% risk. Model 3 B (table 4.2) has the best F test among the different third order attempts, which confirms the previous choice of system.

The parameter uncertainties are not significantly larger in model 3 than in model 2.

Table 4.3 shows the roots of the polynomials of the models. One may suspect common roots of the A and B polynomials in the third order model. However, the Bode plot (figure 4.1) shows a significant difference between the third order model and the abbreviated third order model. The third root of A is quite near to the root of the first order model.

The roots of A in the models are never in the neighbourhood of the negative real axis, so the sampling interval seems to be short enough. However, it may be chosen longer (see chapter 6.7).

In table 4.1 is demonstrated, that the static gain is not very accurate. We find, that both

$$1 + \sum_i a_i \quad \text{and} \quad \sum_i b_i$$

are close to zero. We find the following values:

Model order	1	2	3	4
$1 + \Sigma a_i$	0.9232	0.1353	0.1084	0.4582
Σb_i	0.1436	0.0204	0.0199	0.0719

Consequently an error in any parameter may cause large static gain errors. Thus it is very difficult to conclude anything about the order from the static gain. (Observe, that the gain is defined for the differences of the input and output sequences).
The residual covariance functions (fig 4.2) is satisfactory for both the second and third order models.
Normality can be accepted by the chi-square test within 15 % risk. The tails of the distribution are quite large.

The simulations (fig. 4.3, 4.4) do not show any clear difference between the second and third order systems. In the low frequency range the third order model is somewhat better. Fig. 4.3 and 4.4 also show a large output error. Too many details of the output seem to have been neglected by the deterministic output.

The error can be decreased by a larger input amplitude (see 4.4 and 4.5). The real output has also a very slow variation of several minutes period, which is neglected by the models. The data prefiltering is one important cause. The short sampling interval may also be too short or the input frequency too high.

The continuous transfer function is of the form:

$$G(s) = \frac{B(s)}{A(s)} + D$$

The parameter D is the same as b_0 in the discrete model. The poles and the zeroes are as follows:

Order	1	2	3
Poles	-1.283	-0.1838 ± 0.1215j	-0.1172 ± 0.1538j -1.2575
Zeroes		-0.03279	-0.1460 ± 0.3024j

The third order model has one exponential time constant:

$$T_1 = \frac{1}{1.2575} \approx 0.8 \text{ sec.}$$

which is similar to the time constant of the first order model. One may suspect, that it is too fast, compared to the sampling interval 2 sec. However, simulated systems have shown, that it might be possible to detect a time constant 2 - 3 times shorter than the sampling time. Physically, a time constant of about 1 second is reasonable for the coolant channel dynamics.

The other two complex poles of the third order system will give a damped sine wave with damping time constant T = 8.5 sec. and a period of the sine wave of about 40 seconds. This is quite acceptable in comparison with the theoretical model.

Figure 4.1 shows the Bode plots of three models, viz. the second and third order models, and then the model, which is achieved if the almost common factors in the third order model are omitted.

The third order model has the most probable low frequency gain and phase. The second order model phase seems to be too positive.

To sum up, no clear and unique test exists to determine the system order. Because of the F test and the Bode plot and the simulation we accept the third order system. A control law, based on the second order model, might also give quite a satisfactory result.

The accepted third order model is:

$$(1 - 1.59q^{-1} + 0.75q^{-2} - 0.05q^{-3})\Delta y(t) =$$

$$= (0.14 - 0.22q^{-1} + 0.09q^{-2})\Delta u(t) +$$

$$+ 0.029(1 - 1.42q^{-1} + 0.45q^{-2})e(t) \qquad (4.1)$$

where

$$\Delta y(t) = y(t) - y(t-1) = (1 - q^{-1})y(t)$$

$\Delta u(t)$ is defined analogously.

The continuous transfer function is:

$$\frac{\Delta y(s)}{\Delta U(s)} = \frac{0.0162(s^2 + 0.292s + 0.113)}{s^3 + 1.49s^2 + 0.33s + 0.047} + 0.145 \qquad (4.2)$$

4.3. EXPERIMENT 4, EP-710.

Because of a large output drift, this experiment is shorter than the previous one. 737 data are used. Digital prefiltering is carried out also here.

4.3.1. Accomplishment of the Identification.

The identification result is shown in table 4.4.

As in run 3 we could neglect the parameter b_1 in the first order model (table 4.4).

In the second order model c_2 was very small and uncertain, and it was omitted. Also b_2 was rather small, but not redundant, and we tried to neglect it. The result, however, was very bad. Both the loss function and the parameter variances increased considerably.

In the complete third order model all the parameters a_3, b_2, b_3, and c_3 were found to be redundant. If only b_3 was neglected the result was not satisfactory, and c_3 was still redundant (table 4.5, 3 A). However, if c_3 in model 3 A was neglected a better model (3C) with smaller variances and an acceptable loss function was found. Model 3 C was accepted as the third order model.

If only c_3 was neglected, the parameter variances were larger, and still redundant parameters existed (3B).

A complete fourth order model contains 5 more parameters than the accepted third order model. The loss function is only slightly below that of the third order system (table 4.4). The parameter c_4 is redundant. There is, however, no reason to make more calculations as the loss function will not decrease with fewer parameters. The F test quantity thus can increase at most to 1.3 or to 1.7 if also b_4 is neglected. Thus, the test quantities are too small for the fourth order system.

4.3.2. Test of Order.

The model order discussion is very similar to the previous run 3, so it is made rather briefly.

Even in this case the F test quantity gives a third order system within 5% risk level. The indication is not as clear as in run 3.

The third order model has the same number of parameters as the model in run 3.

The parameter variances are quite large, compared to the second order model and also larger than in corresponding run 3 model (table 4.1). This last fact depends on less number of data.

The root configuration (table 4.6) resembles that of run 3. One may suspect common factors in A and B, in both the second and third order models. The second order system Bode plot (fig. 4.5) is changed only slightly if the almost common roots in the second order model are abbreviated. If one parameter in A and B of the second order model or two parameters from the third order polynomials are neglected, the structure is of first order. This model is too simple to explain the dynamical behaviour of the system. Therefore the roots are not considered common.

The residuals are satisfactorily independent in both the second and third order case (figure 4.6). The hypothesis of normality can be accepted by chi-square test at 50 and 20 % risk level respectively. The tails of the distributions are much smaller than in run 3.

The simulations (fig. 4.7 and 4.8) show, that the third order model has a somewhat better low frequency behaviour.

The continuous models have poles and zeroes as follows:

Order	2	3
Poles	-0.119 -0.510	-0.1866 ± 0.1092j -1.273
Zeroes	-0.0987	-0.1783 ± 0.3516j

Also here we find a fast time constant, 0.8 sec., in the third order system.

The Bode plots (fig. 4.5) indicate a third order model.

A third order model is accepted

$$(1 - 1.42q^{-1} + 0.58q^{-2} - 0.037q^{-3})\Delta y(t) =$$

$$= (0.12 - 0.16q^{-1} + 0.06q^{-2})\Delta u(t) +$$

$$+ 0.033(1 - 1.24q^{-1} + 0.28q^{-2})e(t) \qquad (4.3)$$

The continuous transfer function is:

$$\frac{\Delta Y(s)}{\Delta U(s)} = \frac{0.0124[s^2 + 0.36s + 0.155]}{s^3 + 1.65s^2 + 0.52s + 0.060} + 0.121 \qquad (4.4)$$

4.4. EXPERIMENT 5, EP-710 (DATA PREFILTERED).

The drift of the power in run 5 is insignificant, and no digital prefiltering may be necessary. However, in order to compare the results, two identifications of the same data have been performed one with prefiltering and the other without. 1007 points have been used.

4.4.1. Accomplishment of the identification.

The identification results are shown in table 4.7.

The first order model was found without any problems. In the complete second order model (table 4.8, 2 A) c_2 was found to be redundant. The parameter was neglected and a better model was found (2 B). No better result could be found if b_2 was neglected (2 C), and therefore 2 B was accepted as the second order model.

It was difficult to find a third order model without a pole on the negative real axis. In this case no continuous transfer function is defined.

In the complete third order model (table 4.9, 3 A) rather great uncertainties were obtained and b_3 was small. Neglecting b_3 we got a bad result in the sense that the variances increased. However,

if both b_3 and c_3 were neglected, the convergence was good, and the parameter variances were acceptable (table 4.9, 3 B). The loss function increased only a little.

In the fourth order model all parameters seem to be significant. However, the loss function is not very small, a fact which is reflected in the F test quatity, table 4.7.

4.4.2. Test of Order.

The F test quantity gives a clear indication to a third order system (table 4.7).

This model has the same parameters ~ non zero as the third order models of runs 3 and 4. The parameter uncertainties are smaller than in run 4, probably depending on partly a larger input amplitude, partly more input-output data. The uncertainties are not very much larger than in the second order model.

No common factors can be found in the third order model (table 4.10)

The gain is determined more accurately in this run.

The third order system residuals have a better covariance function than the second order system (fig. 4.10). The normality is established for both model residuals within 2 and 20 % risk respectively.

The simulations (fig. 4.11 and 4.12) have similar behaviour as in run 3 and 4.

The continuous counterparts of systems of order two and three have poles and zeroes as follows:

Order	2	3
Poles	-0.096 -0.636	-0.0767 ± 0.165j -1.345
Zeroes	-0.069	-0.143 ± 0.136j

Also here a fast time constant is found in the third order model.

The Bode plots show very small differences between the two models (figure 4.9).

The main reason to accept the third order model is the F test. The Bode plots are not very different. However, as they show only the deterministic part of the system, we consider the stochastic part better described by the third order system.

The accepted model is:

$$(1 - 1.69q^{-1} + 0.85q^{-2} - 0.05q^{-3})\Delta y(t) =$$

$$= (0.138 - 0.221q^{-1} + 0.099q^{-2})\Delta u(t) +$$

$$+ 0.028(1 - 1.52q^{-1} + 0.58q^{-2})e(t) \qquad (4.5)$$

or

$$(1 - 2.69q^{-1} + 2.54q^{-2} - 0.90q^{-3} + 0.05q^{-4})y(t) =$$

$$= (0.138 - 0.36q^{-1} + 0.32q^{-2} - 0.099q^{-3})u(t) +$$

$$+ 0.028(1 - 1.52q^{-1} + 0.58q^{-2})e(t) \qquad (4.6)$$

In continuous form the transfer function is:

$$\frac{\Delta Y(s)}{\Delta U(s)} = \frac{0.0147[s^2 + 0.29s + 0.039]}{s^3 + 1.50s^2 + 0.24s + 0.046} + 0.138 \qquad (4.7)$$

4.5. EXPERIMENT 5, EP-710 (DATA NOT PREFILTERED).

The same data sequences have been used as in previous section. This time no digital prefiltering with high-pass filter has been made.

4.5.1. Accomplishment of the Identification.

The complete second order model contains two redundant parameters a_2 and b_2. The accuracy is much better if the two parameters are neglected (table 4.11).

In the first third order model (table 4.12, 3 A) both a_3 and b_3 are redundant. With b_3 omitted an acceptable model (3 B) was obtained, although the parameter c_2 is small. Model 3 B was accepted as a third order model.

Model 4 A (table 4.12) has some very small parameters, e.g. c_3, c_4, b_3, and b_4. If c_4 is put zero no change of the loss function is found, and this model must be better. c_3 was also neglected which leads to model 4 B (table 4.12). However, the model has no continuous transfer function, because some roots are real negative.

Therefore the very small parameter b_4 was also omitted (model 4 C, table 4.12). The parameter variances got much smaller, and the loss function was quite good. Model 4 C was accepted as model 4, and it has also a continuous transfer function.

For comparison a result from EP-708, run 84 is shown in table 4.11. The model is from |19|.

4.5.2. Test of Order.

In previous identifications with prefiltered data third order models were found. In this case the F test gives a fourth order system (table 4.11), a fact which could be expected.

Both A and B (table 4.13) have roots near 1. By the prefiltering in previous identifications it was assumed a pole and a zero exactly on the unit circle. In chapter 6 is discussed the consequences of this small difference.

Depending on the dipole near the unit circle the sums $1 + \Sigma a_i$ and Σb_i are almost zero, and therefore it is meaningless to calculate the static gain. This may be an indication of a too short sampling interval. (see chapter 6).
For comparison the roots of the model from EP-708, run 84, are also shown in table 4.13. The model is taken from [19].

The parameter variances are quite acceptable in the fourth order model.

Only the fourth order model has an acceptable residual covariance function (figure 4.14). Normality is only accepted with 90 and 70 % rise.

As previously, the simulations (fig. 4.16 - 4.17) differ mainly in the low frequency range, and the fourth order model is the most accurate one.

The continuous models of third and fourth orders have the following poles and zeroes:

Order	3	4
Poles	-0.0021 -0.113 -1.350	-0.0127 -0.053 ± 0.175j -1.366
Zeroes	-0.0102 -0.263	-0.046 ± 0.142j -0.213

We confirm, that the fast time constant, about 0.75 sec., is found in both models (compare runs 3 and 4).

The Bode plot fig. 4.13 seems a bit oddly shaped for the fourth order model, probably depending on the numerical troubles, caused by the dipole.

We accept the fourth order model:

$$(1 - 2.73q^{-1} + 2.63q^{-2} - 0.95q^{-3} + 0.051q^{-4})y(t) =$$

$$= (0.138 - 0.36q^{-1} + 0.33q^{-2} - 0.11q^{-3})u(t) +$$

$$+ 0.027(1 - 1.62q^{-1} + 0.68q^{-2})e(t) \qquad (4.8)$$

with the continuous transfer function:

$$\frac{Y(s)}{U(s)} = \frac{0.0148[s^3 + 0.30s^2 + 0.042s + 0.005]}{s^4 + 1.49s^3 + 0.20s^2 + 0.048s + 0.0006} + 0.138 \qquad (4.9)$$

The consequences of data prefiltering can be studied, by comparing (4.8) with (4.6). See also section 6.4.

4.6. STEP RESPONSE ANALYSIS - EP-708.

In order to get a more complete comparison between models from different types of experiments, identifications have also been made with deterministic inputs, shown in fig. 3.4.

The rod to nuclear power loop has been analysed, and digital prefiltering has been used.

The plot (fig. 3.5) shows, that the output varies not very much a bit after a step in the rod position.

It is difficult to get accurate values of the output differences, as these are small. This depends on that only the total value of the nuclear is registered.

This value is converted into digital form with 11 bit resolution. When the differences are calculated the quantization errors become large, when compared to the small output variation.

Despite the difficulties mentioned the available data were analysed in order to give some knowledge how useful a simple step response experiment may be.

In table 4.14 the results of the identifications are summed up, assuming first order systems. We can see that the uncertainties are very large. The a_1 values (or pole) vary several standard deviations. In the second order models the results are quite irrelevant in this sense. The large variances are also due to the low number of sampling points (N).

No conclusions about the dynamics can be made from these results. The static gain is comparable to previous results.

5. IDENTIFICATION OF THE REACTIVITY - PRIMARY PRESSURE LOOP

Apart from the nuclear power also the vessel pressure is considered important. As inputs are used the two previously mentioned valves and the rods.

First the primary pressure is identified with the rod input. Generally the gain is very low, so one step amplitude of the rods was not enough (run 3, EP-710) to make the signal-to-noise ratio acceptable (see fig. 3.6). In runs 4 and 5 of EP-710, however, we found higher amplitudes of the pressure (see fig. 3.7 - 3.8). These runs are examined in 5.1 and 5.2 respectively.

5.1. EXPERIMENT 4, EP-710

This identification is based on the same number of data as in chapter 4.3. The input-output sequence consists of 737 data and has been filtered by differences, $1 - q^{-1}$.

The primary pressure is influenced in a similar way as the nuclear power by the neutron kinetics. The fast time constant gives a b_0 parameter significantly nonzero.

In order to increase the numerical accuracy, the output sequence was multiplied with 100 before identification. In the results this factor is reduced again.

5.1.1. Accomplishment of the Identification.

The second order model contained a redundant b_2 parameter from the beginning. When b_2 was omitted, the result got much better. The loss function was changed only in the fourth figure (table 5.1).

Also in the third order model the last b parameter, b_3, was omitted. The uncertainties decreased significantly, while the loss function increased only in the fourth figure.

The complete fourth order model contains four redundant parameters, a_4, b_3, b_4, and c_3 (table 5.1). It was made attempts to neglect one or two parameters, but better result was not achieved. The fourth order model is consequently not significant.

5.1.2. Test of Order.

The F test implies clearly a third order model on the 5% risk level.

There is no indication in table 5.2 of common factors in the polynomials.

Figure 5.2 shows, that the third order system residuals are better than the other residuals, but the second order residuals are also acceptable. The normality is accepted at 20 and 70% risk level respectively.

The static gain is determined very inaccurately, depending on numerical difficulties. The reason is the same as previously (section 4.2), that Σb_i and $1 + \Sigma a_i$ are small.

The continuous second and third order transfer functions are:

$$G(s) = \frac{0.00093(s + 1.011)}{(s + 0.106)(s + 0.547)} + 0.00072 \qquad (5.1)$$

and

$$G(s) = \frac{0.00102(s + 0.218)(s + 1.125)}{(s + 0.041)(s + 0.202)(s + 0.770)} + 0.00081 \qquad (5.2)$$

respectively.

The Bode plots have some minor differences (fig. 5.1).
The simulations show the accuracy of the different models (fig. 5.3 and 5.4). The discrepancies between the real outputs and the deterministic outputs are quite large. The high frequency behaviour is similar in both models, but low frequencies are badly recognized in both cases. The difference in the beginning of the transients is not decisive for the choice of model order.

Apparently the experimental data are bad. The output has some slowly varying mode of about 4 - 5 minutes period and this may depend on the long term control of the pressure, mentioned in section 3.3. Prefiltering of data further decreases the low frequency influence.

Due to the bad accuracy of both models, the best choice, if any, should be that of lowest order. Only fast variations can be explained in any case.

Thus, the model:

$$(1 - 1.14q^{-1} + 0.27q^{-2})\Delta y(t) =$$

$$= (0.00072 + 0.0014q^{-1})\Delta u(t) + 0.0018(1 - 0.91q^{-1} + 0.30q^{-2})e(t) \qquad (5.3)$$

is accepted. with the continuous transfer function (5.1).

5.2. EXPERIMENT 5, EP-710

As previously in run 5 a sequence of 1007 scans has been used. The input - output data have been prefiltered by taking differences.

5.2.1. Accomplishment of the Identification.

The second order model contained a redundant b_2 parameter. If b_2 was omitted the variances decreased significantly, and the loss function changed only in the fourth figure. (Table 5.3).

The third order model contains no redundant parameter. The parameter variances, however, are much larger than in the second order model. No attempt was made to eliminate b_3 as in previous run 4. Even if the variances should decrease, the experimental conditions are too bad to imply a third order model.

In the fourth order model both a_4, b_4, and c_4 were small (table 5.3), while also a_3, b_3, and c_3 were very uncertain. It was impossible to find a fourth order model with all parameters non-redundant, although the F test for the achieved fourth order model (table 5.3) indicates a small loss function.

5.2.2. Test of Order.

The results are quite analogous to the previous section. The roots of the models are shown in table 5.4. In fig. 5.5 the

residuals are plotted. For the same reason as in previous run 4, we accept a second order model. Corresponding simulation is shown in fig. 5.6. The third order model gives no better simulation result.

Thus, the second order model,

$$(1 - 1.12q^{-1} + 0.20q^{-2})\Delta y(t) = \tag{5.4}$$

$$= (0.00074 + 0.0019q^{-1})\Delta u(t) + 0.0016(1 - 0.97q^{-1} + 0.28q^{-2})e(t)$$

with the continuous version

$$G(s) = \frac{0.00113(s + 1.150)}{(s + 0.054)(s + 0.754)} + 0.00074 \tag{5.5}$$

is accepted.

6. COMPARISONS BETWEEN DIFFERENT PROCESS MODELS.

As the identifications of different experiments have given a number of results, some comparison has to be made in order to know something about the accuracy. It is difficult to define accuracy of a model. It may be defined in terms of deviations in the time response or in the transfer function.

As mentioned earlier it is not the goal to get only good process models, but to get the best control law for the reactor, based on the identification results. Therefore the most adequate comparison should be made between the different closed loop systems.

In this chapter the dynamic properties of the different models are compared partly to each other, partly to the state model. The comparison is not completely adequate, as all experiments are not made at the same operating condition. However, the behaviour can be compared qualitatively in these cases.

In order to make it easier, the models are summed up in 6.1. In 6.2 a discussion is made, how to compare different models. The motives for the choice of comparison methods are given. The rest of the chapter is devoted to comparisons between different models with reactivity input. As the EP-710 experiments are made under the same conditions a separate comparison of these models are made in 6.3. The other reactivity power models are discussed in 6.4. The reactivity primary pressure models are then compared in 6.5.

The maximum likelihood identification results can be compared to the state model (appendix). Input - output data has been generated by the state model, and a new model has been identified.

The coefficients are compared to the previous models in 6.6.

Finally, the choice of input is discussed in 6.7.

6.1. SUMMARY OF THE IDENTIFICATION RESULTS.

In order to simplify the references to the models we summarize the reactivity input models in this section.

Nuclear Power Output (C10).

EP-710 Run 3 (prefiltered input-output)

$$(1 - 1.59q^{-1} + 0.75q^{-2} - 0.05q^{-3})\Delta y(t) =$$

$$= (0.14 - 0.22q^{-1} + 0.09q^{-2})\Delta u(t) +$$

$$+ 0.029(1 - 1.42q^{-1} + 0.45q^{-2})e(t) \qquad (6.1)$$

EP-710 Run 4 (prefiltered input-output)

$$(1 - 1.42q^{-1} + 0.58q^{-2} - 0.037q^{-3})\Delta y(t) =$$

$$= (0.12 - 0.16q^{-1} + 0.06q^{-2})\Delta u(t) +$$

$$+ 0.033(1 - 1.24q^{-1} + 0.28q^{-2})e(t) \qquad (6.2)$$

EP-710 Run 5 (prefiltered input-output)

$$(1 - 1.69q^{-1} + 0.85q^{-2} - 0.05q^{-3})\Delta y(t) =$$

$$= (0.138 - 0.221q^{-1} + 0.099q^{-2})\Delta u(t) +$$

$$+ 0.028(1 - 1.52q^{-1} + 0.58q^{-2})e(t) \qquad (6.3A)$$

or

$$(1 - 2.69q^{-1} + 2.54q^{-2} - 0.90q^{-3} + 0.05q^{-4})y(t) =$$

$$= (0.138 - 0.36q^{-1} + 0.32q^{-2} - 0.099q^{-3})u(t) +$$

$$+ 0.028(1 - 1.52q^{-1} + 0.58q^{-2})e(t) \qquad (6.3B)$$

EP-710 Run 5 (no prefiltering)

$$(1 - 2.73q^{-1} + 2.63q^{-2} - 0.95q^{-3} + 0.051q^{-4})y(t) =$$

$$= (0.138 - 0.36q^{-1} + 0.33q^{-2} - 0.11q^{-3})u(t) +$$

$$+ 0.027(1 - 1.62q^{-1} + 0.68q^{-2})e(t) \qquad (6.4)$$

EP-708 Run 84 (from [19])

$$(1 - 2.11q^{-1} + 1.36q^{-2} - 0.25q^{-3})y(t) =$$

$$= (0.15 - 0.30q^{-1} + 0.19q^{-2} - 0.04q^{-3})u(t) +$$

$$+ 0.028|1 - 0.95q^{-1} + 0.21q^{-2} - 0.22q^{-3}|e(t) \qquad (6.5)$$

Primary Pressure Output (P13)

EP-710 Run 4 (prefiltered input-output)

$$(1 - 1.14q^{-1} + 0.27q^{-2})\Delta y(t) =$$

$$= (0.00072 + 0.0014q^{-1})\Delta u(t) +$$

$$+ 0.0018(1 - 0.91q^{-1} + 0.30q^{-2})e(t) \qquad (6.6)$$

EP-710 Run 5 (prefiltered input-output)

$$(1 - 1.12q^{-1} + 0.20q^{-2})\Delta y(t) =$$

$$= (0.00074 + 0.0019q^{-1})\Delta u(t) +$$

$$+ 0.0016(1 - 0.97q^{-1} + 0.28q^{-2})e(t)$$

or

$$(1 - 2.12q^{-1} + 1.32q^{-2} - 0.20q^{-3})y(t) =$$

$$= (0.00074 + 0.0012q^{-1} - 0.0019q^{-2})u(t) +$$

$$+ 0.0016(1 - 0.97q^{-1} + 0.28q^{-2})e(t) \qquad (6.7)$$

EP-708 Run 84 (from |19|)

$$(1 - 1.85q^{-1} + 0.86q^{-2})y(t) =$$

$$= (0.0018 + 0.0006q^{-1} - 0.0019q^{-2})u(t) +$$

$$+ 0.0018(1 - 0.62q^{-1} + 0.19q^{-2})e(t) \qquad (6.8)$$

The variables are given in physical units, that is reactivity in steps (≈7.5pcm)and output nuclear power in MW and pressure in bar. The variables of the state model (app.) are normalized to the stationary values. The reactivity is there written in cent.

6.2. METHODS OF MODEL COMPARISON.

A comparison of process models can be based on a number of different quantities and properties. Such properties are eigenvalues, poles and zeroes, Bode plots, static gain, parameter variance, simulations, and model order. The problem is, that there is no unique measure of accuracy of the open loop of a linear system. Therefore a comparison may sometimes be rather inaccurate, and the complete information of the model accuracy is not achieved, until the loop is closed.

The poles and zeroes in different discrete models may be compared (see chapter 4). However, if the roots are quite near each other, what does it mean for the model accuracy? Moreover, if the model orders are different, the comparison between the roots may be use-

less. The difficulties are even greater when the continuous state model should be compared to the discrete parameter models, as the transformation between continuous and discrete representation must be made. However, the roots may give qualitative hints about the model, as discussed in chapters 4 and 5.

A comparison of the frequency characteristics is also often a bad tool. Other authors, e.g. |24|, have mentioned, that a good agreement between two Bode plots may not cause a similar agreement between the time responses. The transform is an infinite operator, and therefore it may be erronious to use only the Bode plots for comparisons, as they are derived from time domain calculations.

The static gain and the low frequency behaviour may be compared by step responses. As shown later in this chapter the models differ considerably in this sense, but the question is, how the closed loop behaviour is affected by bad accuracy of the static gain.

The parameter accuracy is an important tool, but not a sufficient one to compare two models. In 6.3 an example from run 5, EP-710, will show, that a good parameter agreement can cause quite large deviations in the low frequency behaviour.

The model order comparison is also a very insufficient tool for comparison.

Simulation with different inputs has been the most used tool here for comparison of the models. Both the identifications and the comparisons are based upon the residuals. In order to test the closed loop system accuracy it is, however, not sufficient to make residual tests. The output variance may be the most adequate performance index.

6.3. COMPARISON BETWEEN THE REACTIVITY-POWER MODELS FROM EXPERIMENT EP-710.

The models (6.1) - (6.4), resulting from chapter 4, will be discussed in this section. The operation conditions are almost the same in all three runs, so the models ought to be similar.

First the parameters of the fourth order models (6.3B) and (6.4) are compared.
The parameters are based on the same data, but in the former case the data are prefiltered. From table 4.11 we find the sigma limits of the model order 4. (6.4) It is clear that the A and B polynomials of (6.3B) differ less than one sigma limit, while the C parameters differ a little bit more.
Despite the small differences of the parameters we will show in the next section, that the low frequency responses are quite different. This depends on the fact, that (6.3B) has zeroes exactly on the unit circle, but (6.4) has the corresponding zeroes of A and B in 0.975 and 0.957 respectively (table 4.13).

Obviously the parameters do not differ significantly if the input-output sequence has been prefiltered or not. However, the low frequency modes have been neglected by the filter, so the poles close to the unit circle have been moved to the circle exactly.

The parameters from the models (6.1), (6.2), and (6.3A) are then compared. The parameters in the models (6.1) and (6.3A) are closer to each other than to (6.2). One reason is, that run 4 (6.2) contained only 737 scans, so the parameters in (6.2) are also less accurate than those of the other models (see tables 4.1, 4.4, 4.7).

It is quite difficult to conclude very much from the pole patterns (tables 4.3, 4.6, 4.10). The pole configurations resemble each other, but frequency contents or simulations have to be studied in order to get better information.

From the simulations the most interesting detail may be the low frequency behaviour in run 5 (fig. 4.12 and 4.15). In fig. 4.12 the low frequencies are almost completely neglected. In the next section more simulation results are given.
The normality of the residuals has been tested in chapter 4. However, in most cases it has not been possible to verify normality. Probably this is not very crucial.

6.4. SIMULATIONS OF THE REACTIVITY-POWER MODELS.

The different identification results and the state model are compared by simulation in this section.

Three different inputs have been chosen. First the PRBS input from EP-710 has been applied to the model (6.5) and the theoretical model. Then the random reactivity input from EP-708, run 84, has been tried on the models (6.1) - (6.4) and the deterministic outputs as well as the residuals are plotted. Finally, the step responses are compared to each other.

Fig. 6.1 and 6.2 show simulations with the PRBS input (EP-710) applied to model (6.5) and to the theoretical model. The outputs (condition a) can be compared e.g. with that of fig. 4.16. The high frequencies are satisfactory, while there are some differences in the low frequencies.

The second input (from EP-708, run 84) shows more clearly the discrepancy in the low frequencies. Fig. 6.3 is a simulation of the model (6.5) based on the experiment 84 |19|. In fig. 6.4 - 6.7 the same input is applied to the different models achieved from EP 710.

The residuals of the different models are not very different from the "right" model in fig. 6.3. However, the deterministic outputs differ considerably. The low frequency modes are completely neglected in the models, based on prefiltered input-output data (fig. 6.4 - 6.6). The low frequency in fig. 6.7 is not very good either. However, the output from model (6.5) in fig. 6.3 is quite similar to that of the theoretical model (fig. 6.8).

Finally, the models are tested with step inputs (fig. 6.9). The static gain is not accurate, a fact, which was emphasized in chapter 4. Then it is demonstrated also here, that the low frequencies are badly recognized. The state model step response is shown in fig. 2.3. (Upper curve. Observe that other units are used.)

The bad low frequency behaviour of the models (6.1) - (6.4) may also depend on the choice of input, However, the input is not the only reason. Model (6.5) has also a very inaccurate static gain, although it is based on a low frequency input. The gain is almost of the form $\frac{0}{0}$, because of a dipole near the

unit circle. This in turn depends on a too small sampling interval. However, no common factors were found in this model either |19|.

6.5. COMPARISON BETWEEN THE REACTIVITY-PRIMARY PRESSURE MODELS FROM EXPERIMENT EP-710.

As in section 6.3 the models from the experiments EP-710 are considered, and they are previously discussed in chapters 5.1 and 5.2 (see (6.6) and (6.7)).

In general the parameter variances are larger in model (6.6) than in (6.7) depending on a shorter sample record (tables 5.1 and 5.3).

The step responses (fig. 6.10) are a bit faster than the state model step response (fig. 2.3, second curve). The static gain is not very accurate, a fact, which is shown in chapter 8.

The simulations of the state model (fig. 6.2, 6.8, condition a) should be compared to the experimental results.

The EP-710 models are shown in fig. 5.3 and 5.7, while the EP-708 model (from |19|) is simulated in fig. 6.11.

6.6. COMPARISONS WITH THE STATE MODEL BY IDENTIFICATION.

In the previous section 6.4 the identification results were compared by simulation. Here is considered another more relevant way of comparison between the reactivity - power models, viz. identification of the state model. The Åström model (section 4.1) is then achieved from data, generated by the state model, and the different parameters may be compared directly. The identification

method may also be used as a model reduction method.

As input to the state model the PRBS signal from run 5, EP-710 was used during 1000 sampling intervals.

A deterministic 11th order model should, of course, give a parametric model of the same order. Already for order five, however, great numerical difficulties arose, and the convergence speed was unsatisfactorily low. Therefore a fourth order model was tried,

$$A^{*}(q^{-1})y(t) = B^{*}(q^{-1})u(t)$$

where

$$A^{*}(q^{-1}) = 1 - 2.7953q^{-1} + 2.6069q^{-2} - 0.8141q^{-3} + 0.0028q^{-4} \qquad (6.9)$$

$$B^{*}(q^{-1}) = 1.0203 - 2.8339q^{-1} + 2.6245q^{-2} - 0.8108q^{-3} \qquad (6.10)$$

As the data has not been prefiltered, the model may be compared to the model (6.4). In order to compare the models the input has to be scaled, so $B^{*}(q^{-1})$ is divided with a constant. Thus the b_o parameter of (6.10) is made equal to b_o of (6.4).

$$\tilde{B}^{*}(q^{-1}) = 0.1379 - 0.3830q^{-1} + 0.3547q^{-2} - 0.1096q^{-3} \qquad (6.11)$$

Now the system has both a pole and a zero close to the unit circle, so the polynomials (6.9) and (6.10) are split up into

$$A^{*}(q^{-1}) = A_1^{*}(1 - q^{-1}) + o(q^{-4}) =$$

$$= (1 - 1.7953q^{-1} + 0.8116q^{-2} - 0.0025q^{-3})(1 - q^{-1}) +$$

$$+ 0.0003q^{-4} \qquad (6.12)$$

$$B^{*}(q^{-1}) = B_1^{*}(1 - q^{-1}) + o(q^{-3}) =$$

$$= (1.0203 - 1.8136q^{-1} + 0.8109q^{-2})(1 - q^{-1}) +$$

$$+ 0.0001q^{-3} \qquad (6.13)$$

The rest terms are neglected, and the polynomials A_1^* and B_1^* may be compared to the identification results of runs 3 - 5, (6.1) - - (6.3). Again B_1^* has to be scaled to

$$\tilde{B}_1^*(q^{-1}) = 0.1379 - 0.2451q^{-1} + 0.1096q^{-2}$$

The static gain of the scaled difference system is

$$\frac{\tilde{B}_1^*(1)}{A_1^*(1)} = 0.172 \qquad (6.14)$$

A simple noise model has been used in Halden |21| for the plant. Every state variable is corrupted by independent noise. This noise model showed a bad agreement with the experimental results, as was expected. Only the amplitude was almost correct. Also here numerical troubles occured in the identification of the fifth order model.

6.7. DISCUSSION OF THE INPUT CHOICE

The comparisons show that the high frequency performance is quite acceptable in all models. The low frequencies, however, are not very good.

The step responses have given bad accuracies, so we can confirm, that the input has to be persistently exciting |26| in this case.

The choice of bandwidth of the input and choice of sampling interval have to receive more attention. Recent reports in this area |3|, |17|, show the need of more knowledge.

The simulations have shown, that the identification result may depend very much on the choice of input frequency.

In section 6.4 was shown, that the slow input from EP-708, run 84, gave more accurate low frequency behaviour than the PRBS input in EP-710.

The low frequency limit of the EP-710 PRBS signal was $0.5 \cdot 10^{-3}$ Hz (section 3.3). Consequently time constants of several minuts would be identified |9|. However, the longest pulse length of the input is only 9 sampling intervals or 18 seconds.

It is reasonable to assume that time constants longer than about twice the longest pulse are badly identified |3|. In this case this means, that time constants greater than 30 - 40 seconds are not detected.

The longest pulse of run 84, EP-708, is about 240 seconds, i.e. about 13 times longer than the PRBS pulse.

If differences of the output are calculated, the slow modes are almost neglected. In order to eliminate drift, other methods have to be used, if the slow modes should remain. The simplest way would be a subtraction of a straight line from the output. Other suggestions are made in |2|, |20|.

7. SUBJECTS FOR FUTURE STUDIES.

The identifications of the HBWR dynamics have revealed some general problems. They may be split up into three classes, experiment planning, identification, and control.

The results have shown clearly, that the choice of sampling interval is crucial. It is also obvious, that a step input is not sufficient to give an accurate model desired. The type of random input must be taken into account, and also other types of inputs than PRBS may be useful |3|. If the model shall be used for control purposes, the most interesting frequency range must be stated. Then the instrument equipment has to be considered. For example, on the HBWR only the total nuclear power and not its difference values can be measured (section 4.6). Of this reason, quantization errors in the AD conversion as well as instrument noise are significant.

Drift elimination at the identification may be crucial |20|. High pass prefiltering eliminates the low frequency modes, and it is interesting to know the consequences for the closed loop behaviour.

Redundant parameters have occured many times here. A method for automatic parameter elimination should simplify the identification procedure.

The static gain has been calculated with bad accuracy. A dipole has occured close to the unit circle, which causes the static gain to be the quotient of two small numbers. The pole close to the unit circle is a result of the short sampling interval. The closed loop sensitivity for the gain error has to be known. Probably a larger sampling interval should be the best correction to make in this case.

Multiple mode control of the reactor may be interesting to try, as the reactor time constants cover a very broad range.

REFERENCES.

|1| Brouwers, A.: Step Perturbation Experiments with the HBWR Second Fuel Charge, HPR-51 OECD Halden Reactor Project, 1964.

|2| Brown, R.F.: Effects of Drift and Nonlinearity upon Pseudo-random Binary Crosscorrelation Estimates, Paper 9.5, Preprints IFAC Symp., Prague, 1970.

|3| Cumming, I.G.: Frequency of Input Signal in Identification, Paper 7.8, Preprints IFAC Symp., Prague, 1970.

|4| Cummins, J.D.: Parameter Estimation from Dragon High Temperature Gas Cooled Reactor Dynamic Experiments, Report AEEW - R 571, Atomic Energy Establishment, Winfrith, Dorset.

|5| Eurola, T.: Noise Experiments with the HBWR Second Fuel Charge, HPR-53, OECD Halden Reactor Project, 1964.

|6| Eurola, T.: Dynamics Model of the HBWR Heat Removal Circuits, HPR-62 OECD Halden Reactor Project, 1964.

|7| Fishman, Y.: Pseudorandom Reactivity Perturbation Experiments with the HBWR Second Fuel Charge, HPR-50 OECD Halden Reactor Project, 1964.

|8| Fleck, J.A.Jr.: The Dynamic Behaviour of Boiling Water Reactors, J. Nucl. Energy, Part A, Reactor Science, 11, 1960.

|9| Godfrey, K.R.: The Application of Pseudo-Random Sequences to Industrial Processes and Nuclear Power Plant, Paper 7.1, Preprints IFAC Symp., Prague, 1970.

|10| Grumbach, R. et.al.: Application of Modern Control Theory to Digital Control of HBWR, Paper to the Seminar on "Applications of On-line Computers to Nuclear Reactors", Sandefjord, Norway, 1968.

|11| Grumbach, R.: Covariance Analysis in the Design of Models and Monitor Patterns for On-line Computer Control of Multivariable Processes, HPR-106 OECD Halden Reactor Project, Norway, 1969.

|12| Grumbach, R.: Personal Communication, 1969, 1970.

|13| Gustavsson, I.: Maximum Likelihood Identification of Dynamics of the Ågesta Reactor and Comparison with Results of Spectral Analysis, Report 6903, Div. of Aut. Control, Lund Inst. of Techn., Lund, 1969.

|14| Gustavsson, I.: Parametric Identification of Multiple Input, Single Output Linear Dynamical Systems, Report 6907, Div. of Aut. Control, Lund Inst. of Techn., Lund, 1969.

|15| Gustavsson, I.: Identification of Dynamics of a Distillation Column, Report 6916, Div. of Aut. Control, Lund Inst. of Techn., Lund, 1969.

|16| Gustavsson, I.: Comparison of Different Methods for Identification of Linear Models for Industrial Processes, Preprints IFAC Symp., Prague, 1970.

|17| Gustavsson, I., Choice of Sampling Interval for Parametric Identification. Report 7103, Div. of Autom. Cont., Lund Inst. of Techn., Lund, Sweden 1971

|18| Klöver, L., Olsson, L.E.: Identifiering av Halden-reaktorns dynamik, Master thesis, Div. of Aut. Control, Lund Inst. of Techn., Lund, 1969, Sweden.

|19| Nikiforuk, P.N. et.al.: Identification of Linear Discrete Systems in the Presence of Drift Using Pseudorandom Sequences, Paper 7.4, Preprints IFAC Symp., Prague, 1970.

|20| Sato, Kazuo: Personal Communication, 1969, 1970.

|21| Tosi, V., Åkerhielm, F.: Sinusoidal Reactivity Perturbation Experiments with the HBWR Second Fuel Charge, HPR-49, OECD Halden Reactor Project, 1964.

|22| Uhrig, R.E. (ed.): Symposium on Neutron Noise, Waves and Pulse Propagation, Univ. of Florida, Gainesville, Florida, 1966, published as CONF 660206 by the USAEC, 1967.
Especially: Johnson, J.A.: pp. 271-284
Wasserman, A.A., Steiner,G.H., Bodenschatz, C.A., Honka, E.K.: pp. 285-314
Rajagopal, V., Gallagher, J.M.: pp. 487-501

|23| Unbehauen, H., Schlegel, G.: Estimation of the Accuracy in the Identification of Control Systems Using Deterministic Test Signals, IFAC Symposium, Prague, Paper 1.12, 1967.

|24| Vollmer, H., and Andersson, A.J.W.: Development of a Dynamic Model for Heavy Water Boiling Reactors and its Application to the HBWR, HPR-54 OECD Halden Reactor Project, 1964.

|25| Åström, K.J., and Bohlin, T.: Numerical Identification of Linear Dynamic Systems from Normal Operating Records, Paper IFAC Symp., Theory of Self-Adaptive Control Systems, Teddington, 1965.

|26| Åström, K.J.: Computer Control of a Paper Machine - An Application of Linear Stochastic Control Theory, IBM Journal of Research and Dev., 11, 389-405.

|27| Åström, K.J.: Lectures on the Identification Problem. The Least Squares Method, Report 6806, Div. of Aut. Control, Lund Inst. of Techn., Lund, 1968.

|28| Åström, K.J., Eykhoff, P.: System Identification, a Survey, IFAC Symposium, Prague, June, 1970.

|29| Åström, K.J.: Introduction to Stochastic Control Theory, N.Y. Academic Press, 1970.

|30| Øvreeide, M.: Siffermaskinstyringseksperimenter ved HBWR, Seminar in Lund, 1967.

APPENDIX

THE SYSTEM MATRICES OF THE LINEAR STATE MODEL.

The matrices A, B, and C of the reactor model are found in an analog computer scheme in |18|, but are repeated here for convenience.

Two reactor conditions a and b with 2 MW and 1.1 MW subcooling respectively are defined. Condition b is consequently less stable (see table A.1).

The A matrices are different in the two cases, while B and C are constant.

The explanation of the state variables is found on page 9. The control variables are

u_1 = subcooling valve VA770. Δu_1 corresponds to change of the opening of the valve. u_1 can vary 1 unit.

u_2 = tertiary steam flow valve VB282

u_3 = reactivity $\frac{\delta k}{\beta}$

Reactor condition a.

$$
\begin{array}{c}
\begin{pmatrix} n^* & p_1^* & p_2^* & p_3^* & c^* & \theta_F & \theta_W & \theta_{sub} & x_9 & x_{10} & x_{11} \end{pmatrix} \\
A = \begin{bmatrix}
-10.0 & -30.0 & 27.0 & 0 & 10.0 & -5.368 & -47.0 & 0.648 & 1.572 & 0 & 0 \\
0 & -0.15 & 0.0225 & 0 & 0 & 0.01011 & 0.12 & 0.00024 & 0.00036 & 0 & 0 \\
0 & 0.0723 & -0.10 & 0.0244 & 0 & 0 & 0 & -0.0003 & 0 & 0 & 0 \\
0 & 0 & 0.02 & -0.025 & 0 & 0 & 0 & 0 & 0 & 0 & 0 \\
0.08 & 0 & 0 & 0 & -0.08 & 0 & 0 & 0 & 0 & 0 & 0 \\
0.125 & 0 & 0 & 0 & 0 & -0.125 & 0 & 0 & 0 & 0 & 0 \\
0 & 0 & 0.0075 & 0 & 0 & 0.00087 & -0.01 & -0.0002 & -0.0003 & 0 & 0 \\
0 & 0 & 0 & 0 & 0 & 0 & 0 & -0.05 & -0.05 & 0 & 0 \\
0 & 0 & 0 & 0 & 0 & 0 & 0 & 0 & -0.05 & 0 & -0.2625 \\
0 & 0 & 0 & 0 & 0 & 0 & 0 & 0 & 0 & 0 & -0.2625 \\
0 & 0 & 0 & 0 & 0 & 0 & 0 & 0 & 0 & 0.2625 & -0.04
\end{bmatrix}
\end{array}
$$

A 2.

$$B = \begin{pmatrix} 0 & 0 & 10.0 \\ 0 & 0 & 0 \\ 0 & 0 & 0 \\ 0 & -0.0975 & 0 \\ 0 & 0 & 0 \\ 0 & 0 & 0 \\ 0 & 0 & 0 \\ 0 & 0 & 0 \\ 0 & 0 & 0 \\ 0.1 & 0 & 0 \\ 0 & 0 & 0 \end{pmatrix}$$

$$C = \begin{pmatrix} 1 & 0 & \cdots & 0 \\ 0 & 1 & 0 & \cdots & 0 \\ 0 & 0 & 1 & 0 & \cdots & 0 \\ 0 & 0 & 0 & 1 & 0 & \cdots & 0 \end{pmatrix}$$

Reactor condition b.

$$A = \begin{pmatrix} n^* & p_1^* & p_2^* & p_3^* & c^* & \theta_F & \theta_W & \theta_{sub} & x_9 & x_{10} & x_{11} \\ -10.0 & \underline{-80.0} & \underline{72.0} & 0 & 10.0 & \underline{2.352} & \underline{-46.0} & \underline{1.6792} & \underline{1.7688} & 0 & 0 \\ 0 & -0.15 & 0.0225 & 0 & 0 & 0.1011 & 0.12 & \underline{0.00034} & \underline{0.0005} & 0 & 0 \\ 0 & 0.0723 & -0.1 & 0.0244 & 0 & 0 & 0 & -0.0003 & 0 & 0 & 0 \\ 0 & 0 & 0.02 & -0.025 & 0 & 0 & 0 & 0 & 0 & 0 & 0 \\ 0.08 & 0 & 0 & 0 & -0.08 & 0 & 0 & 0 & 0 & 0 & 0 \\ 0.125 & 0 & 0 & 0 & 0 & -0.125 & 0 & 0 & 0 & 0 & 0 \\ 0 & 0 & 0.0075 & 0 & 0 & 0.00087 & -0.01 & \underline{-0.00028} & \underline{-0.00042} & 0 & 0 \\ 0 & 0 & 0 & 0 & 0 & 0 & 0 & -0.05 & -0.05 & 0 & 0 \\ 0 & 0 & 0 & 0 & 0 & 0 & 0 & 0 & -0.05 & 0 & -0.2625 \\ 0 & 0 & 0 & 0 & 0 & 0 & 0 & 0 & 0 & 0 & -0.2625 \\ 0 & 0 & 0 & 0 & 0 & 0 & 0 & 0 & 0 & 0.2625 & -0.04 \end{pmatrix}$$

A 4.

The underlined figures are changed compared to condition a.

EIGENVALUES.

The system matrix A can be subdivided, which simplifies the eigenvalue calculation.

Thus we find:

$$|sI - A| = (s + 0.05)^2\{(s + 0.04)s + 0.2625^2\}|sI - A_7|$$

where A_7 denotes the submatrix of order seven. The eigenvalues are given in table A.1.

Table A.1 - Eigenvalues.

Cond A	Cond B
-0.01967 ± j • 0.004438	-0.003651 ± j • 0.02166
-0.02266	-0.02084
-0.08823	-0.08545
-0.1633 ± j • 0.06129	-0.1331 ± j • 0.07871
-10.013	-10.110
-0.02000 ± j 0.2617	-0.02000 ± j 0.2617
-0.05000	-0.05000
-0.05000	-0.05000

The first six eigenvalues correspond to time constants between 6 and 44 seconds (condition A) and 7.5 and 300 seconds (condition B). The seventh eigenvalue corresponds to the neutron kinetics with a time constant of about 0.1 second. This eigenvalue is impossible to detect with a 2 sec. sampling interval. Therefore we find a direct term from input to output in the identifications.

The last four eigenvalues correspond to the fictitious states and hav no physical interpretation.

Table 3.1 - Summary of the analysed experiments.

Run No.	Input	Input type/ /amplitude	Number of scans	Stationary			Comments
				Power MW	Sub-cooling MW	Pressure bar	
EP-706							
681001-10	VB282	step/	900	9.7	2.0	33.0	
11	VB282	step/	900	10.0	2.0	32.8	
14	VA770	step/65→83%	900	9.9	1.9	32.3	
15	VA770	step/83→47%	900	10.1	2.1	32.4	
EP-708							
57	Rod 15	a, ΔT=60/4	240	8±0.5		31.9	
60	" 15	" =30/4	150	"		"	
63	" 15	" =20/4	100	"		"	
65	" 11	" =60/4	185	"		"	
66	" 11	" =30/4	150	"		"	
67	" 11	" =20/4	100	"		"	
84	" 11	b/1	780	"		"	Analysed in [19]
EP-710							
3	Rod 15	PRBS/1	1019	9.69	1.36	30.5	+0.5 MW drift.
4	" 15+17	-"-	749	9.92	1.39	30.6	Positive drift.
5	" 13+15+17	-"-	1019	9.48	1.35	30.5	+0.3 MW drift.

Table 4.1 - Experiment EP-710, run 3. Output nuclear power. Estimates of the parameters and their variances for different model orders. The calculation is based on 1007 scans (prefiltered).

n	1	2	3	4
a_1	-0.0768 ± 0.0111	-1.3441 ± 0.1037	-1.5887 ± 0.0895	0.3072 ± 0.1207
a_2		0.4794 ± 0.0942	0.7477 ± 0.0884	-1.0561 ± 0.0847
a_3			-0.0506 ± 0.0148	-0.2967 ± 0.0895
a_4				0.5038 ± 0.0758
b_0	0.1436 ± 0.0015	0.1445 ± 0.0018	0.1447 ± 0.0018	0.1445 ± 0.0018
b_1		-0.1812 ± 0.0150	-0.2164 ± 0.0130	0.0575 ± 0.0176
b_2		0.0571 ± 0.0131	0.0916 ± 0.0114	-0.1432 ± 0.0132
b_3				-0.0511 ± 0.0131
b_4				0.0642 ± 0.0106
c_1	0.1768 ± 0.0313	-1.1674 ± 0.1173	-1.4209 ± 0.1037	0.4896 ± 0.1335
c_2		0.1993 ± 0.1152	0.4497 ± 0.1016	-1.0465 ± 0.0940
c_3				-0.6246 ± 0.1142
c_4				0.2945 ± 0.1047
λ	0.03016	0.02906	0.02891	0.02882
V	0.45787	0.42526	0.42085	0.41828
Gain	0.155	0.181	0.184	0.157
$F_{n,n-1}$		19.2	10.4	1.2

Table 4.2 - Experiment EP-710, run 3. Output nuclear power. Estimates of parameters and their variances for different third order model structures.

n	3 A	3 B = 3	3 C
a_1	-1.1294 ± 0.2939	-1.5887 ± 0.0895	-1.6648 ± 0.1803
a_2	0.0382 ± 0.3802	0.7477 ± 0.0884	0.8419 ± 0.2183
a_3	0.2516 ± 0.1405	-0.0506 ± 0.0148	-0.0811 ± 0.0698
a_4			
b_0	0.1446 ± 0.0018	0.1447 ± 0.0018	0.1447 ± 0.0018
b_1	-0.1500 ± 0.0425	-0.2164 ± 0.0130	-0.2274 ± 0.0261
b_2	-0.0049 ± 0.0510	0.0916 ± 0.0114	0.1043 ± 0.0293
b_3	0.0377 ± 0.0168		-0.0039 ± 0.0089
b_4			
c_1	-0.9549 ± 0.2951	-1.4209 ± 0.1037	-1.4943 ± 0.1791
c_2	-0.2091 ± 0.3216	0.4497 ± 0.1016	0.5202 ± 0.1725
c_3	0.2060 ± 0.0853		
c_4			
λ	0.02886	0.028911	0.02891
V	0.41938	0.42085	0.42077
Gain	0.171	0.184	0.184
$F_{n,n-1}$	4.6	10.4	5.3

Table 4.3 - Experiment EP-710, run 3. Output nuclear power.
Roots of the discrete models of different order.

n	A	B	C
1	0.077		-0.177
2	0.672 ± 0.167j	0.627	0.208
		0.627	0.960
3	0.081	0.748 ± 0.272j	0.476
	0.754 ± 0.240j		0.945
4	0.720 ± 0.217j	0.679 ± 0.182j	0.334
	-0.873 ± 0.360j	-0.878 ± 0.358j	0.954
			-0.889 ± 0.367j

Table 4.4 - Experiment EP-710, run 4. Output nuclear power. Estimates of the parameters and their variances for different model orders. The calculation is based on 737 scans (prefiltered).

n	1	2	3	4
a_1	-0.0650 ± 0.0087	-1.1489 ± 0.0374	-1.4229 ± 0.1311	-1.9370 ± 0.1629
a_2		0.2842 ± 0.0349	0.5796 ± 0.1280	1.9992 ± 0.2882
a_3			-0.0372 ± 0.0128	-1.1691 ± 0.2448
a_4				0.2546 ± 0.1053
b_0	0.1197 ± 0.0010	0.1205 ± 0.0012	0.1206 ± 0.0012	0.1204 ± 0.0012
b_1	0	-0.1290 ± 0.0047	-0.1619 ± 0.0158	-0.2239 ± 0.0197
b_2		0.0265 ± 0.0041	0.0596 ± 0.0142	0.2257 ± 0.6334
b_3				-0.1250 ± 0.0282
b_4				0.0230 ± 0.0117
c_1	0.1825 ± 0.0367	-0.9603 ± 0.0150	-1.2360 ± 0.1443	-1.7507 ± 0.1678
c_2		0	0.2764 ± 0.1415	1.5927 ± 0.2848
c_3				-0.8198 ± 0.2366
c_4				0.0235 ± 0.1149
λ	0.03377	0.03290	0.03274	0.03263
V	0.42020	0.39881	0.39506	0.39235
Gain	0.128	0.133	0.153	0.137
$F_{n,n-1}$		13.1	3.5	1.0
$1+\Sigma a_i$	0.9350	0.1353	0.1195	0.1477
Σb_i	0.1197	0.0180	0.0183	0.0202

Table 4.5 - Experiment EP-710, run 4. Output nuclear power. Estimates of parameters and their variances for different third order model structures.

n	3 A	3 B	3 C = 3
a_1	-1.4908 ± 0.2083	-1.3591 ± 0.3037	-1.4229 ± 0.1311
a_2	0.6363 ± 0.1832	0.5046 ± 0.3452	0.5796 ± 0.1280
a_3	-0.0386 ± 0.0131	-0.0168 ± 0.0873	-0.0372 ± 0.0128
b_0	0.1206 ± 0.0012	0.1206 ± 0.0012	0.1206 ± 0.0012
b_1	-0.1700 ± 0.0251	-0.1542 ± 0.0366	-0.1619 ± 0.0158
b_2	0.0658 ± 0.0200	0.0512 ± 0.0388	0.0596 ± 0.0142
b_3	0	0.0021 ± 0.0088	
c_1	-1.3015 ± 0.2112	-1.1725 ± 0.3083	-1.2360 ± 0.1443
c_2	0.3094 ± 0.1514	0.2158 ± 0.2964	0.2764 ± 0.1415
c_3	0.0288 ± 0.0766	0	
λ	0.03274	0.03274	0.03274
V	0.39499	0.39504	0.39506
Gain	0.153	0.153	0.153
$F_{n,n-1}$	2.3	2.3	3.5

Table 4.6 - Experiment EP-710, run 4. Output nuclear power.
Roots of the discrete models of different order.

n	A	B	C
1	0.065		-0.183
2	0.360	0.277	0.960
	0.788	0.793	
3	0.078	0.671 ± 0.209j	0.293
	0.672 ± 0.149j		0.943
4	0.439	0.321	0.030
	0.744	0.754	0.955
	0.377 ± 0.799 j	0.392 ± 0.797j	0.383 ± 0.814j

Table 4.7 - Experiment EP-710, run 5. Output nuclear power. Estimates of the parameters and their variances for different model orders. The calculation is based on 1007 scans (prefiltered).

n	1	2	3	4
a_1	-0.1645 ± 0.0566	-1.1051 ± 0.0330	-1.6908 ± 0.0615	-0.4396 ± 0.1402
a_2		0.2313 ± 0.0277	0.8458 ± 0.0614	-0.9257 ± 0.0759
a_3			-0.0499 ± 0.0064	0.5267 ± 0.1252
a_4				0.1161 ± 0.0674
b_0	0.1373 ± 0.0005	0.1375 ± 0.0006	0.1375 ± 0.0006	0.1376 ± 0.0006
b_1	-0.0112 ± 0.0073	-0.1400 ± 0.0046	-0.2206 ± 0.0085	-0.0486 ± 0.0193
b_2		0.0214 ± 0.0036	0.0989 ± 0.0077	-0.1299 ± 0.0095
b_3				0.0623 ± 0.0171
b_4				0.0193 ± 0.0078
c_1	0.0525 ± 0.0633	-0.9340 ± 0.0165	-1.5184 ± 0.0732	-0.2664 ± 0.1444
c_2			0.5775 ± 0.0702	-0.9631 ± 0.0735
c_3				0.2806 ± 0.1354
c_4				0.1033 ± 0.0580
λ	0.02856	0.02817	0.02767	0.02755
V	0.41081	0.39944	0.38544	0.38226
Gain	0.151	0.150	0.150	0.147
$F_{n,n-1}$		14.2	18.2	1.65

Table 4.8 - Experiment EP-710, run 5. Output nuclear power. Estimates of parameters and their variances for different second order model structures.

n	2 A	2 B = 2	2 C
a_1	-1.0448 ± 0.0832	-1.1051 ± 0.0330	-0.9213 ± 0.0296
a_2	0.1765 ± 0.0743	0.2313 ± 0.0277	0.0602 ± 0.0053
b_0	0.1375 ± 0.0006	0.1375 ± 0.0006	0.1375 ± 0.0006
b_1	-0.1317 ± 0.0115	-0.1400 ± 0.0046	-0.1147 ± 0.0041
b_2	0.0145 ± 0.0093	0.0214 ± 0.0036	
c_1	-0.8680 ± 0.0839	-0.9340 ± 0.0165	-0.7529 ± 0.0371
c_2	-0.0623 ± 0.0774		-0.1713 ± 0.0288
λ	0.02816	0.02817	0.02819
V	0.39919	0.39944	0.40018
Gain	0.154	0.150	0.164
$F_{n,n-1}$	8.9	14.2	12.0

Table 4.9 - Experiment EP-710, run 5. Output nuclear power. Estimates of parameters and their variances for different third order structures.

n	3 A	3 B = 3
a_1	-1.4270 ± 0.1386	-1.6908 ± 0.0615
a_2	0.4693 ± 0.1803	0.8458 ± 0.0614
a_3	0.0985 ± 0.0666	-0.0499 ± 0.0064
b_0	0.1376 ± 0.0006	0.1375 ± 0.0006
b_1	-0.1844 ± 0.0191	-0.2206 ± 0.0085
b_2	0.0502 ± 0.0232	0.0989 ± 0.0077
b_3	0.0173 ± 0.0077	
c_1	-1.2598 ± 0.1424	-1.5184 ± 0.0732
c_2	0.2680 ± 0.1638	0.5775 ± 0.0702
c_3	0.0699 ± 0.0553	
λ	0.02761	0.02767
V	0.38377	0.38544
Gain	0.147	0.150
$F_{n,n-1}$	10.2	18.2

Table 4.10 - Experiment EP-710, run 5. Output nuclear power.
Roots of the discrete models of different order.

n	A	B	C
1	0.165	0.082	-0.053
2	0.281	0.187	0.934
	0.825	0.831	
3	0.068	0.802	0.759 ± 0.033j
	0.811 ± 0.278j	0.275	
4	-0.174	-0.221	-0.220
	0.787 ± 0.275j	0.768 ± 0.264j	0.841
	-0.962	-0.961	0.590
			-0.945

Table 4.11 - Experiment EP-710, run 5. Output nuclear power. Estimates of the parameters and their variances for different model orders.
The calculation is based on 1007 scans (data not prefiltered).
3^x is the model from |19|, based on EP-708, run 84 (for comparison).

n	2	3 B = 3	4	3^x
a_1	-0.8134 ± 0.0202	-1.8610 ± 0.0336	-2.7297 ± 0.0466	-2.108 ± 0.165
a_2		0.9152 ± 0.0366	2.6295 ± 0.0917	1.364 ± 0.316
a_3		-0.0534 ± 0.0054	-0.9483 ± 0.050	-0.254 ± 0.152
a_4			0.0513 ± 0.0056	
b_0	0.1394 ± 0.0007	0.1380 ± 0.0006	0.1379 ± 0.0006	0.148 ± 0.006
b_1	-0.0979 ± 0.0029	-0.2444 ± 0.0047	-0.3638 ± 0.0065	-0.298 ± 0.029
b_2		0.1066 ± 0.0046	0.3320 ± 0.0120	0.187 ± 0.052
b_3			-0.1054 ± 0.0057	-0.037 ± 0.025
c_1	0.2799 ± 0.0389	-0.7724 ± 0.0426	-1.6242 ± 0.0572	0.954 ± 0.163
c_2	0.2097 ± 0.0334	-0.0276 ± 0.0419	0.6848 ± 0.0587	0.210 ± 0.126
c_3		-0.1633 ± 0.0322		-0.218 ± 0.056
λ	0.02961	0.02744	0.02710	0.02805
V	0.44181	0.37936	0.37022	0.30653
$F_{n,n-1}$		41	24.7	

Table 4.12 - Experiment EP-710, run 5. Output nuclear power. Estimates of parameters and their variances for different third and fourth order model structures (data not prefiltered).

n	3 A	3 B = 3	4 A	4 B	4 C = 4
a_1	-1.8173 ± 0.0987	-1.8610 ± 0.0336	-2.4643 ± 0.1244	-2.5222 ± 0.1100	-2.7297 ± 0.0466
a_2	0.8338 ± 0.1756	0.9152 ± 0.0366	1.9841 ± 0.2922	2.1420 ± 0.2430	2.6295 ± 0.0917
a_3	-0.0158 ± 0.0794	-0.0534 ± 0.0054	-0.4042 ± 0.2403	-0.5567 ± 0.1749	-0.9483 ± 0.050
a_4			-0.1118 ± 0.0730	-0.0600 ± 0.0439	0.0513 ± 0.0056
b_0	0.1380 ± 0.0006	0.1380 ± 0.0006	0.1379 ± 0.0006	0.1380 ± 0.0006	0.1379 ± 0.0006
b_1	-0.2383 ± 0.0137	-0.2444 ± 0.0047	-0.3273 ± 0.0172	-0.3353 ± 0.0152	-0.3638 ± 0.0065
b_2	0.0959 ± 0.0230	0.1066 ± 0.0046	0.2463 ± 0.0387	0.2673 ± 0.0322	0.3320 ± 0.0120
b_3	0.0046 ± 0.0097		-0.0365 ± 0.0302	-0.0560 ± 0.0217	-0.1054 ± 0.0057
b_4			-0.0194 ± 0.0086	-0.0131 ± 0.0051	
c_1	-0.7282 ± 0.1026	-0.7724 ± 0.0426	-1.3849 ± 0.1279	-1.4497 ± 0.1108	-1.6242 ± 0.0572
c_2	-0.0647 ± 0.0884	-0.0276 ± 0.0419	0.4081 ± 0.1663	0.5223 ± 0.1114	0.6848 ± 0.0587
c_3	-0.1688 ± 0.0340	-0.1633 ± 0.0322	0.0612 ± 0.0788		
c_4			-0.0020 ± 0.0398		
λ	0.02743	0.02744	0.02700	0.02702	0.02710
V	0.37927	0.37936	0.36755	0.36784	0.37022
$F_{n,n-1}$	33	41	8.0	15.6	24.7

Table 4.13 - Experiment EP-710, run 5. Output nuclear power. Roots of the discrete models of different order (data not prefiltered).

n	A	B	C
2	0.813	0.702	-0.140 ± 0.436j
3	0.067	0.778	-0.100 ± 0.397j
	0.996	0.993	0.973
	0.798		
4	0.065	0.840 ± 0.303j	0.812 ± 0.159j
	0.845 ± 0.308j	0.957	
	0.975		
3 x)(84)	0.322	0.424	-0.008 ± 0.474j
	0.985	0.589	0.969
	0.801	1.000	

x) from |19|, run 84, EP-708.

Table 4.14 - Experiment EP-708, runs 57-67. Input reactivity steps. Output nuclear power. Estimates of parameters and their variances for first order models.

Run	Input rod	N	a_1	b_0	c_1	λ	G_{st}
57	15	238	-0.1377 ± 0.0447	0.1196 ± 0.0059	-0.0182 ± 0.0704	0.02236	0.139
60	15	148	-0.0796 ± 0.0458	0.1118 ± 0.0055	-0.0588 ± 0.0835	0.02402	0.122
63	15	98	-0.1088 ± 0.0482	0.1173 ± 0.0061	0.0124 ± 0.0998	0.02546	0.131
65	11	169	-0.0885 ± 0.0504	0.1363 ± 0.0071	0.1152 ± 0.0907	0.02220	0.150
66	11	148	-0.2026 ± 0.0495	0.1146 ± 0.0066	0.1067 ± 0.0833	0.02762	0.142
67	11	98	-0.1051 ± 0.0362	0.1244 ± 0.0049	-0.0282 ± 0.0921	0.02122	0.139

Table 5.1 - Experiment EP-710, run 4. Output primary pressure. Estimates of the parameters and their variances for different model orders.
The calculation is based on 737 scans (prefiltered).

n	1	2	3	4
a_1	-0.9142 ± 0.0175	-1.1443 ± 0.0368	-1.8032 ± 0.0901	-2.0402 ± 0.5374
a_2		0.2709 ± 0.0361	0.9556 ± 0.1270	1.3028 ± 1.1341
a_3			-0.1319 ± 0.0457	-0.1267 ± 0.8317
a_4				-0.1183 ± 0.2278
b_0	0.00072 ± 0.00007	0.00072 ± 0.00006	0.00081 ± 0.00006	0.00082 ± 0.00006
b_1	0.00161 ± 0.00007	0.00143 ± 0.00007	0.00098 ± 0.00011	0.00080 ± 0.00044
b_2		0	-0.00096 ± 0.00012	-0.00128 ± 0.00042
b_3			0	0.00021 ± 0.00070
b_4				0.00027 ± 0.00028
c_1	-0.6512 ± 0.0414	-0.9057 ± 0.0494	-1.6443 ± 0.0909	-1.8758 ± 0.5360
c_2		0.3029 ± 0.0535	0.9587 ± 0.1184	1.2328 ± 1.0398
c_3			-0.2882 ± 0.0480	-0.2257 ± 0.7755
c_4				-0.1052 ± 0.2576
λ	0.00183	0.00177	0.00173	0.00172
V	0.00124	0.001153	0.001097	0.001087
Gain	0.027	0.017	0.040	0.047
$F_{n,n-1}$		29	12.4	1.7

Table 5.2 - Experiment EP-710, run 4. Output primary pressure.
Roots of the discrete models of different order.

n	A	B	C
1	0.9142	-2.236	0.6512
2	0.335 0.810	-1.986	0.453 ± 0.313j
3	0.215 0.667 0.922	0.641 -1.850	0.957 0.343 ± 0.428j
4	-0.223 0.940 0.662 ± 0.355j	-0.387 0.633 ± 0.340j -1.879	-0.194 0.952 0.559 ± 0.508j

Table 5.3 - Experiment EP-710, run 5. Output primary pressure. Estimates of the parameters and their variances for different model orders.
The calculation is based on 1007 scans.

n	1	2	3	4
a_1	-0.9526 ± 0.0070	-1.1176 ± 0.0150	-2.1304 ± 0.1141	-2.3654 ± 0.2389
a_2		0.1984 ± 0.0154	1.5257 ± 0.2026	1.8645 ± 0.5441
a_3			-0.3813 ± 0.0922	-0.3901 ± 0.4359
a_4				-0.0972 ± 0.1279
b_0	0.00076 ± 0.00004	0.00074 ± 0.00003	0.00077 ± 0.00003	0.00078 ± 0.00003
b_1	0.00202 ± 0.00004	0.00187 ± 0.00004	0.00111 ± 0.00010	0.00093 ± 0.00019
b_2		0	-0.00179 ± 0.00018	-0.00213 ± 0.00025
b_3			0.00055 ± 0.00020	0.00066 ± 0.00048
b_4				0.00037 ± 0.00022
c_1	-0.8082 ± 0.0395	-0.9698 ± 0.0323	-2.0822 ± 0.1081	-2.3115 ± 0.2448
c_2		0.2882 ± 0.0432	1.6268 ± 0.1734	1.9309 ± 0.5468
c_3			-0.5294 ± 0.0705	-0.5617 ± 0.4642
c_4				-0.0423 ± 0.1582
λ	0.00169	0.00158	0.00152	0.00151
V	0.001442	0.001250	0.001165	0.001142
Gain	0.059	0.032	64/1400 = 0.046	0.052
$F_{n,n-1}$		78	24.3	6.1

Table 5.4 - Experiment EP-710, run 5. Output primary pressure.
Roots of the discrete models of different orders.

n	A	B	C
1	0.953	-2.658	0.808
2	0.221 0.896	-2.527	0.485 ± 0.230j
3	0.163 0.638 0.921	0.607 -2.428	0.249 0.963 0.473 ± 0.505j
4	-0.139 0.942 0.781 ± 0.362j	-0.281 0.758 ± 0.346j -2.428	-0.061 0.952 0.710 ± 0.468j

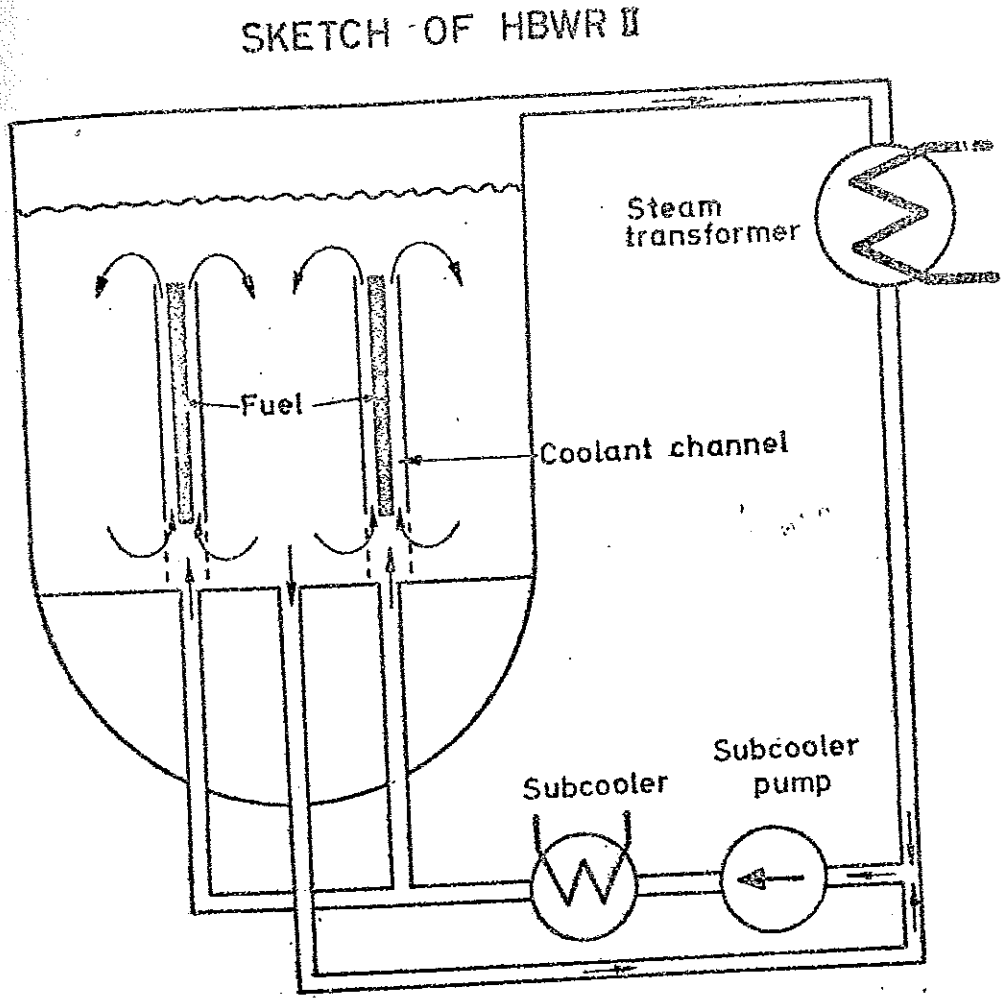

Fig. 2.1 - Sketch of the core of HBWR.
(The figure is fetched from ref. |25|.)

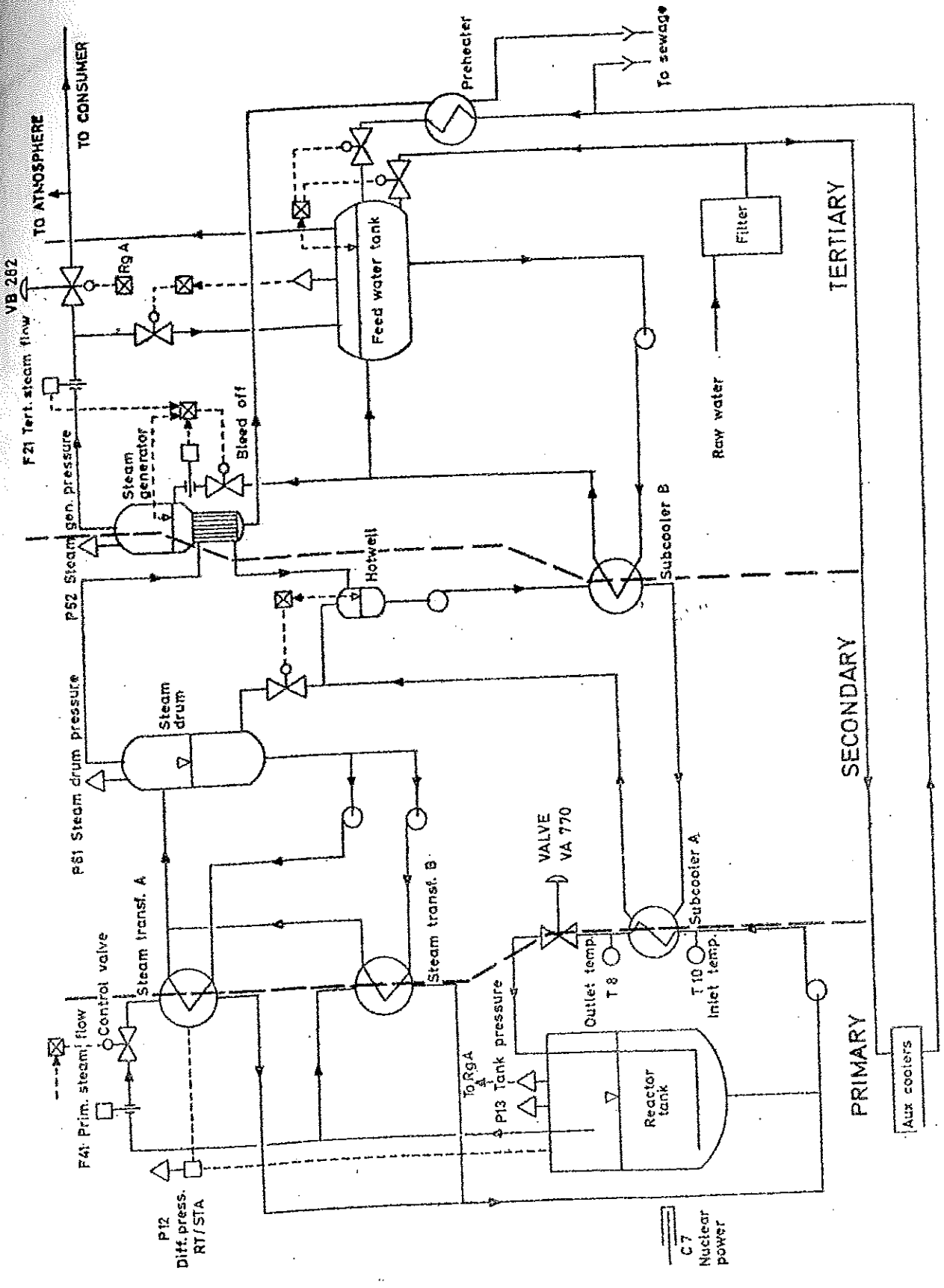

Fig. 2.2 - Diagram of the HBWR II plant circuits.

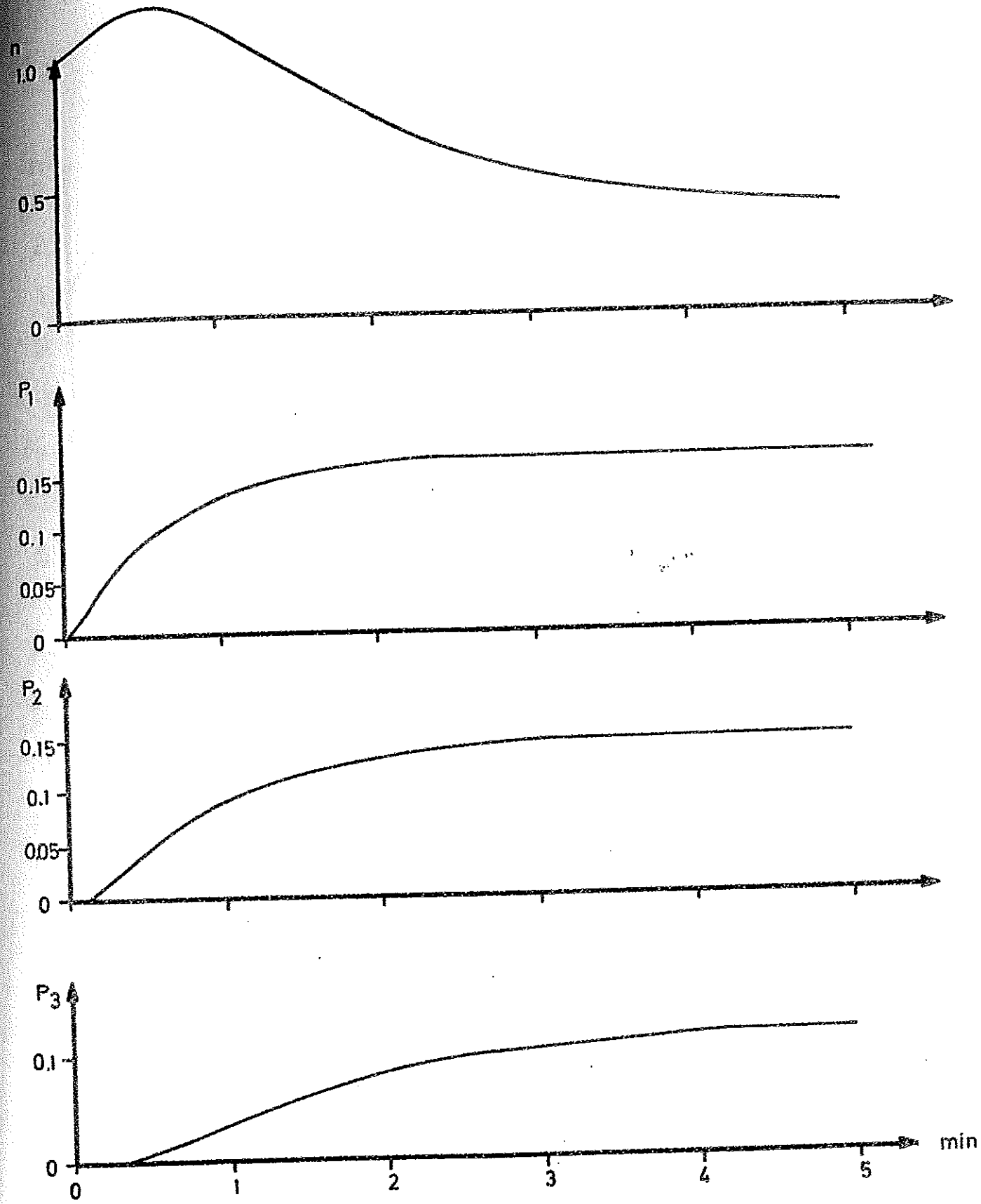

Fig. 2.3 - (See page 8 and App.)
Response of the reactor system after a unit positive step in reactivity, condition a.

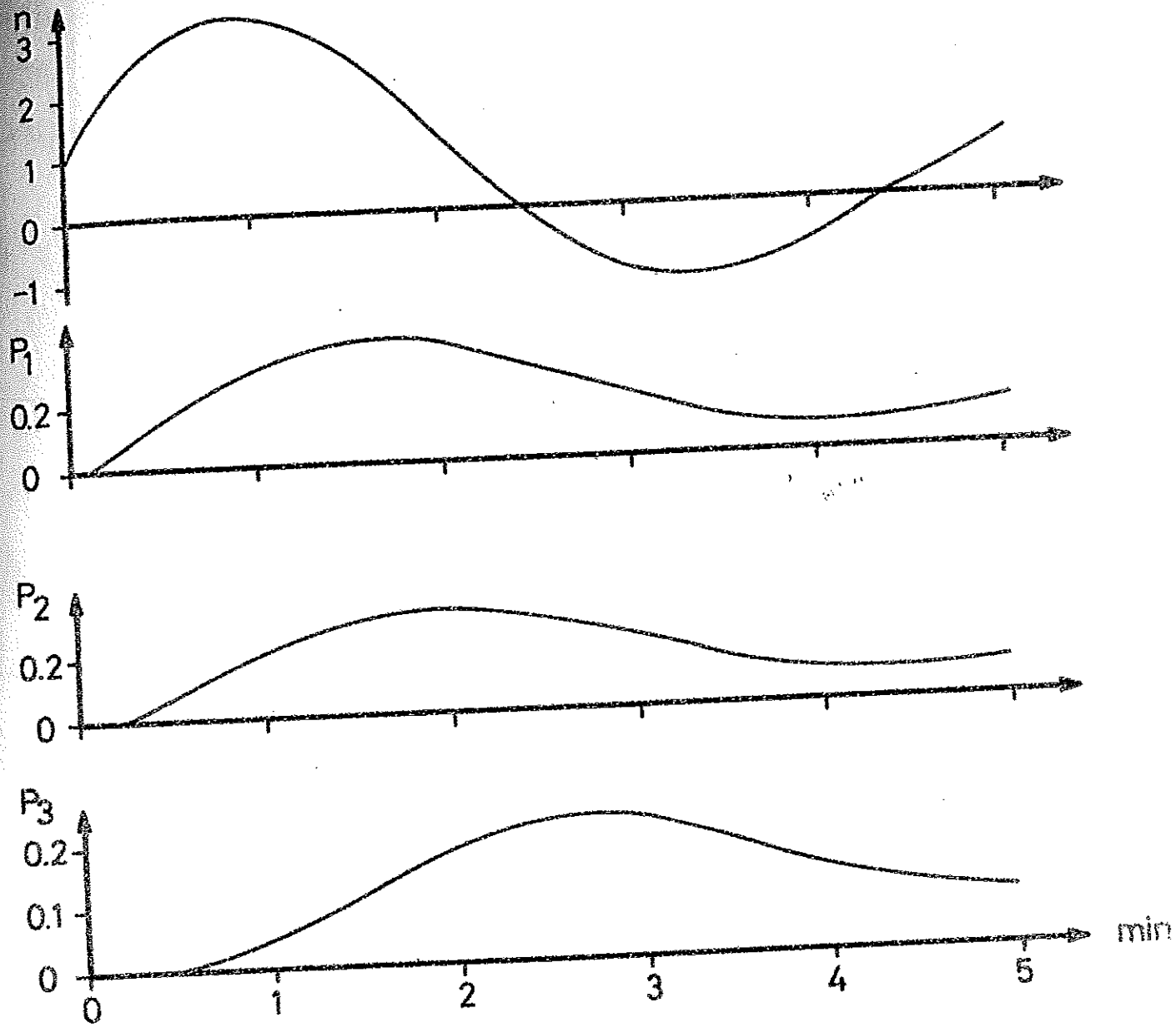

Fig. 2.4 - (See page 8 and App.)
Response of the reactor after a unit positive reactivity step, condition b.

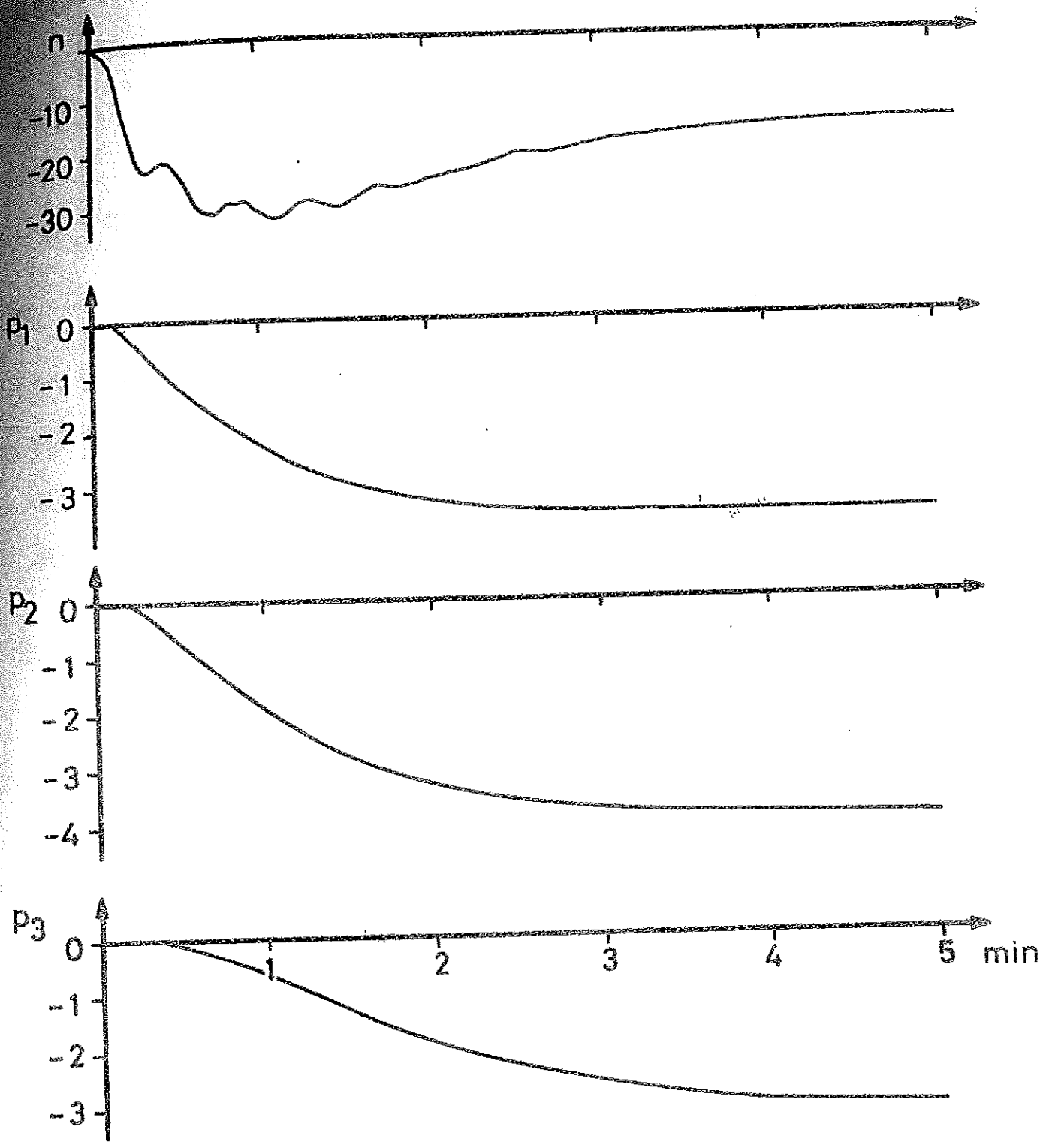

Fig. 2.5 - (See page 8 and App.)
Response of the reactor after a step of 100 units of the subcooling valve VA770 (closing the valve).

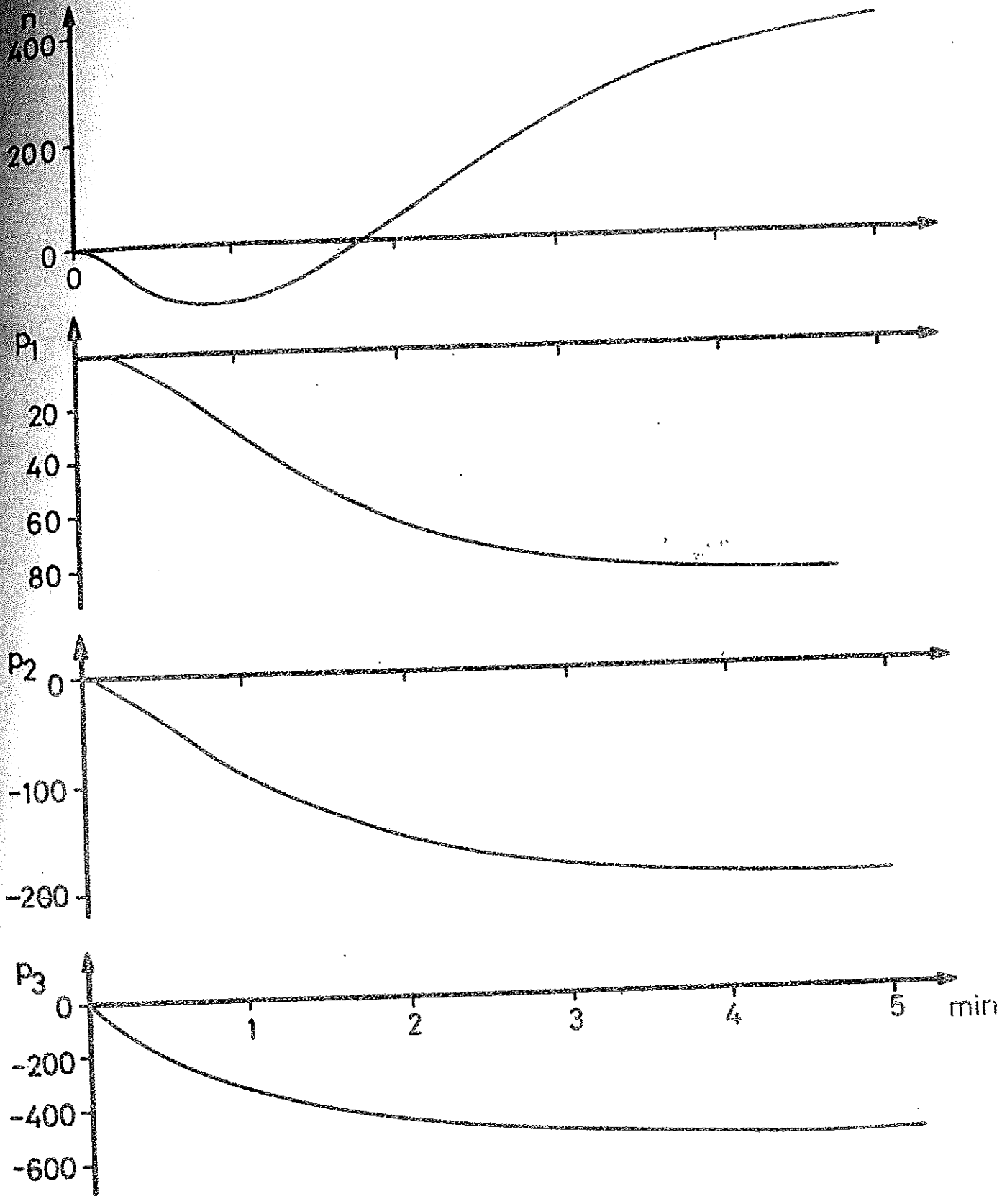

Fig. 2.6 - (See page 8 and App.)
Response of the reactor after a step of 100 units of the tertiary steam valve VB282 (opening the valve).

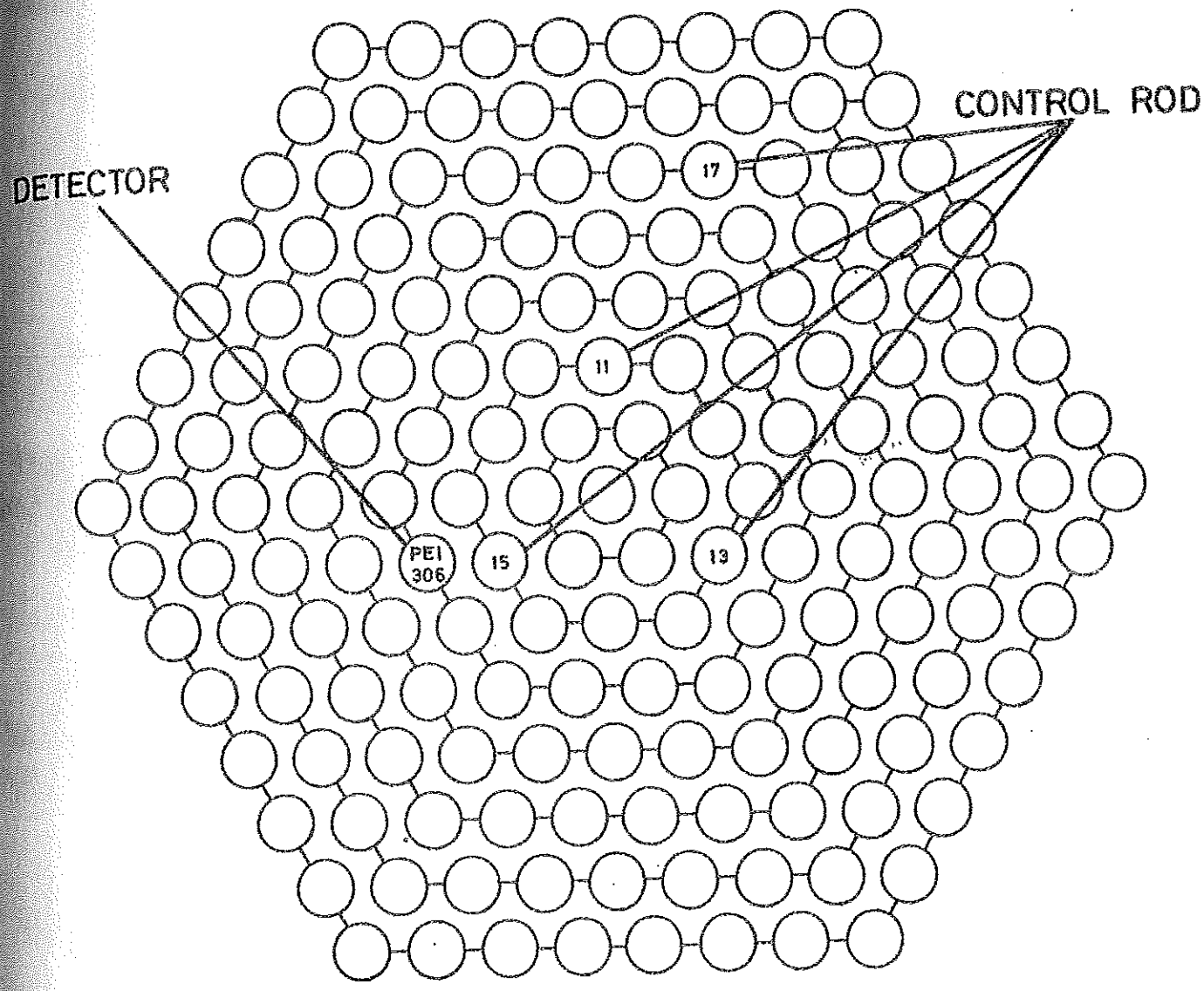

Fig. 3.1 - Sketch of the HBWR core loading.

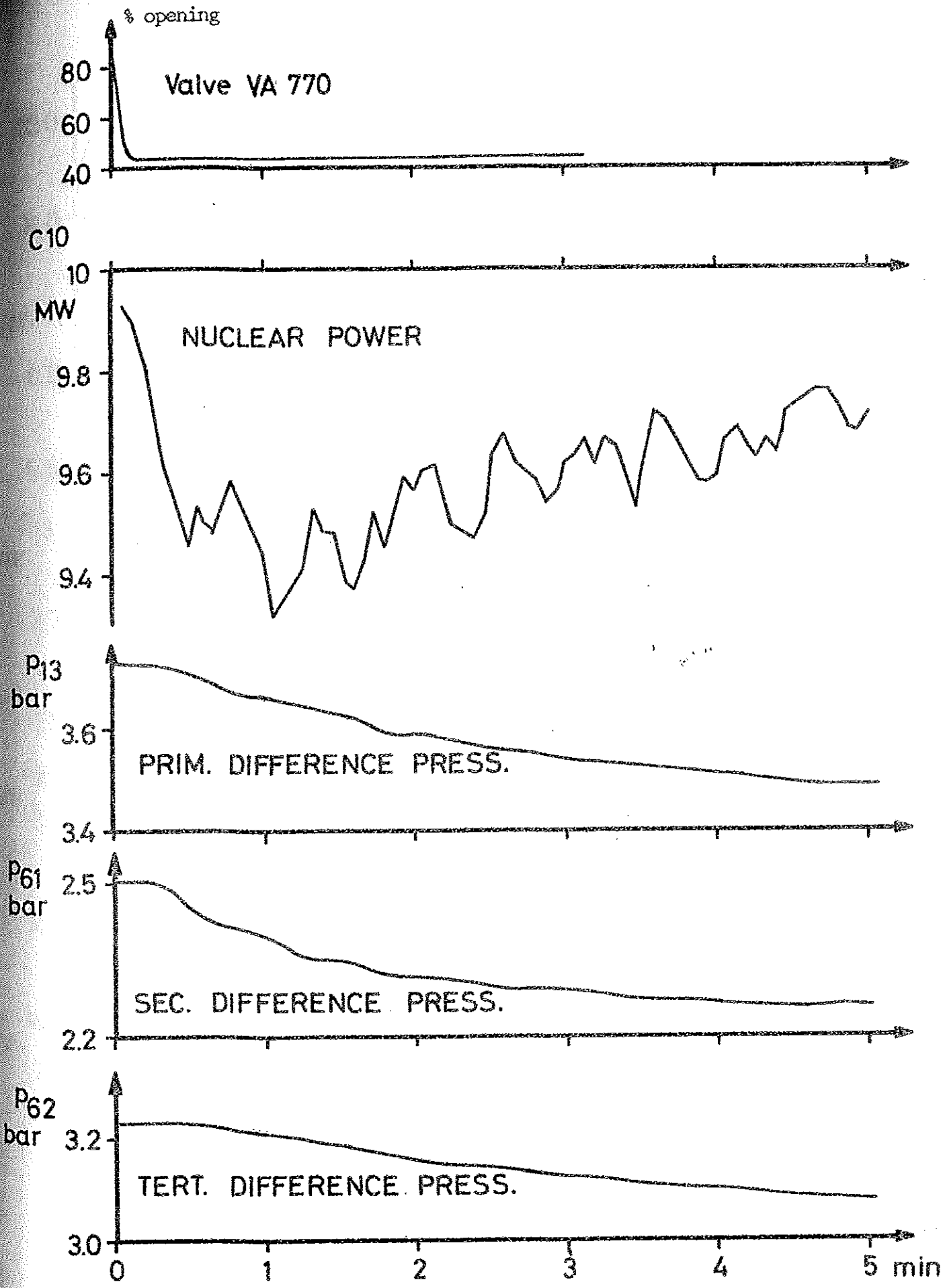

Fig. 3.2 - (See page 13)
The dynamic responses of the nuclear power and the pressures after a disturbance in the subcooling flow (VA770). Run 681001-15, EP-706.

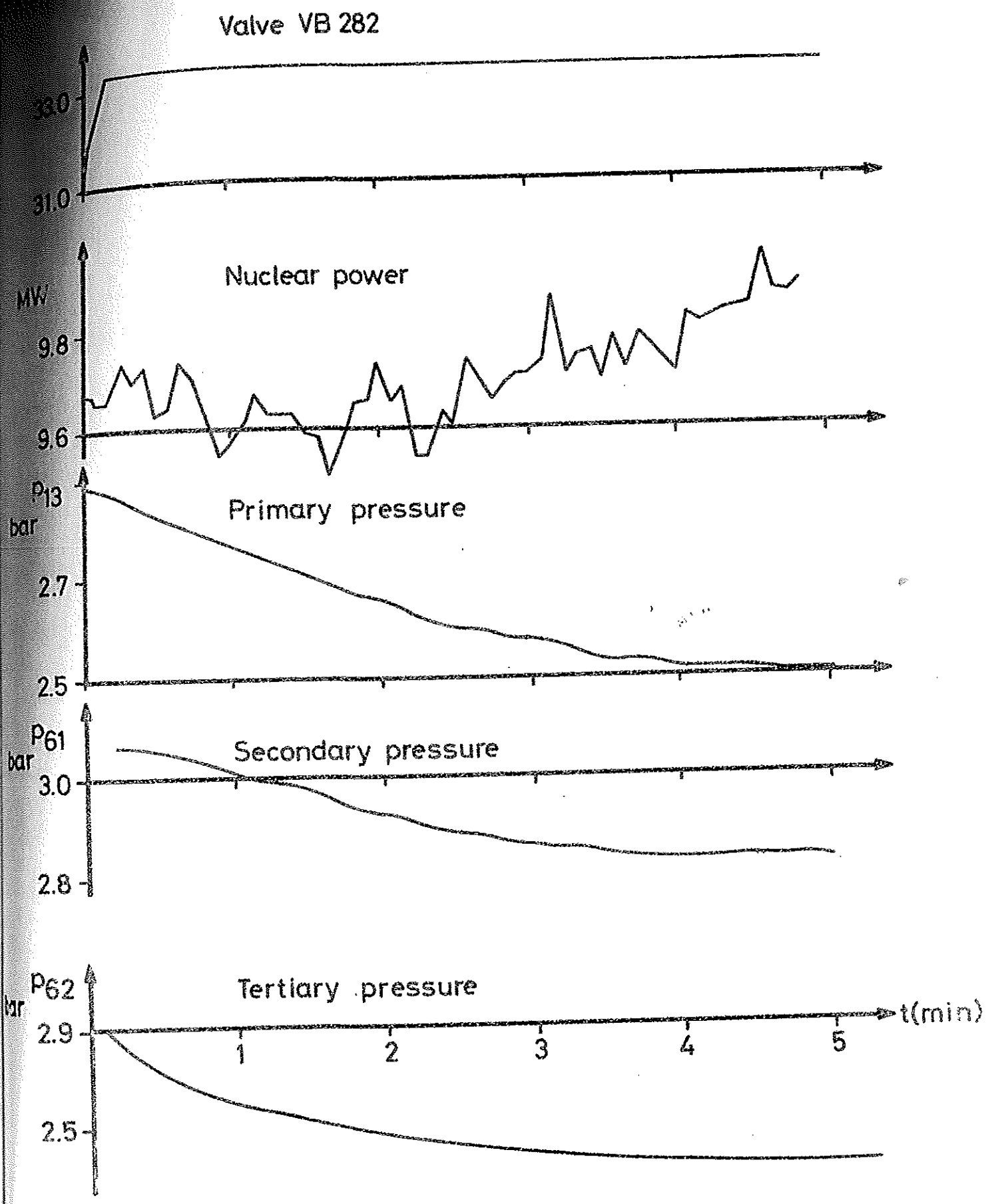

Fig. 3.3 - (See page 13)
The dynamic responses of the nuclear power and the pressures after a tertiary steam load disturbance (VB282). Run 681001-10, EP-706.

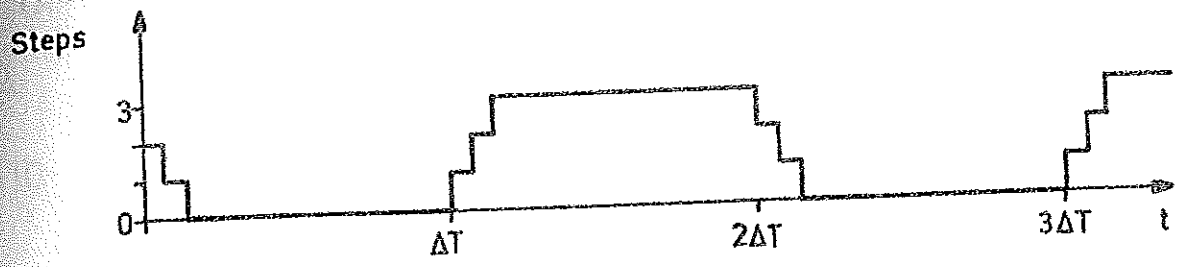

Fig. 3.4 - (See page 13)
Sketch of the rod input for some experiments in EP-708.

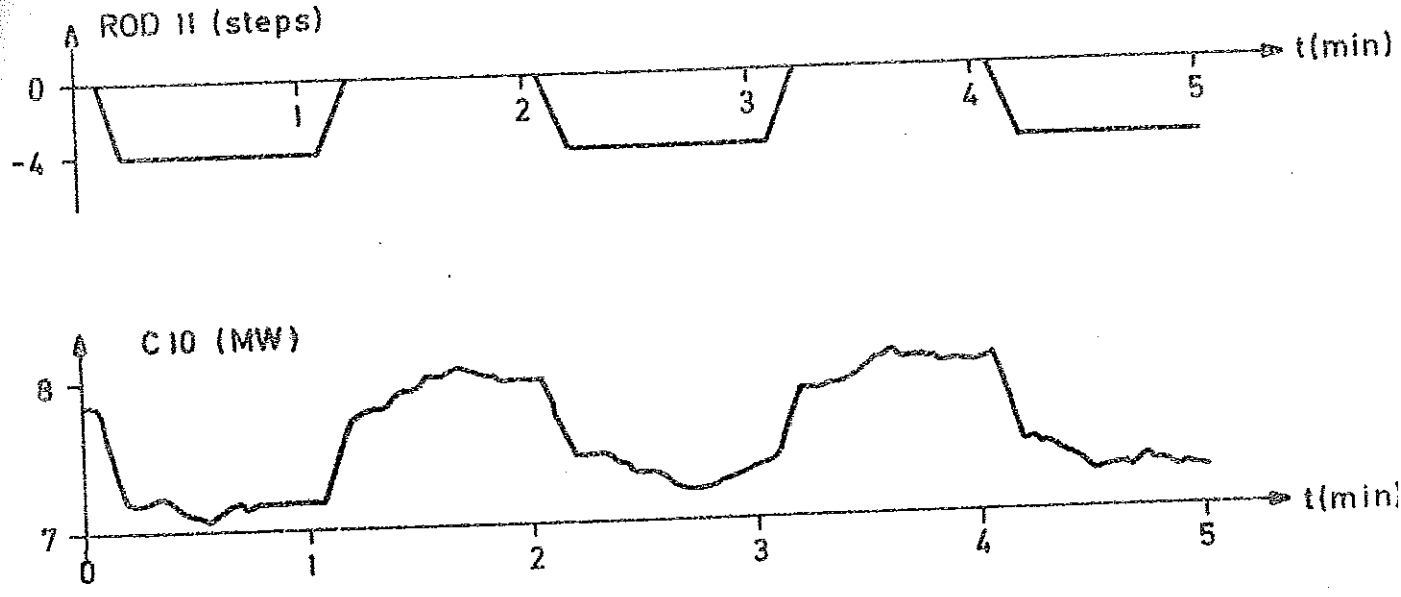

Fig. 3.5 - (See page 13)
The dynamic response of the nuclear power after a regular rod movement. Run 65, EP-708.

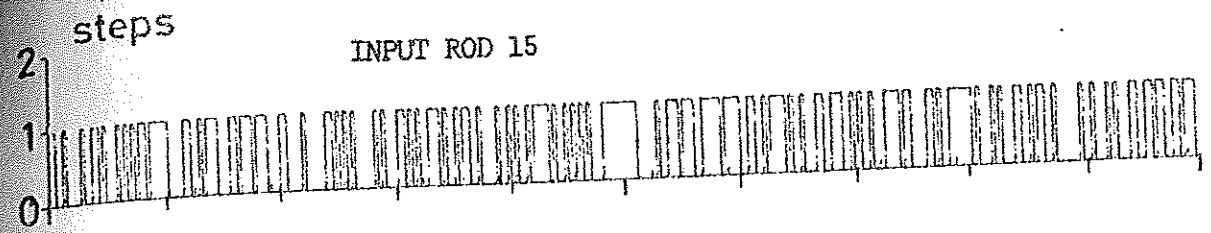

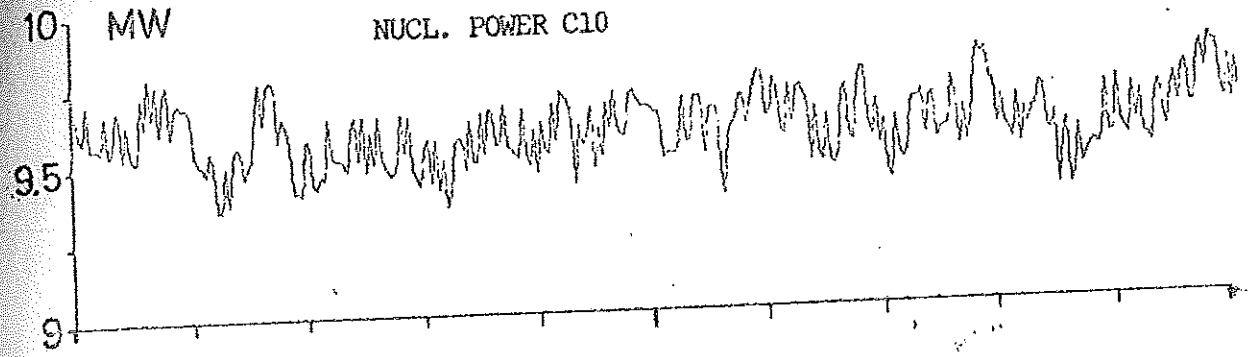

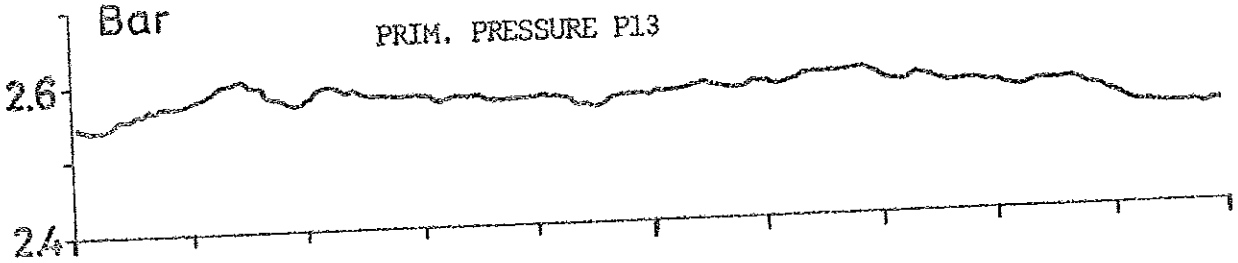

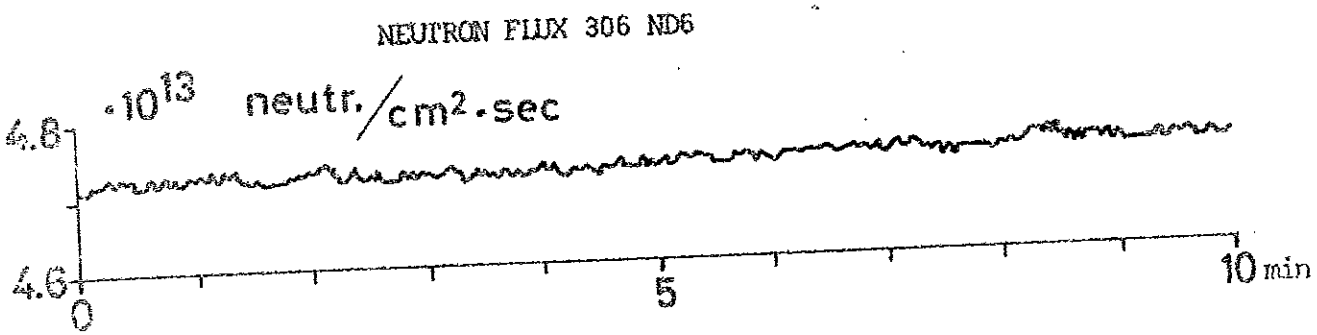

Fig. 3.6 - (See page 14)
Plot of the first part of experiment EP-710, run 3.

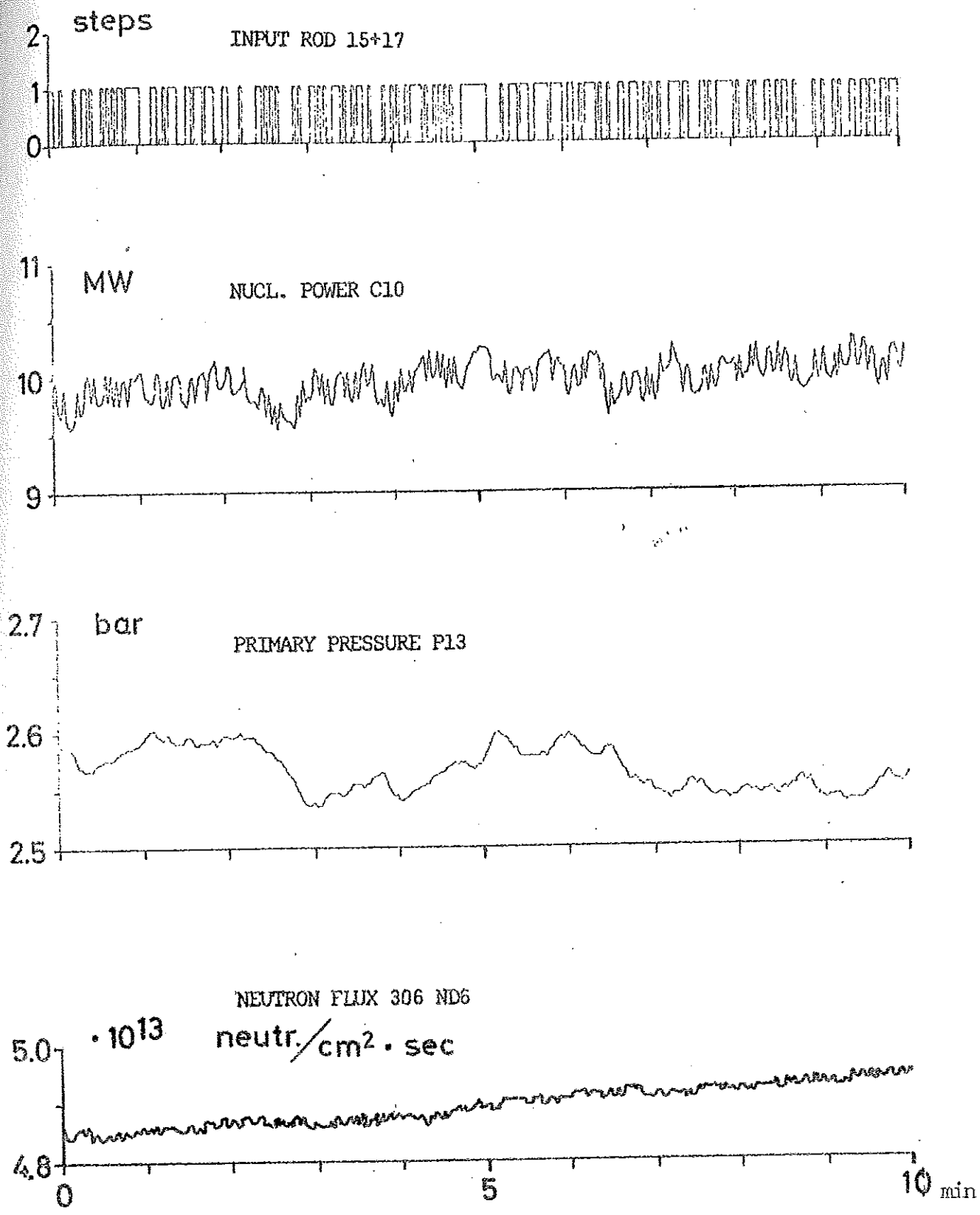

Fig. 3.7 - (See page 14)
Plot of the first part of experiment EP-710, run 4.

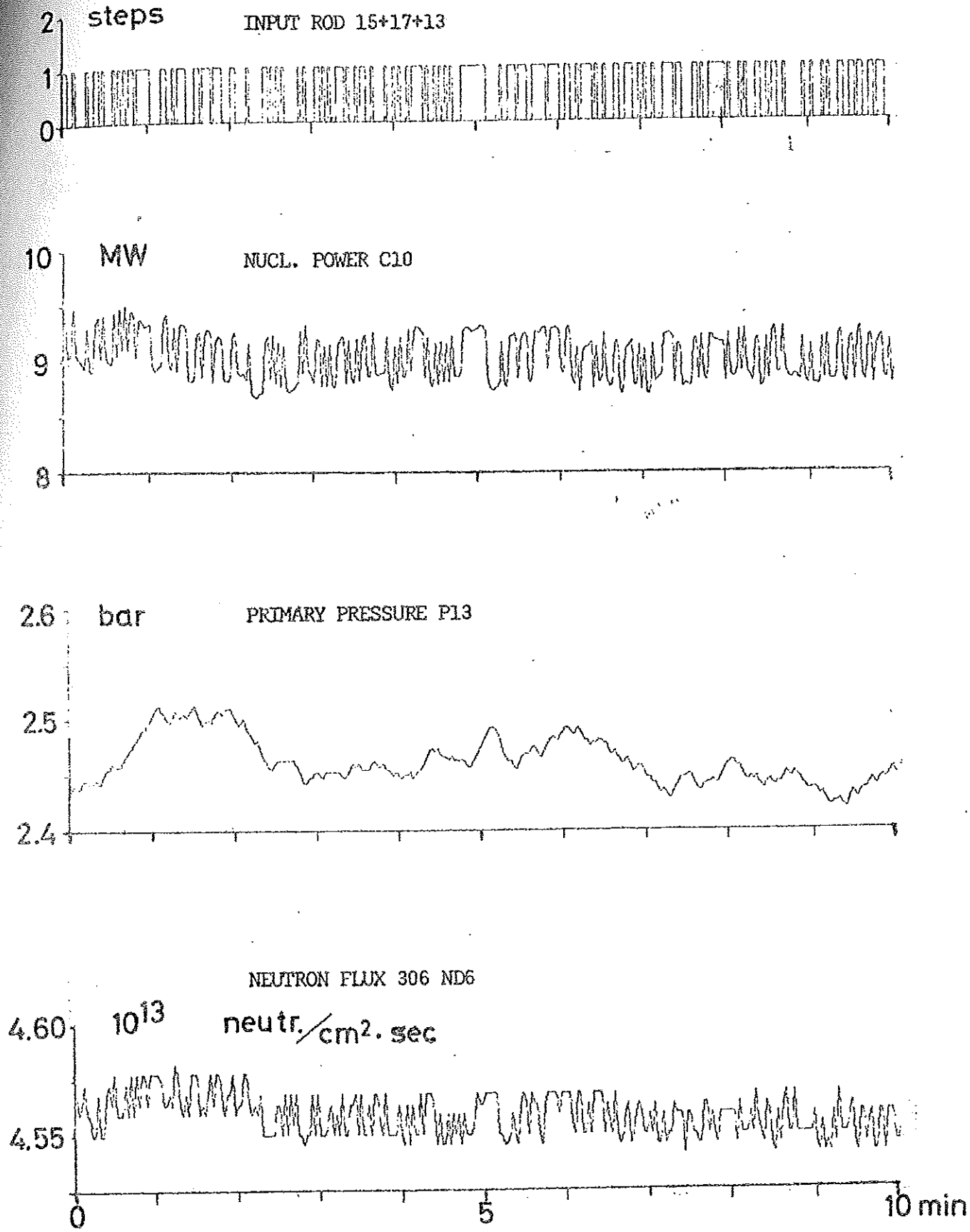

Fig. 3.8 - (See page 14)
Plot of the first part of experiment EP-710, run 5.

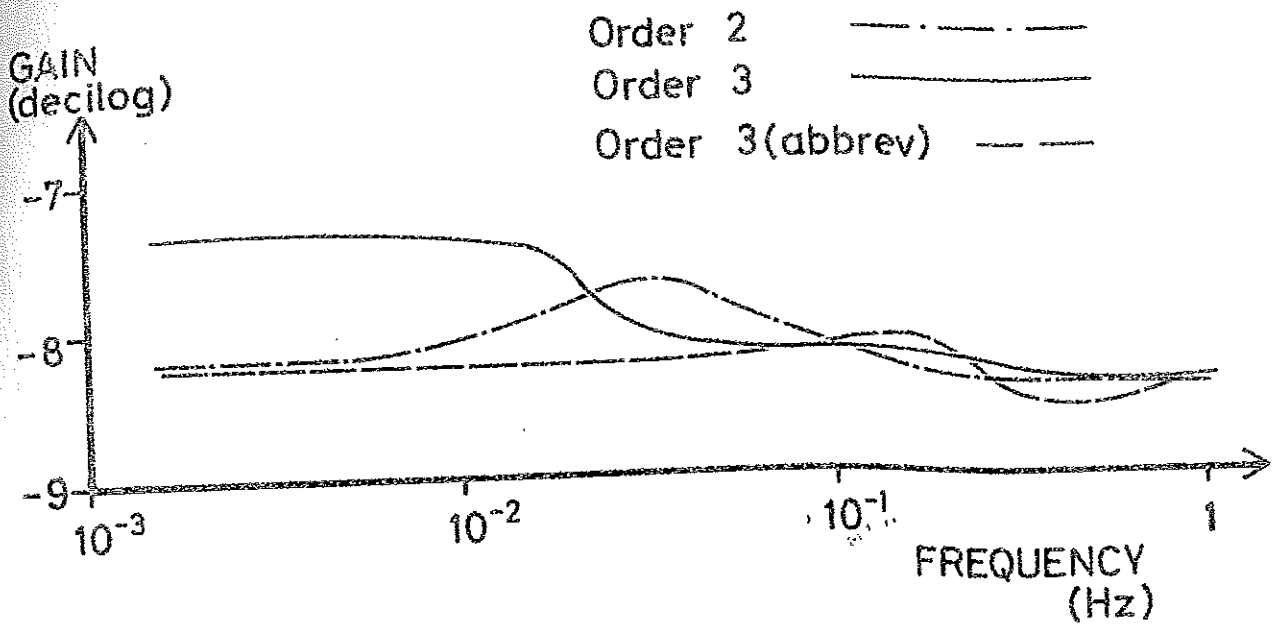

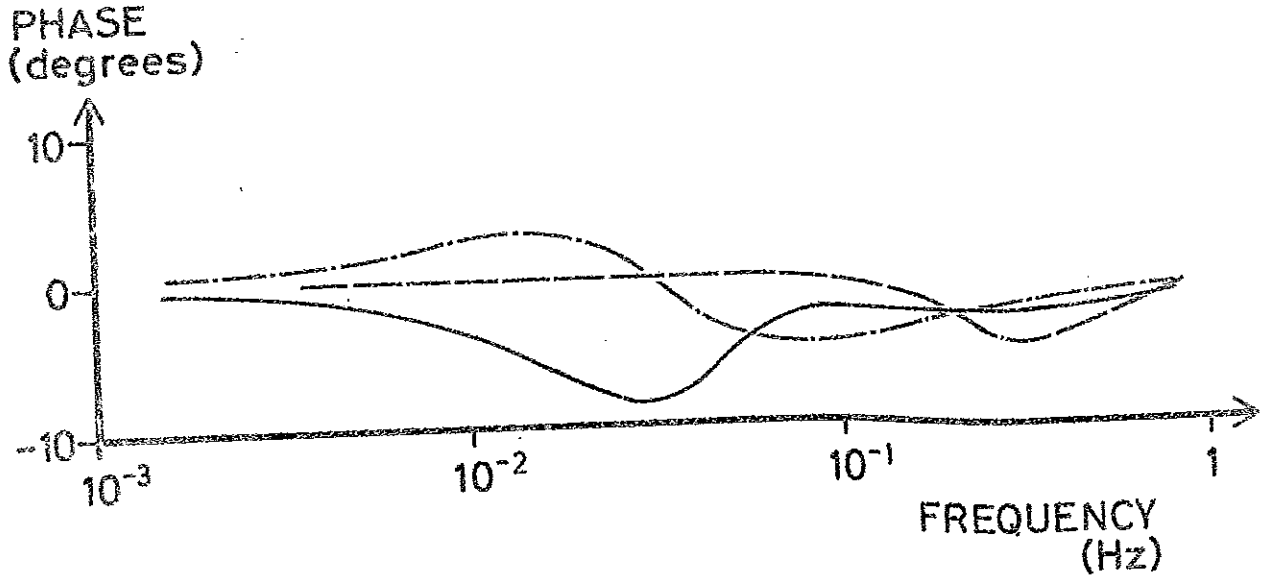

Fig. 4.1 - (See page 19)
Experiment EP-710, run 3. Output nuclear power. Bode plot of the 2nd and 3rd order models.

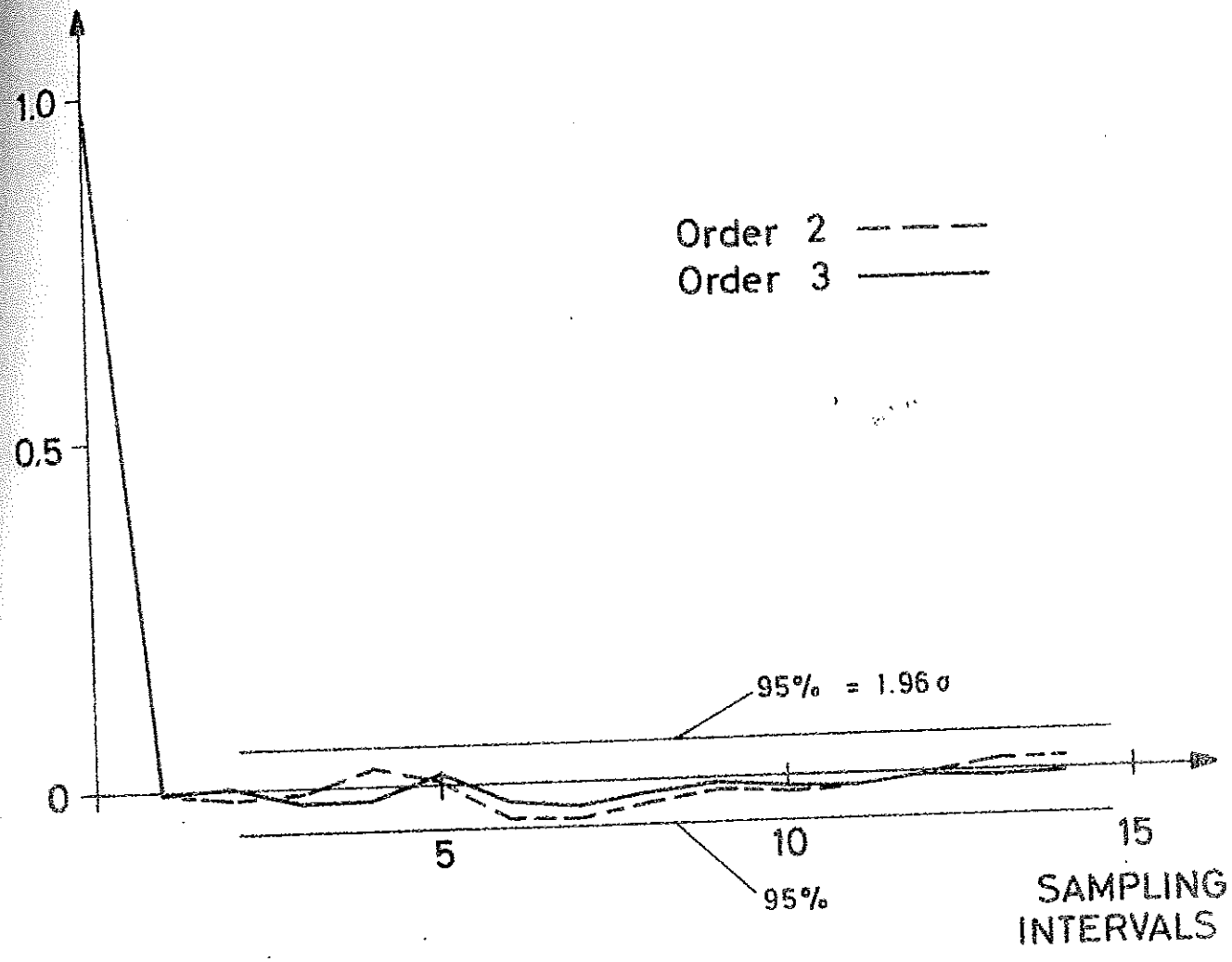

Fig. 4.2 - (See page 20)
Experiment EP-710, run 3. Output nuclear power. Covariance functions and the 95% significance limit of the 2nd and 3rd order system residuals.

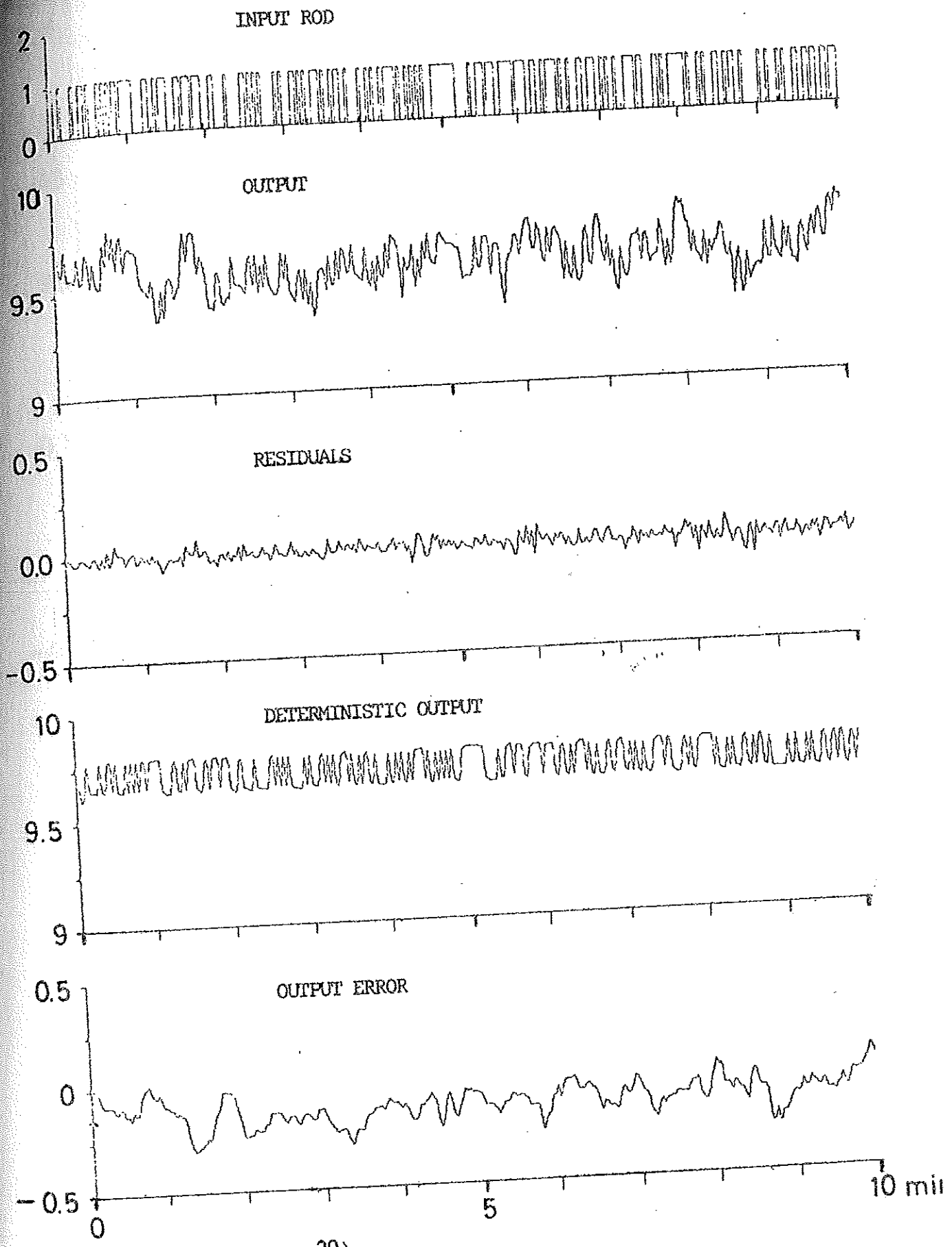

Fig. 4.3 - (See page 20)
Experiment EP-710, run 3. Output nuclear power. Experimental and simulated outputs of the 2nd order model.

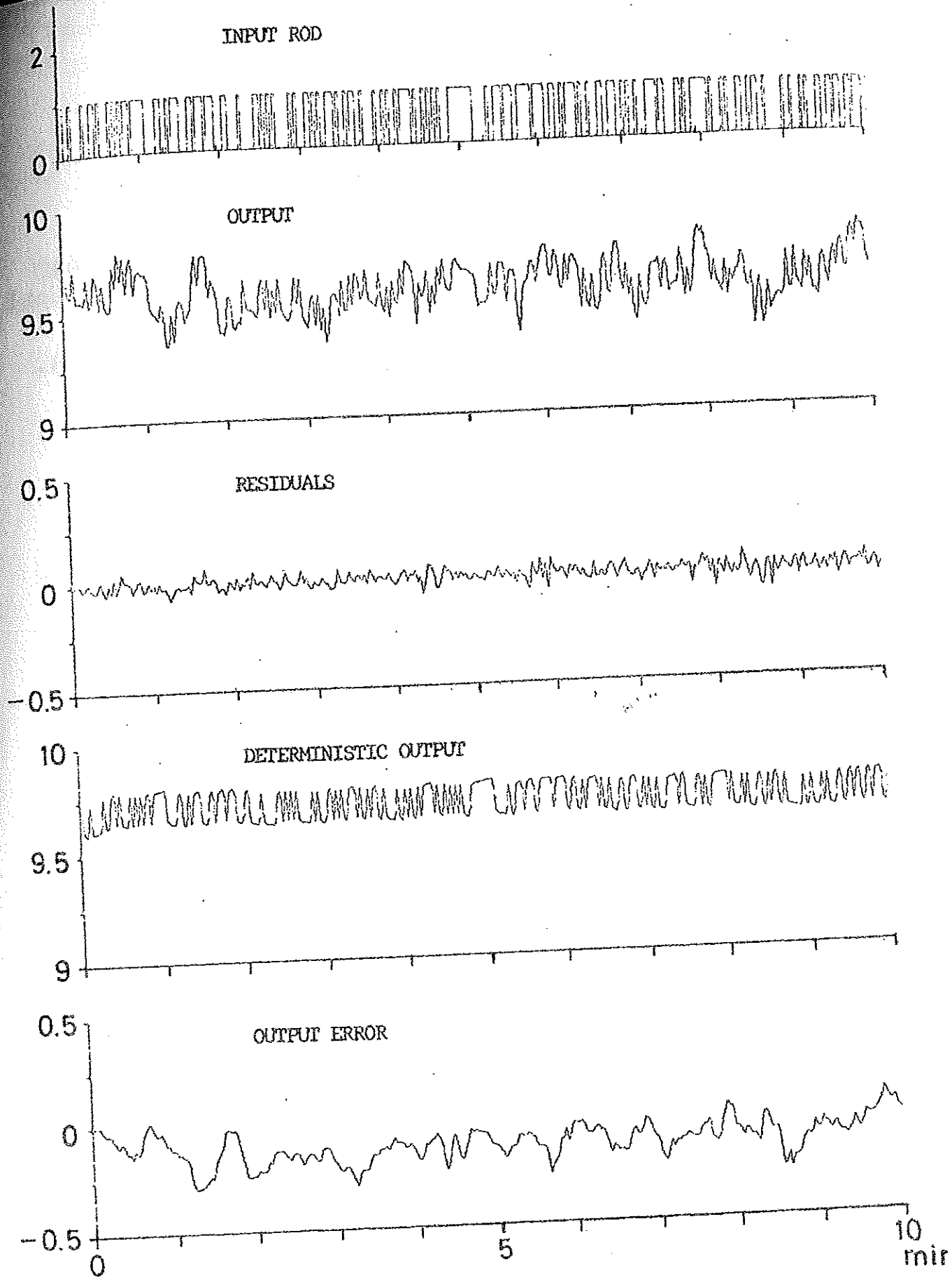

Fig. 4.4 - (See page 20)
Experiment EP-710, run 3. Output nuclear power. Experimental and simulated outputs of the 3rd order model.

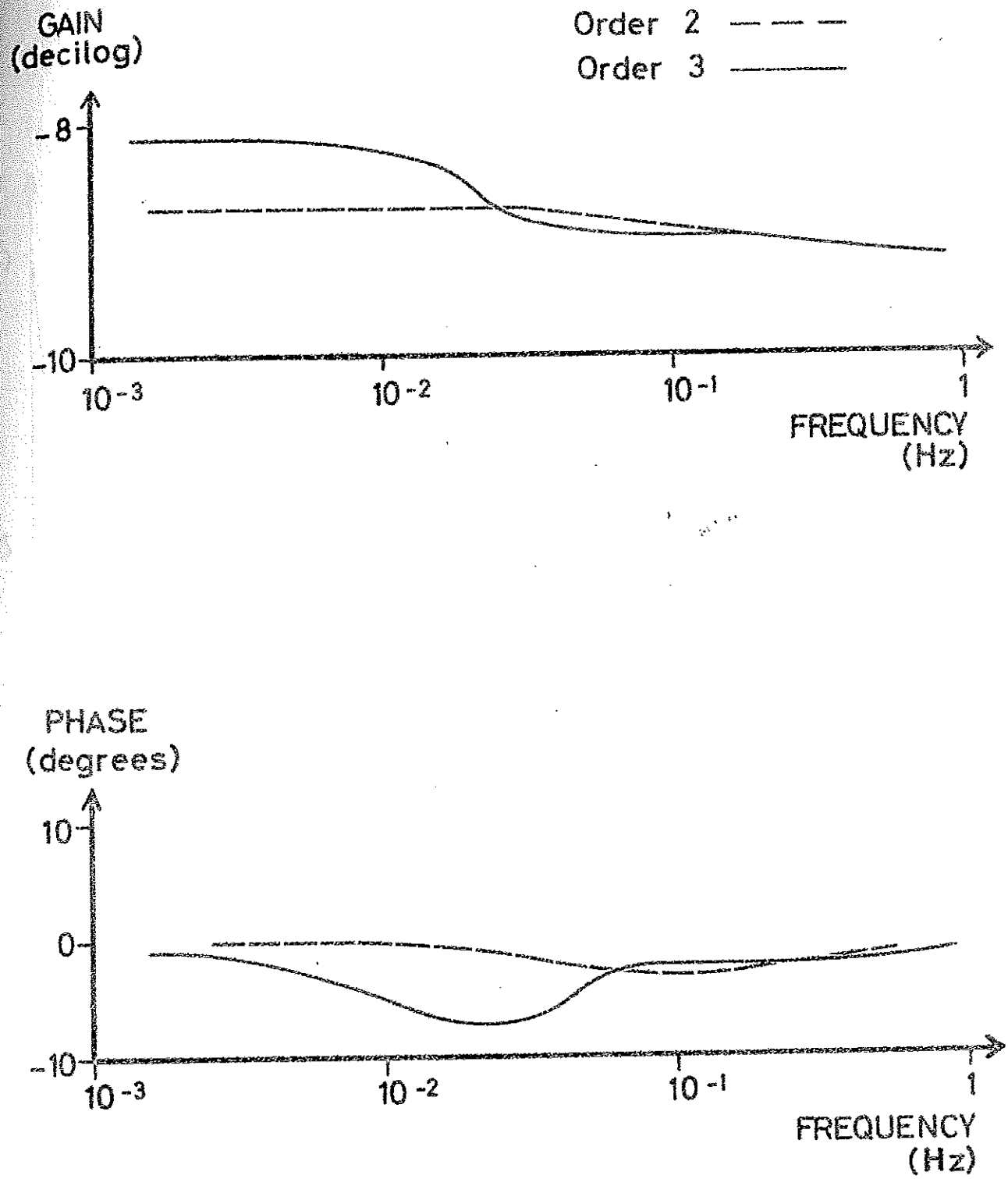

Fig. 4.5 - (See page 24)
Experiment EP-710, run 4. Output nuclear power. Bode plot of the 2nd and 3rd order models.

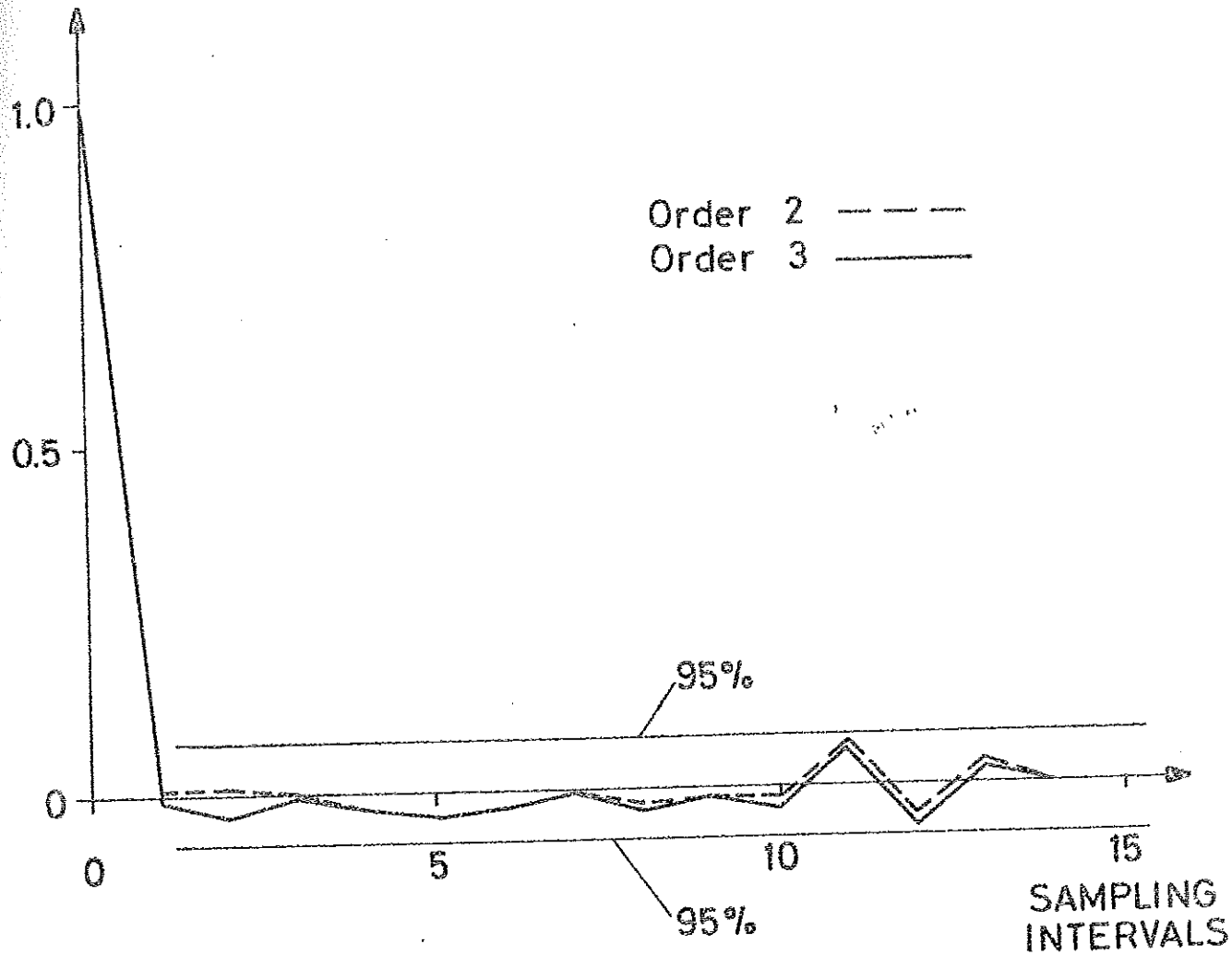

Fig. 4.6 - (See page 24)
Experiment EP-710, run 4. Output nuclear power. Covariance functions and the 95% significance limit of the 2nd and 3rd order system residuals.

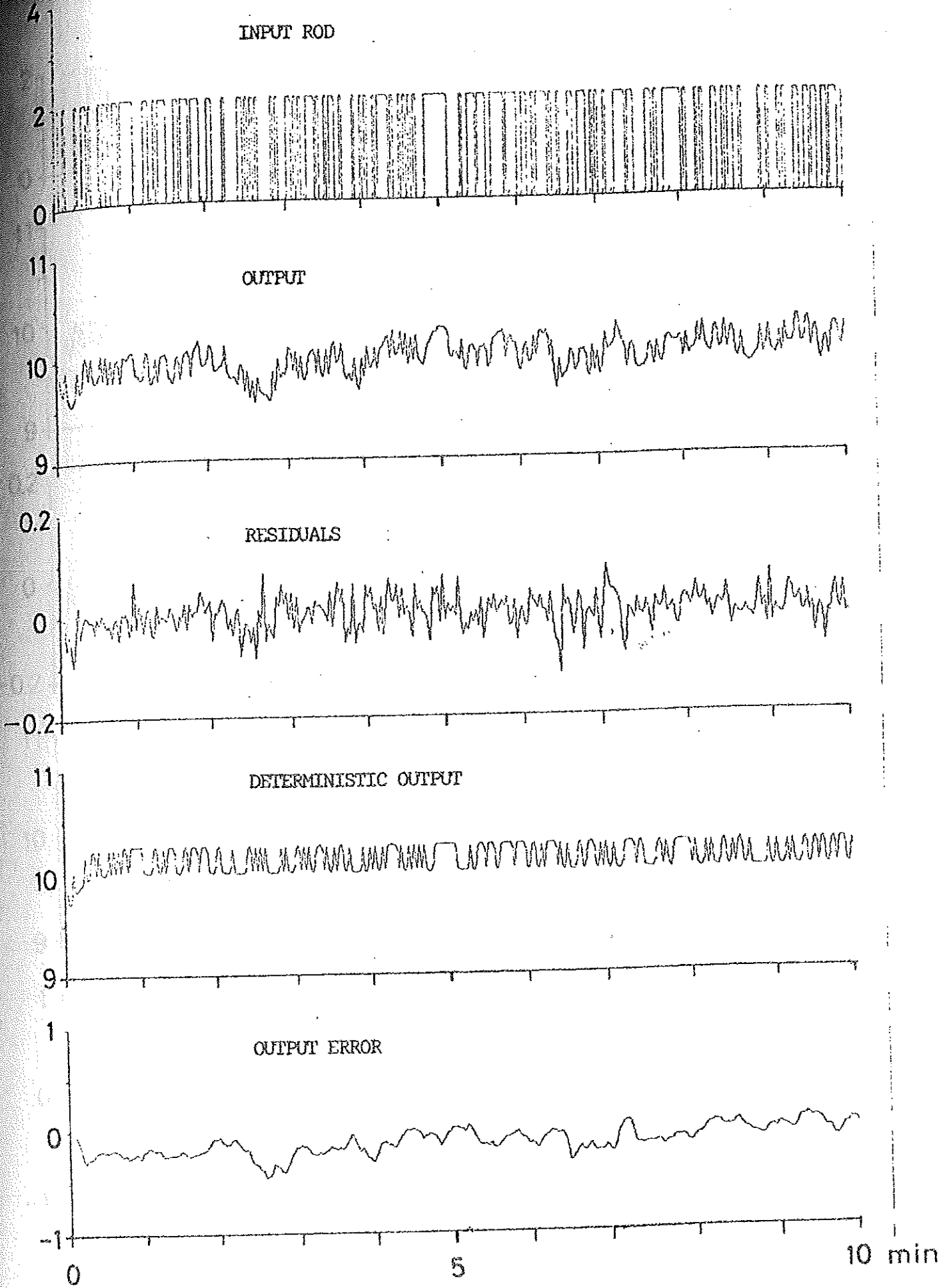

Fig. 4.7 - (See page 24)
Experiment EP-710, run 4. Output nuclear power. Experimental and simulated outputs of the 2nd order model.

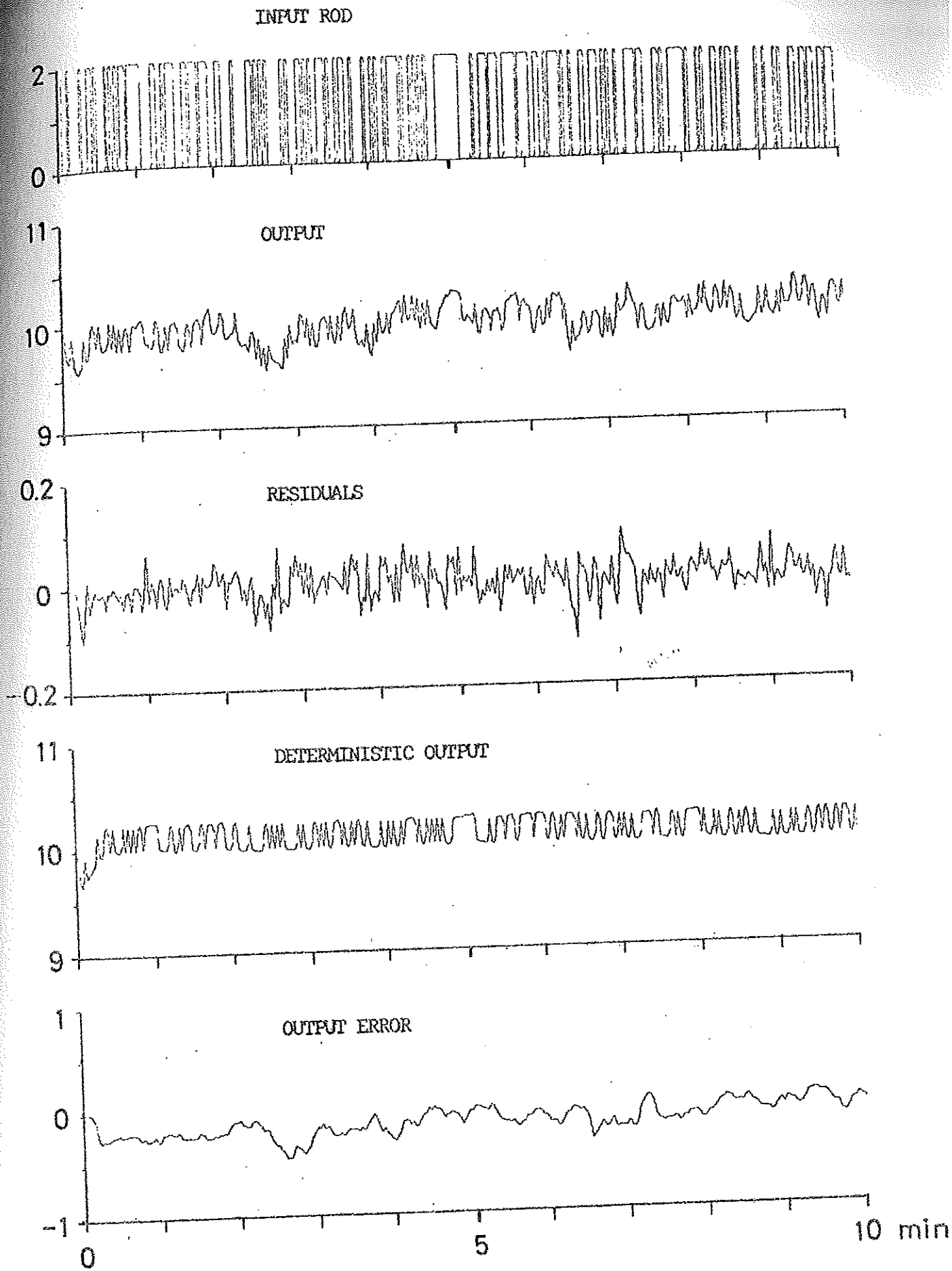

Fig. 4.8 - (See page 24)
Experiment EP-710, run 4. Output nuclear power. Experimental and simulated outputs of the 3rd order model.

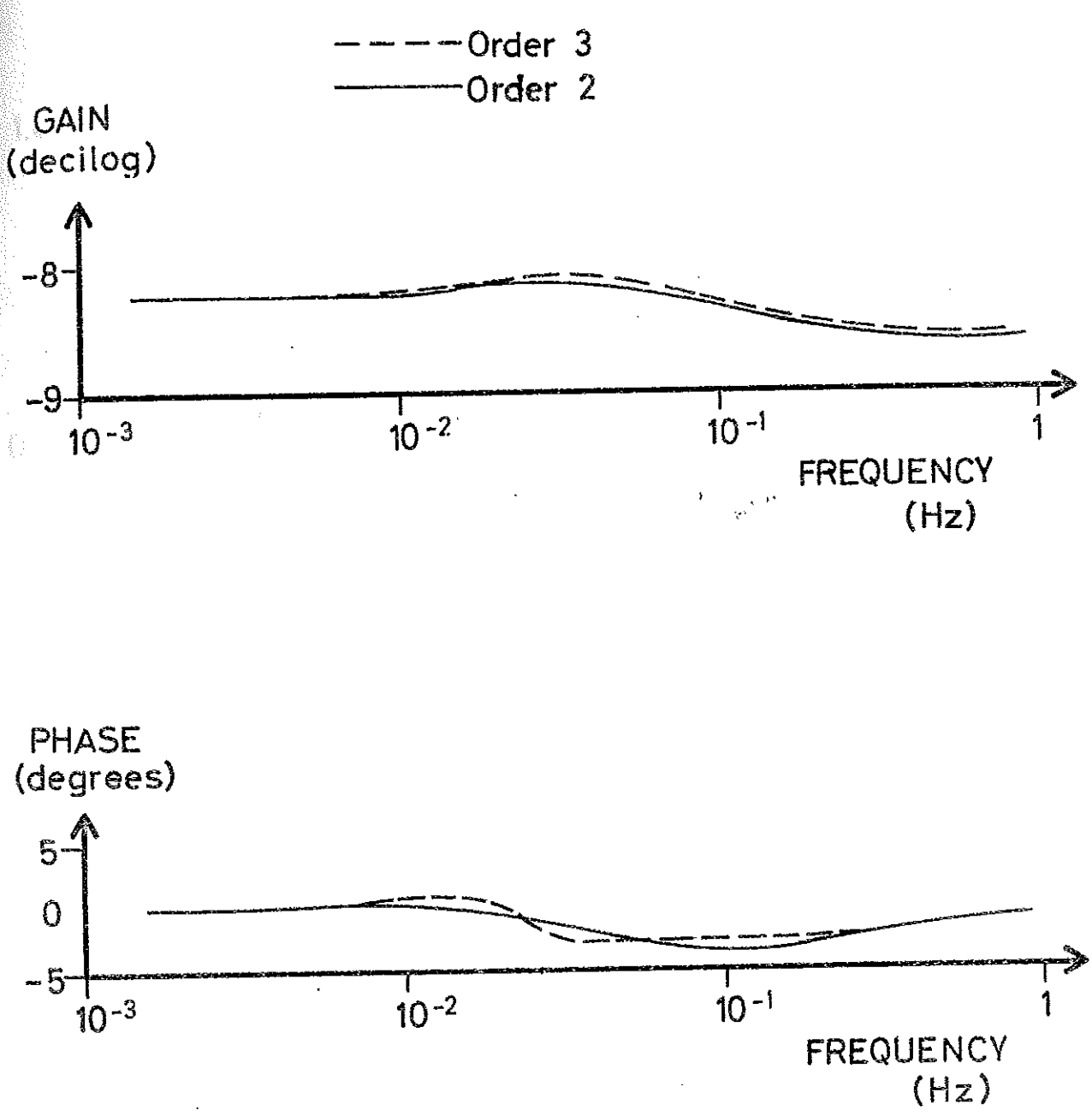

Fig. 4.9 - (See page 26)
Experiment EP-710, run 5. Output nuclear power. Bode plot of the 2nd and 3rd order models (prefiltered data).

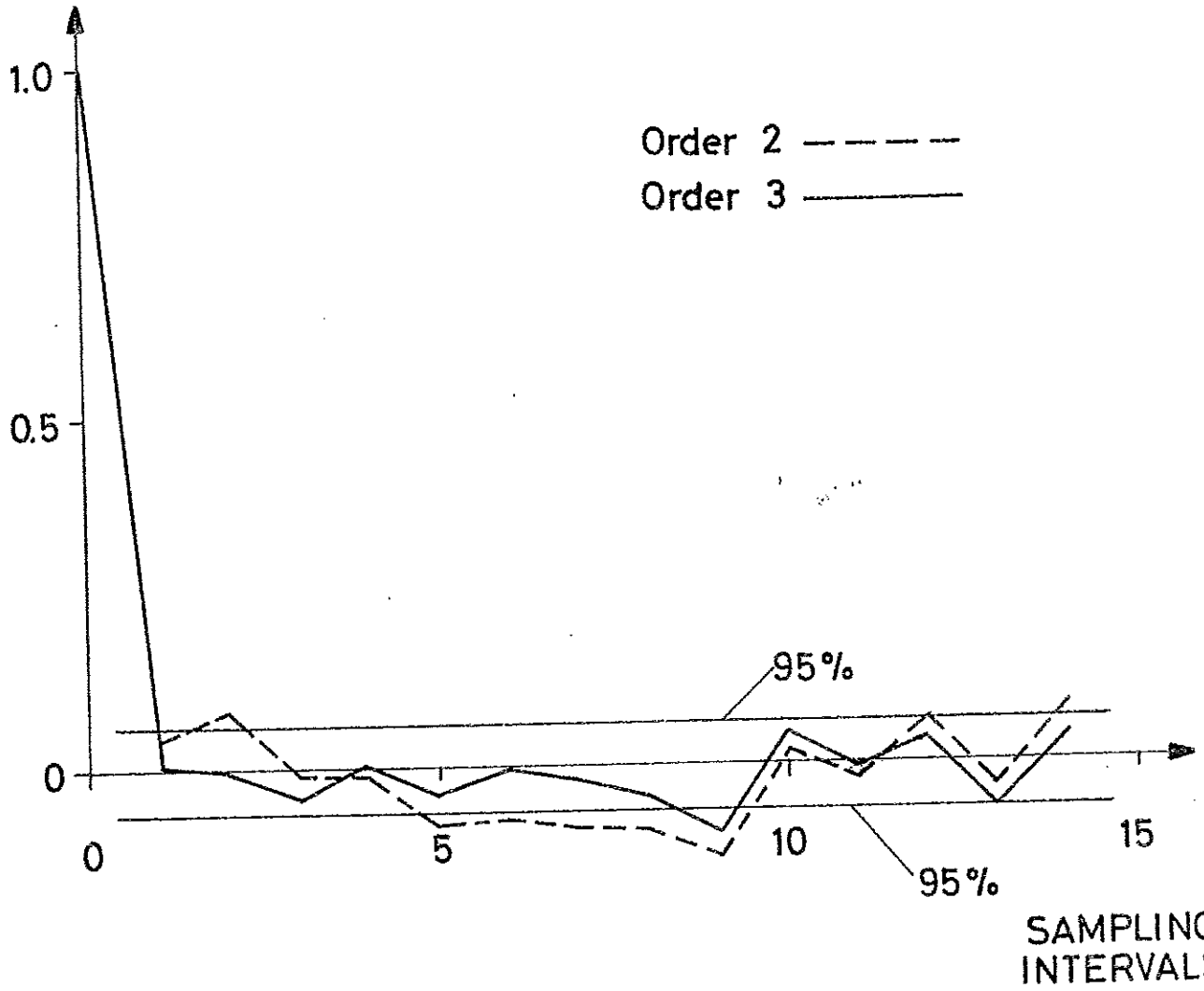

Fig. 4.10 - (See page 26)
Experiment EP-710, run 5. Output nuclear power. Covariance functions and the 95% significance limit of the 2nd and 3rd order system residuals (prefiltered data).

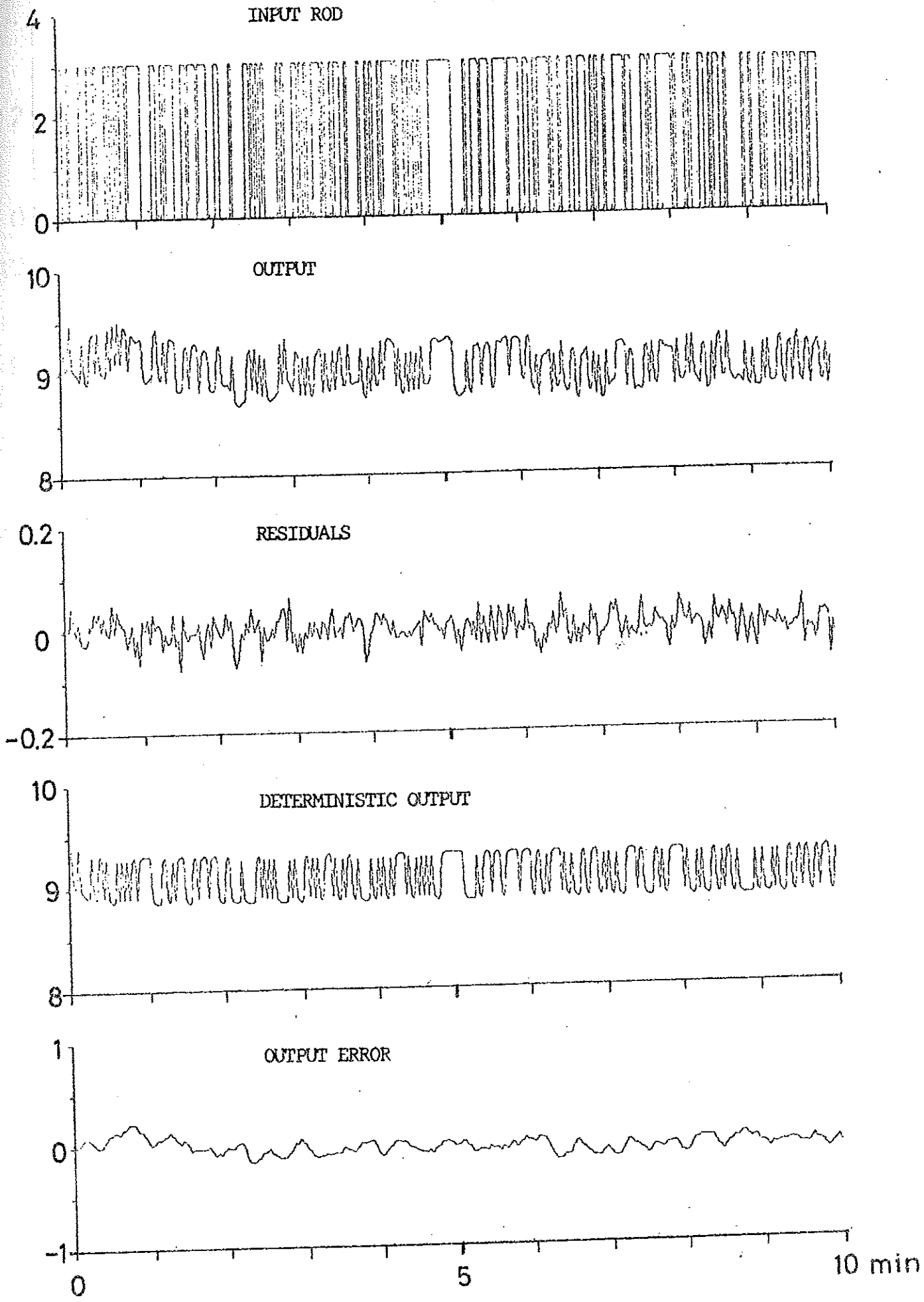

Fig. 4.11 - (See page 27)
Experiment EP-710, run 5. Output nuclear power. Experimental and simulated outputs of the 2nd order model (prefiltered data).

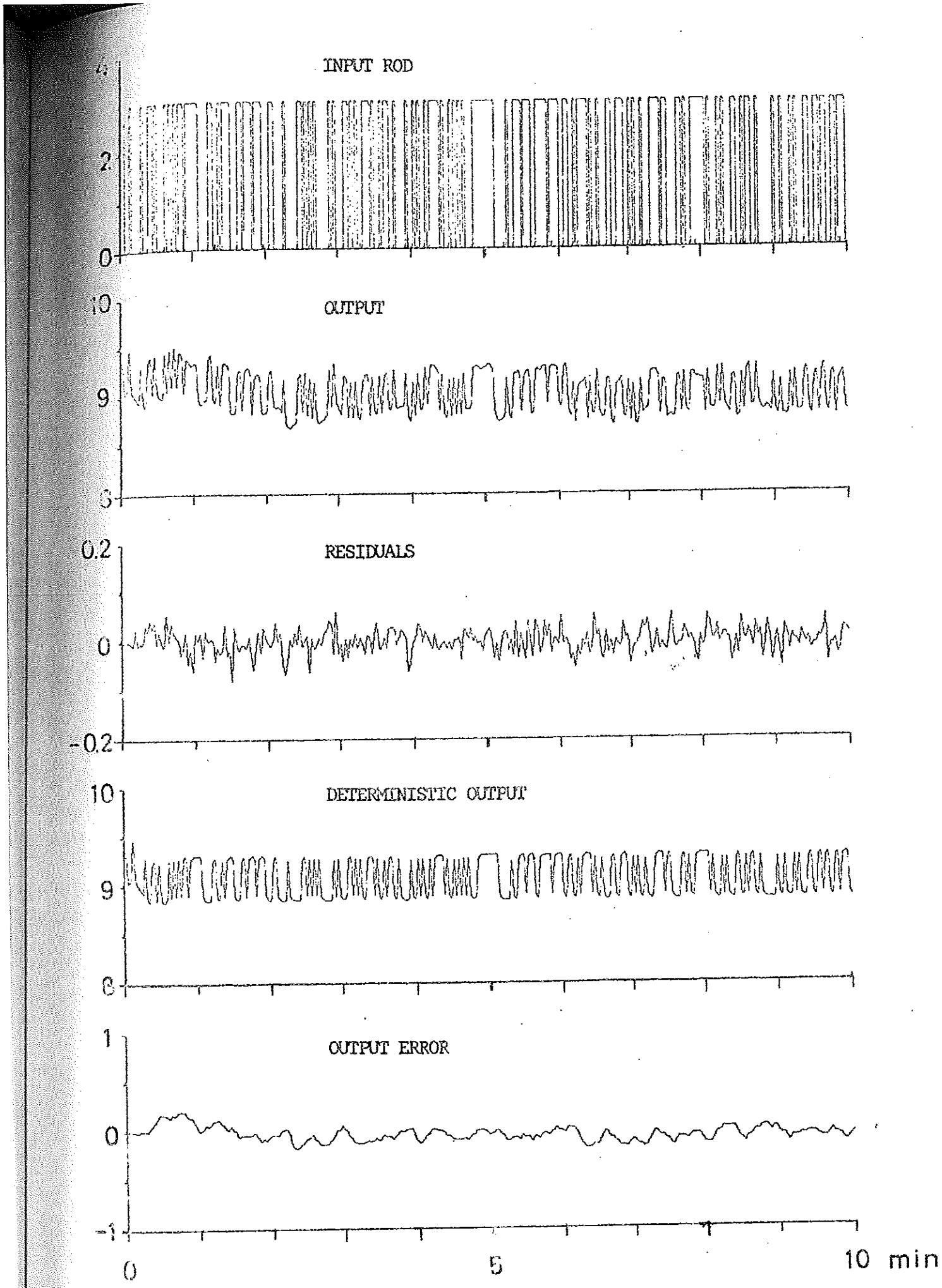

Fig. 4.12 - (See page 27)
Experiment EP-710, run 5. Output nuclear power. Experimental and simulated outputs of the 3rd order model (prefiltered data).

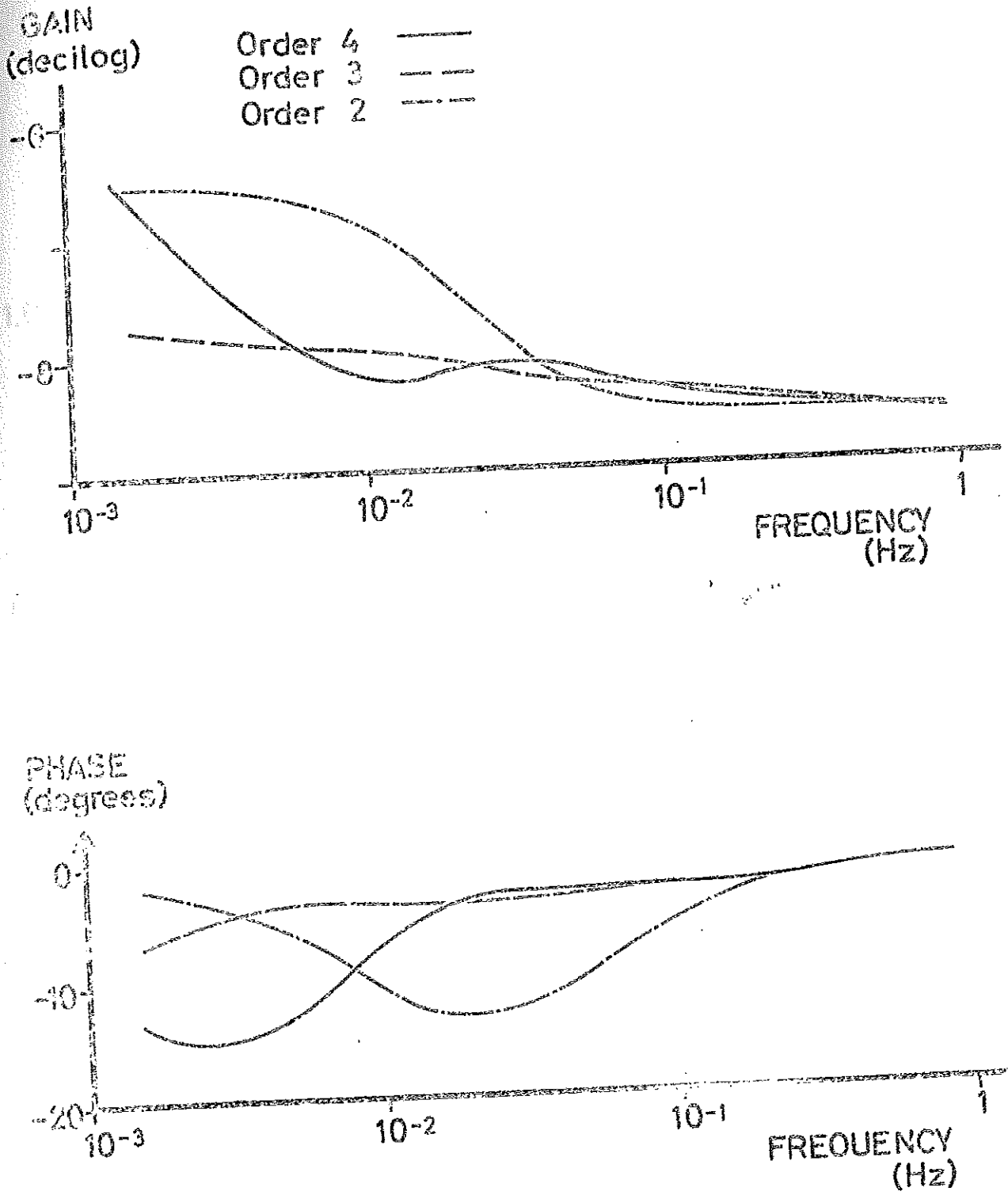

Fig. 4.13 - (See page 29)
Experiment EP-710, run 5. Output nuclear power. Bode plot of the 2nd and 3rd and 4th order models (no input-output differences).

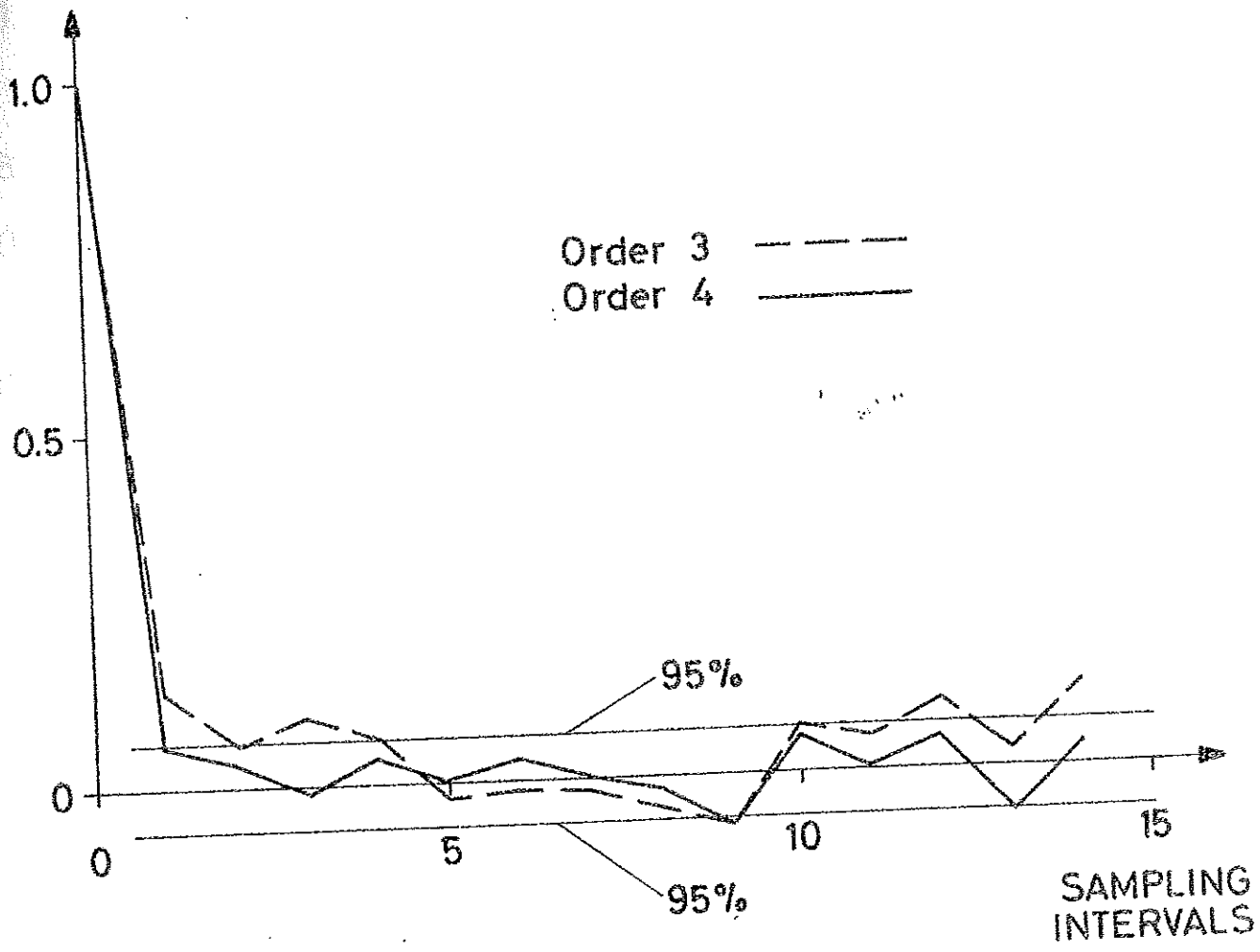

Fig. 4.14 - (See page 29)
Experiment EP-710, run 5. Output nuclear power. Covariance functions and the 95% significance limit of the 3rd and 4th order system residuals (no input-output differences).

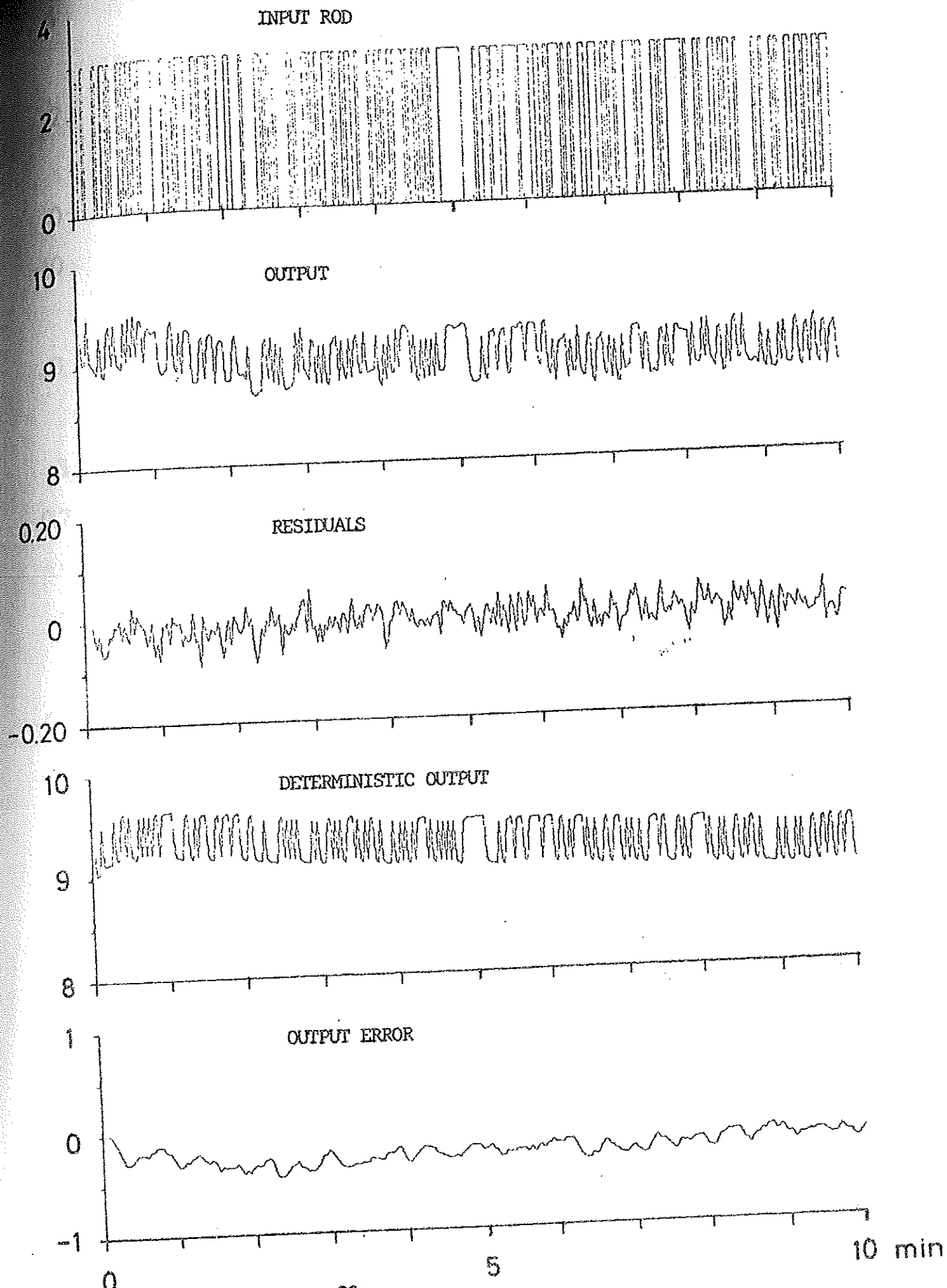

Fig. 4.15 - (See page 29)
Experiment EP-710, run 5. Output nuclear power. Experimental and simulated outputs of the 3rd order model (no input-output differences).

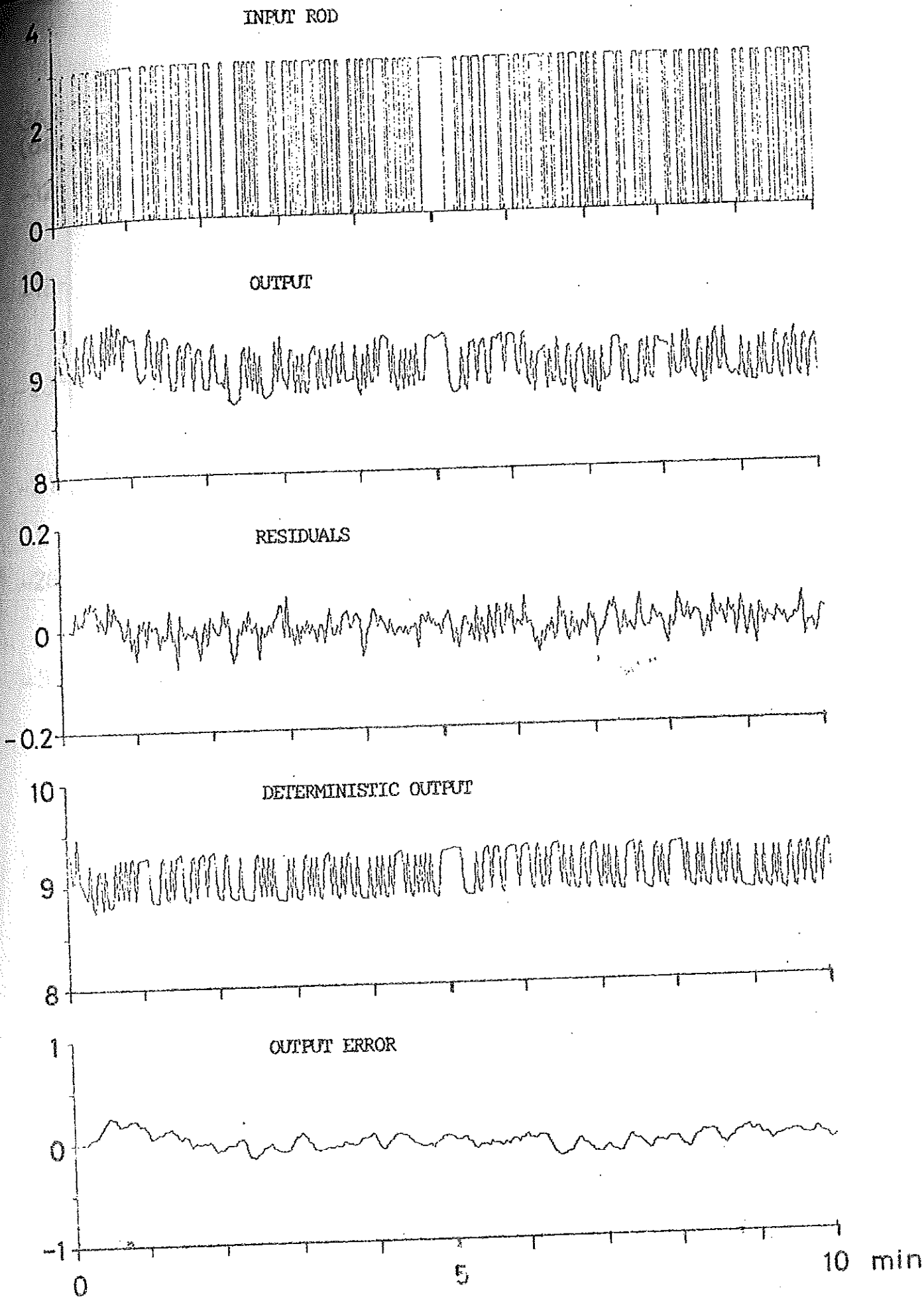

Fig. 4.16 - (See page 29)
Experiment EP-710, run 5 (no input-output differences). Output nuclear power. Experimental and simulated outputs of the 4th order model.

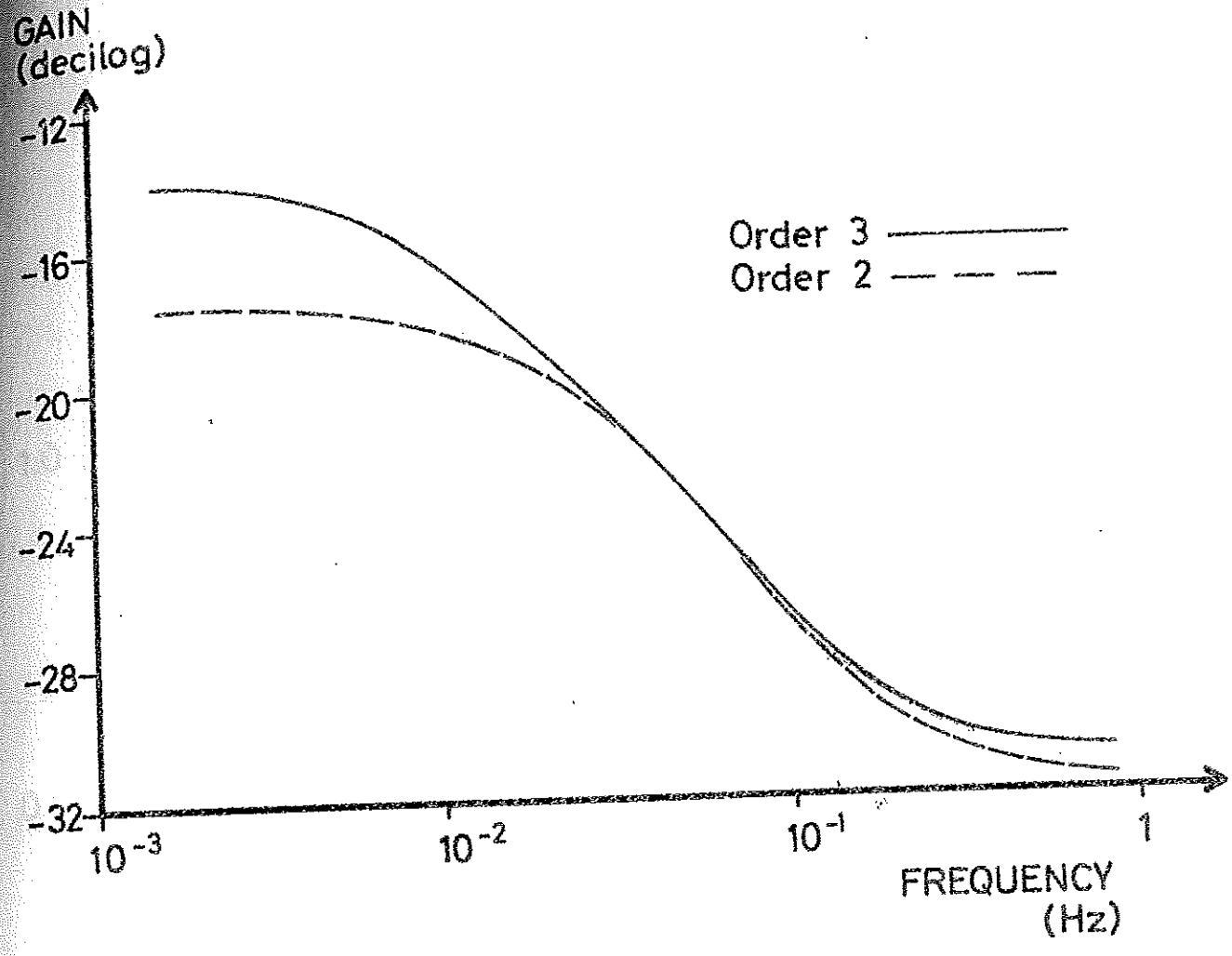

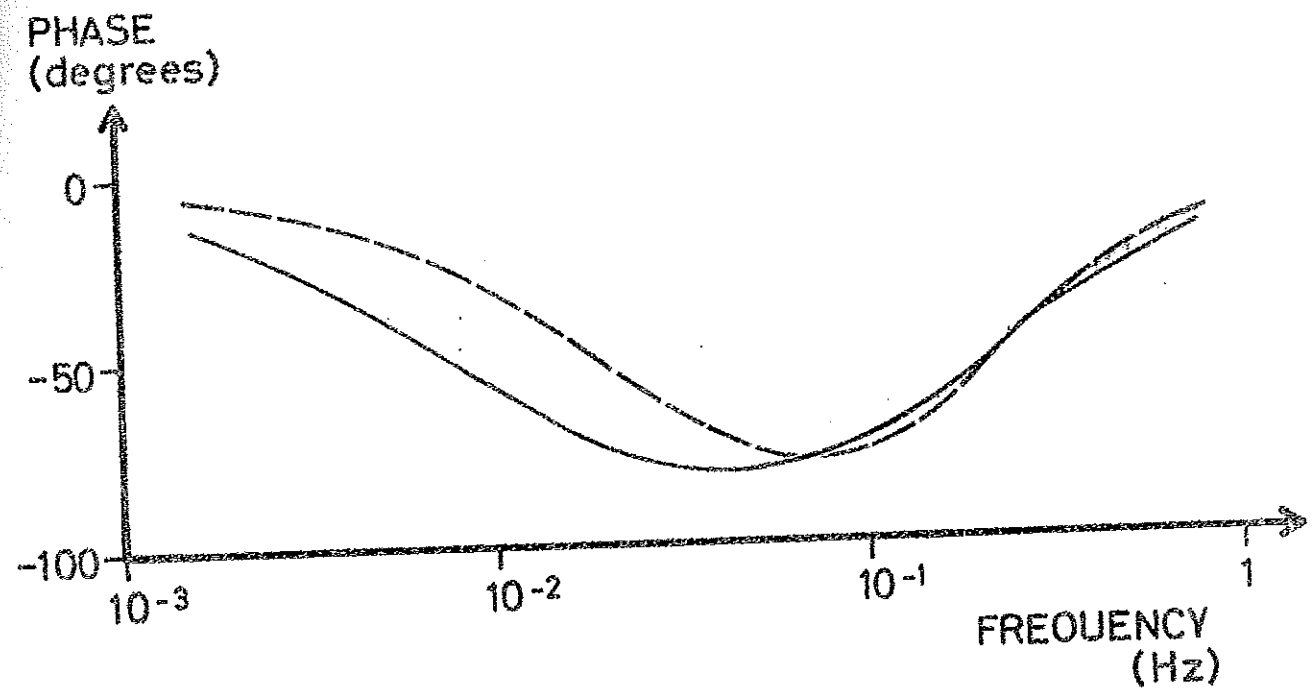

Fig. 5.1 - (See page 33)
Experiment EP-710, run 4. Output primary pressure. Bode plot of the 2nd and 3rd order models.

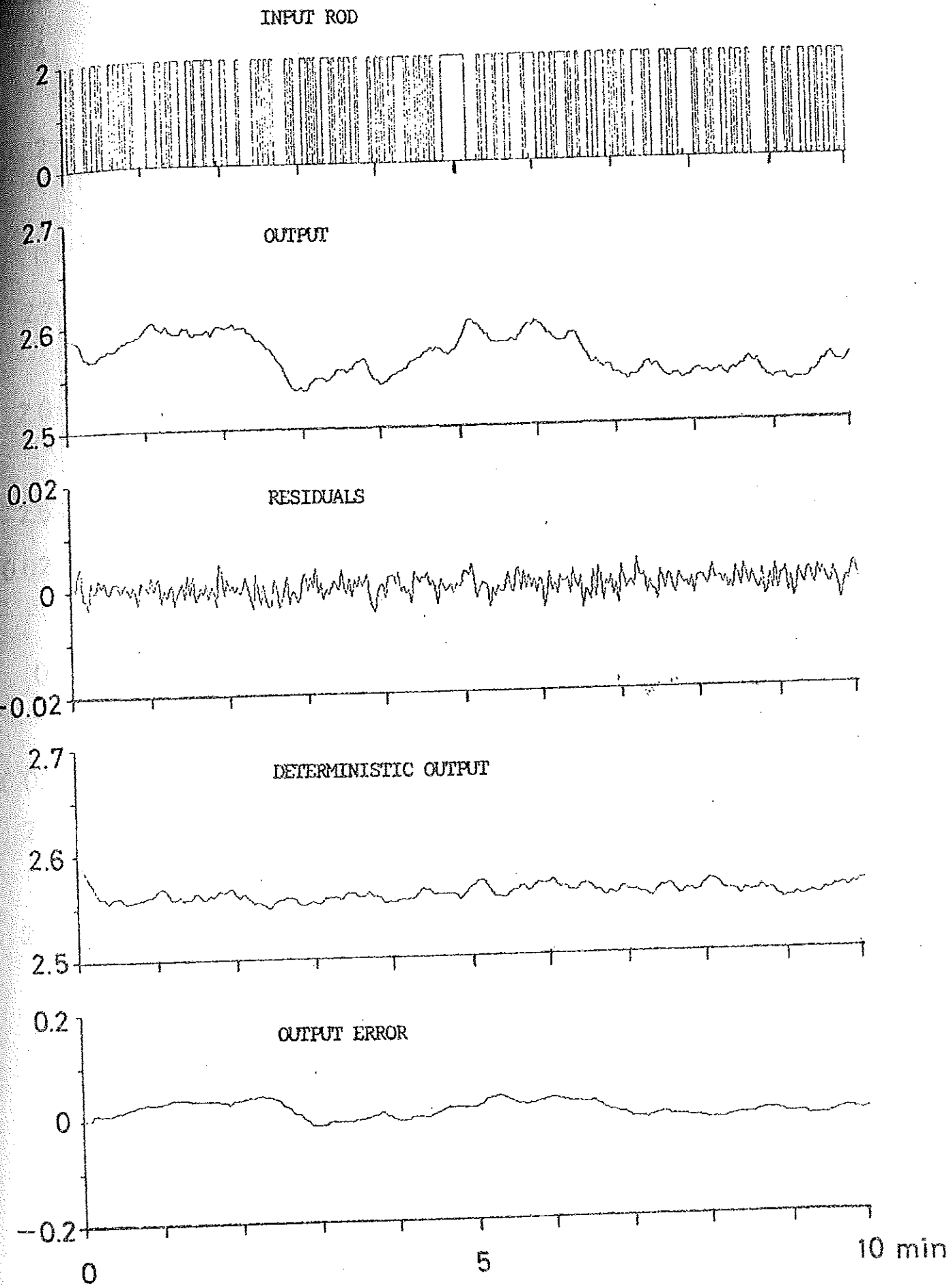

Fig. 5.3 - (See page 33)
Experiment EP-710, run 4. Output primary pressure. Experimental and simulated outputs of the 2nd order model.

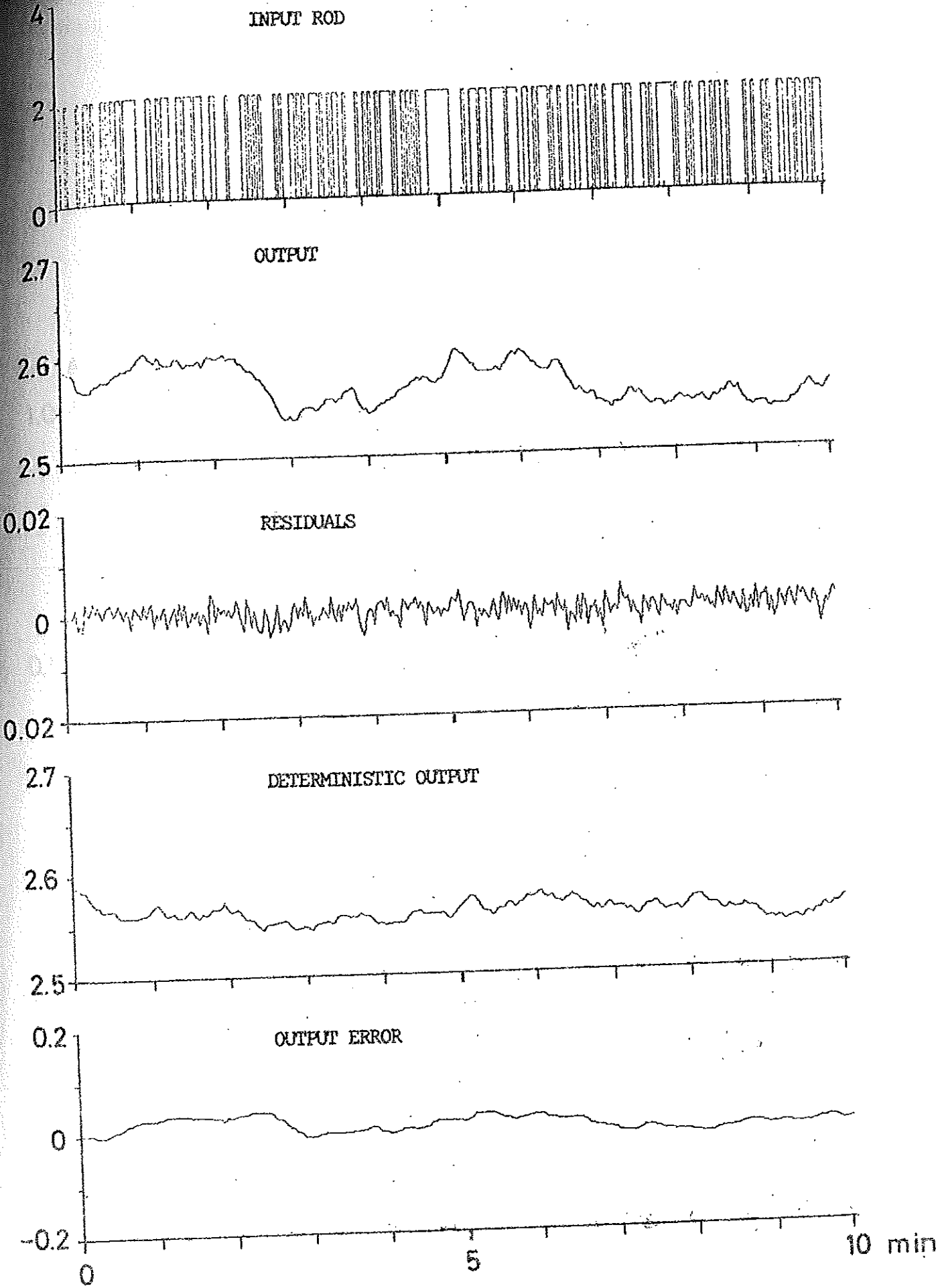

Fig. 5.4 - (See page 33)
Experiment EP-710, run 4. Output primary pressure. Experimental and simulated outputs of the 3rd order model.

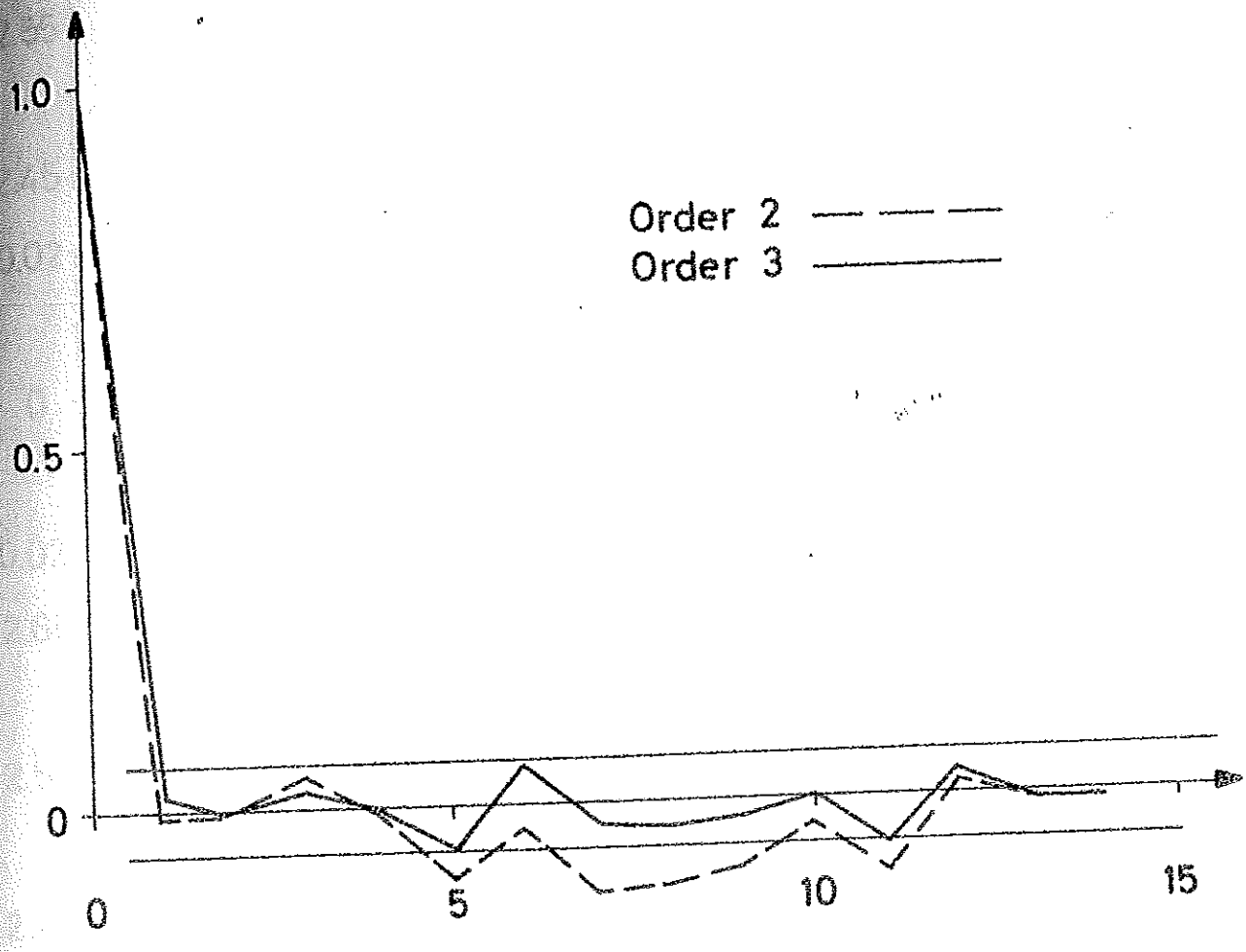

Fig. 5.5 - (See page 35)
Experiment EP-710, run 5. Output primary pressure. Covariance functions and the 95% significance limit of the 2nd and 3rd order system residuals.

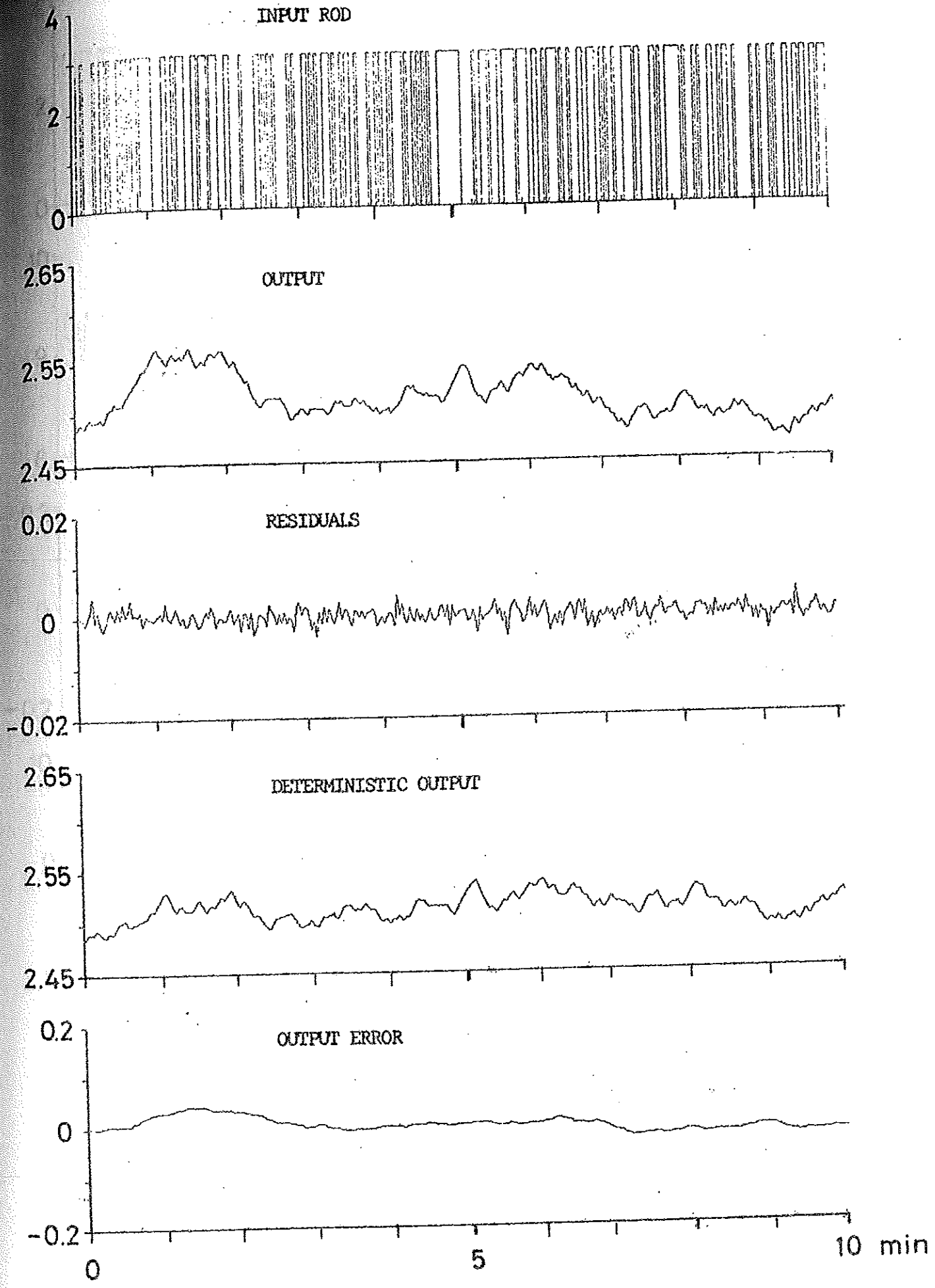

Fig. 5.6 - (See page 35)
Experiment EP-710, run 5. Output primary pressure. Experimental and simulated outputs of the 2nd order model.

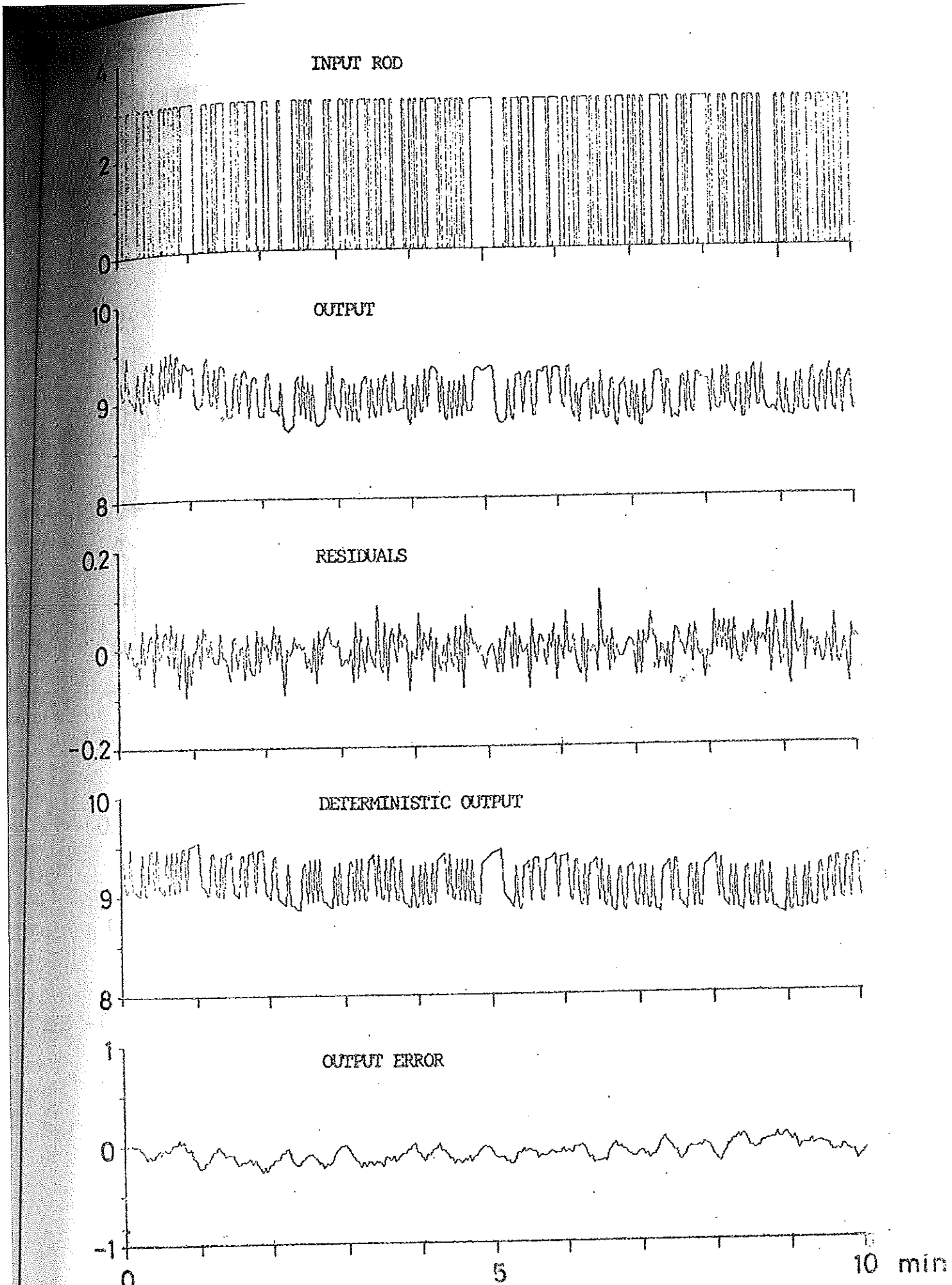

Fig. 6.1 - (See page 42)
Reactivity input, power output. Experimental output from EP-710, run 5. Simulated output from a 3rd order model, based on experimental data from EP-708, run 84 (ref. |19|).

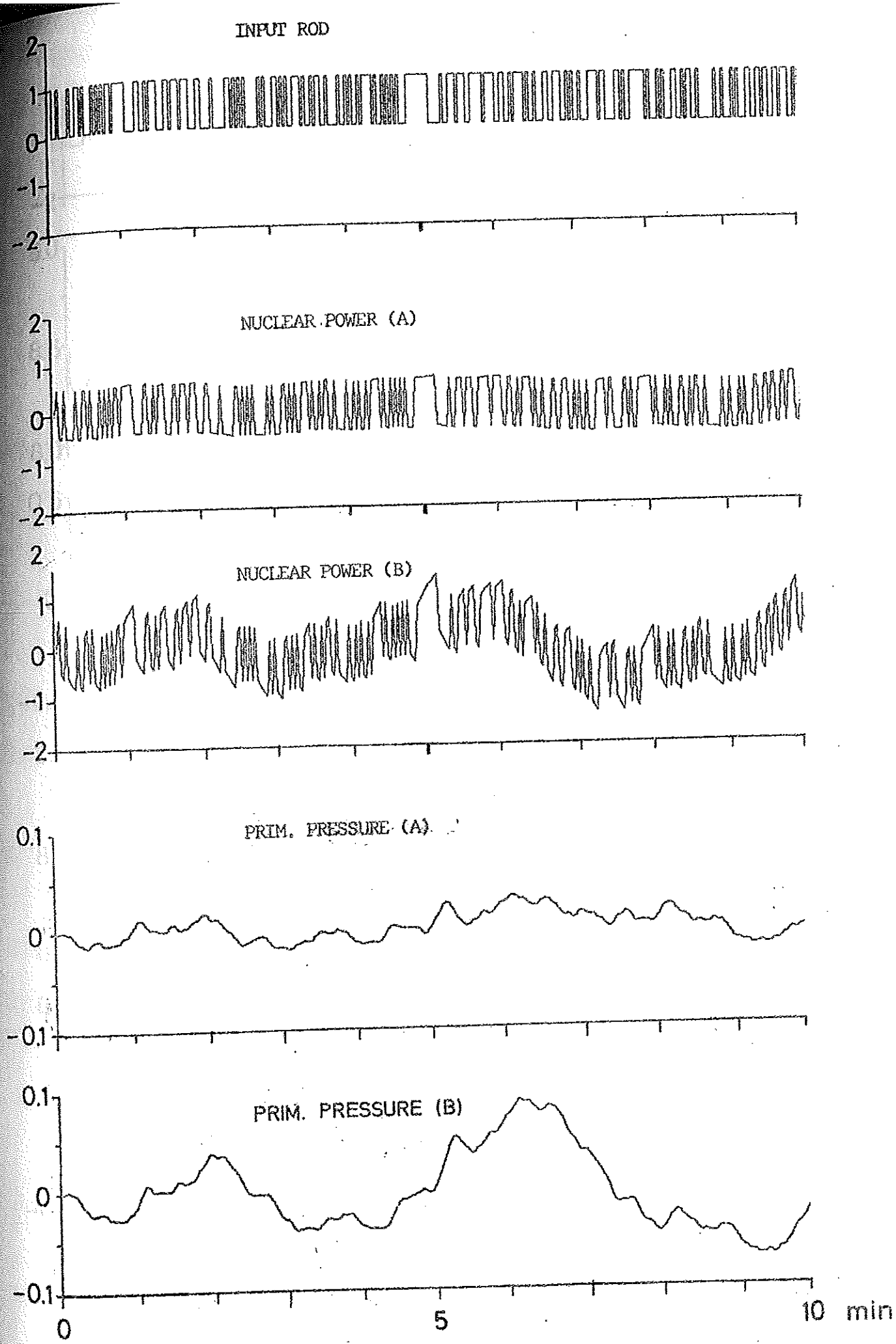

Fig. 6.2 - (See page 42)
Deterministic simulation of the theoretical state model. Reactivity input PRBS from EP-710. Output nuclear power and primary pressure, conditions a and b.

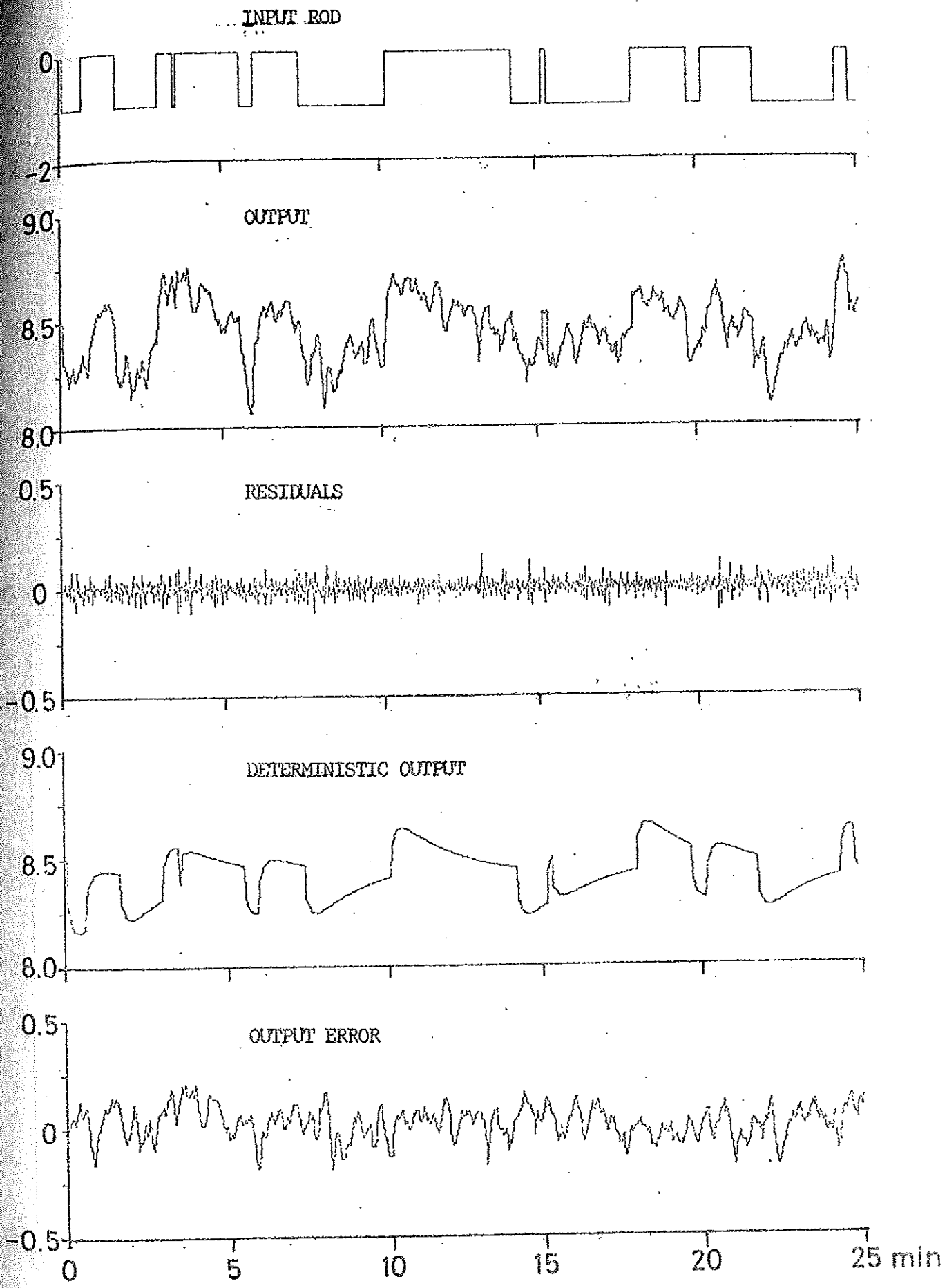

Fig. 6.3 - (See page 42)
Experiment EP-708, run 84. Reactivity input, nuclear power output. Experimental and simulated outputs of a 3rd order model (from |19|).

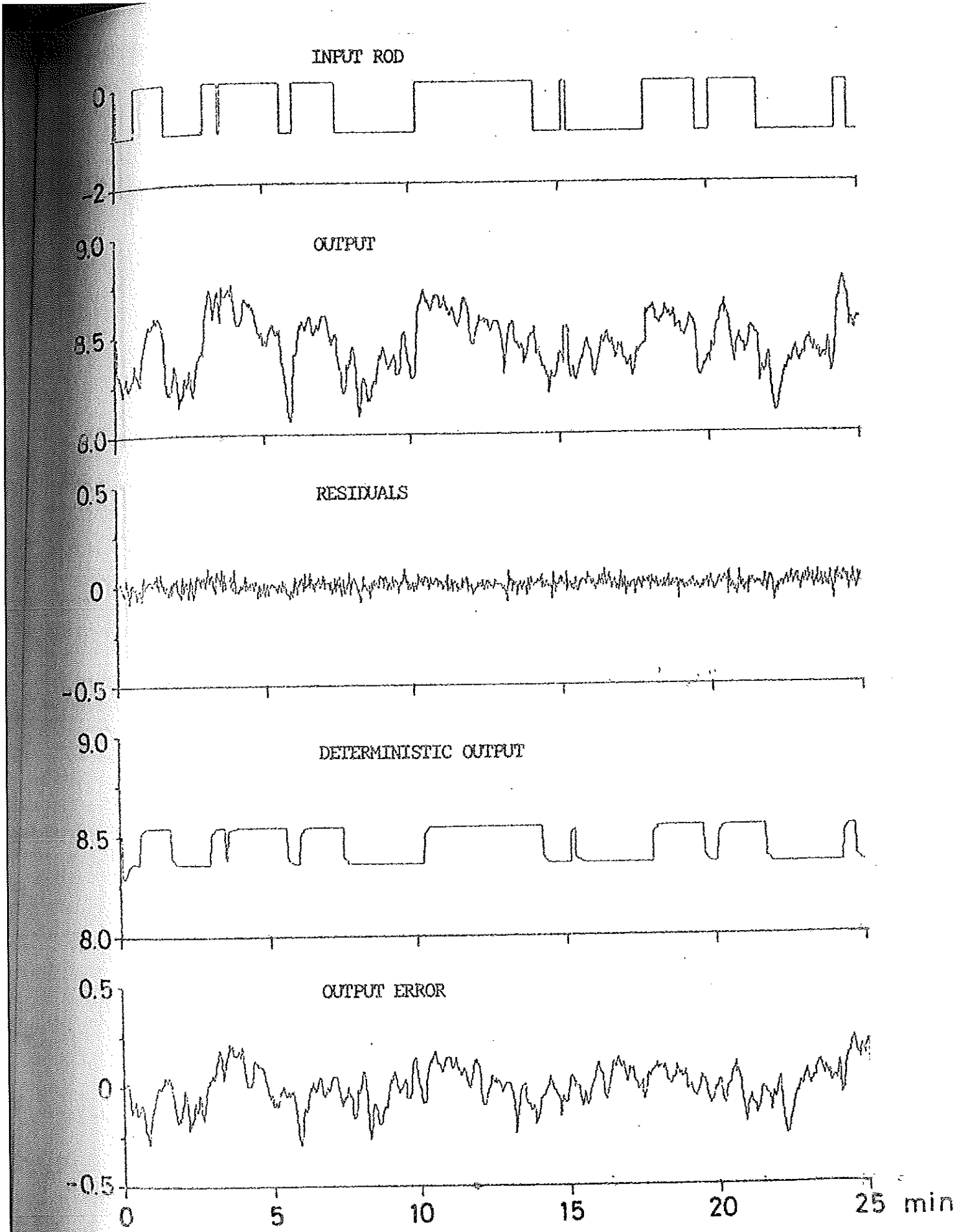

Fig. 6.4 - (See page 43)
Reactivity input, nuclear power output. Experimental output from EP-708, run 84. Simulated output from the 3rd order model from EP-710, run 3.

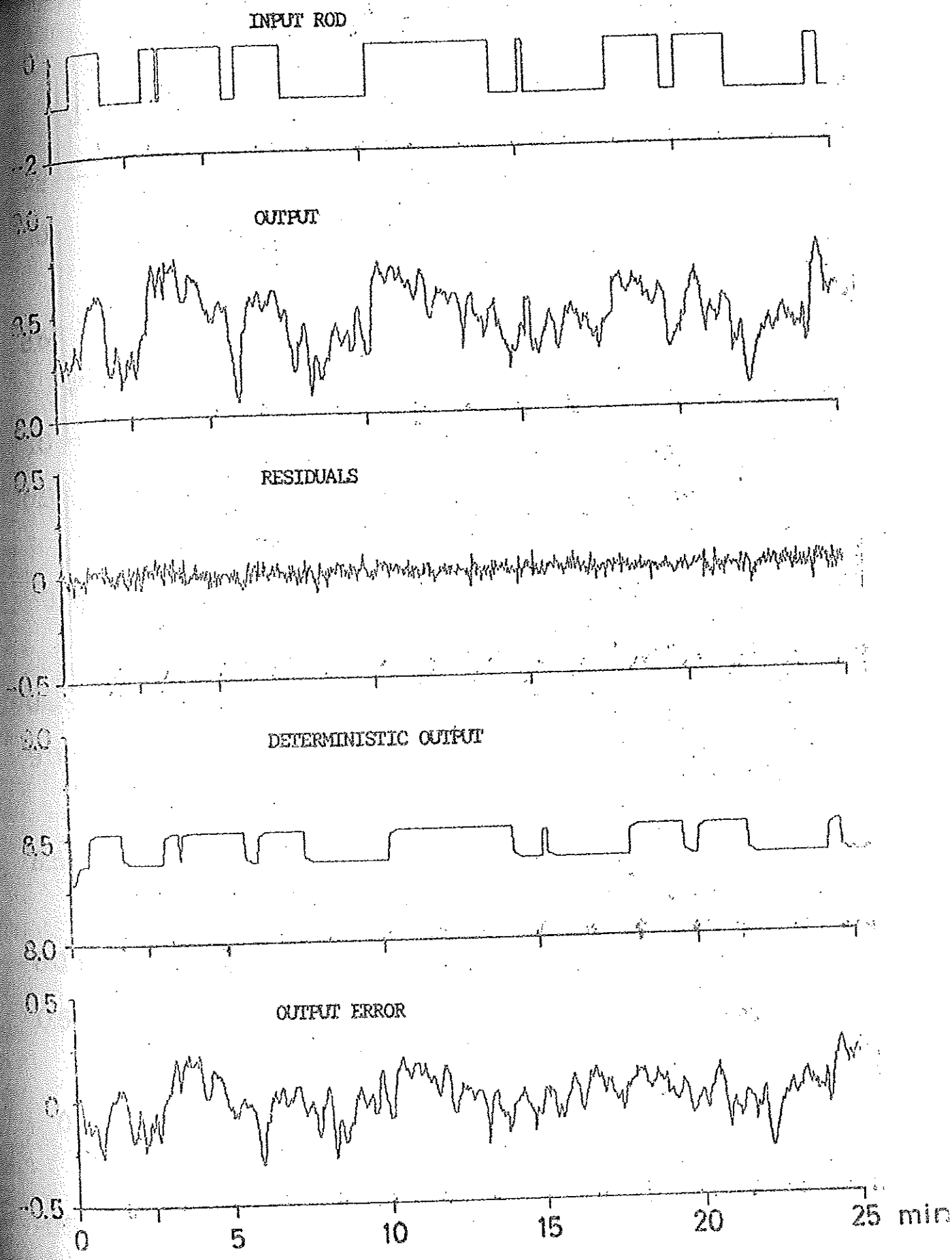

Fig. 6.5 - (See page 42)
Reactivity input, nuclear power output. Experimental output from EP-708, run 84. Simulated output from the 3rd order model from EP-710, run 4.

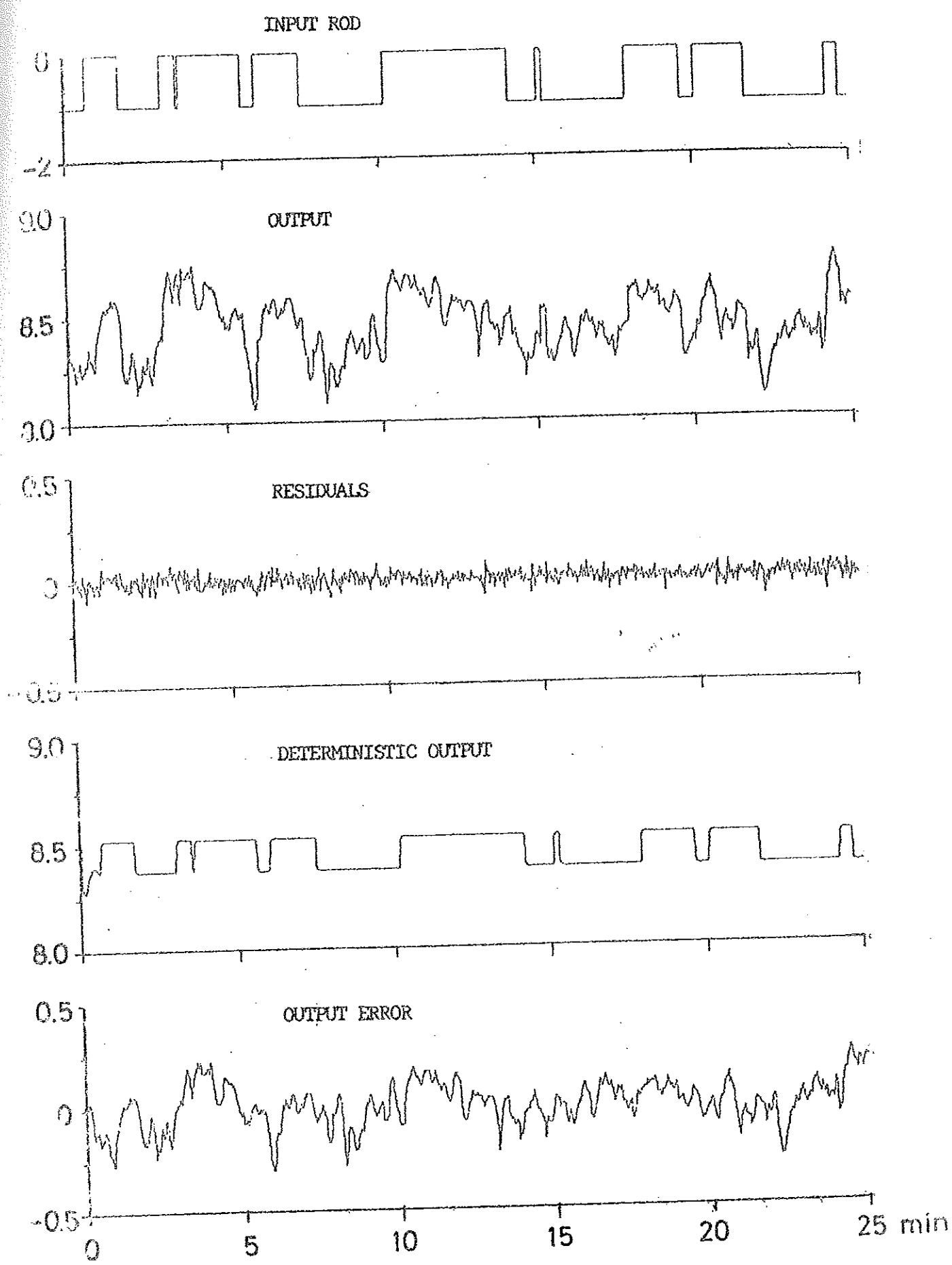

Fig. 6.6 - (See page 42)
Reactivity input, nuclear power output. Experimental output from EP-708, run 84. Simulated output from the 3rd order model from EP-710, run 5 (prefiltered).

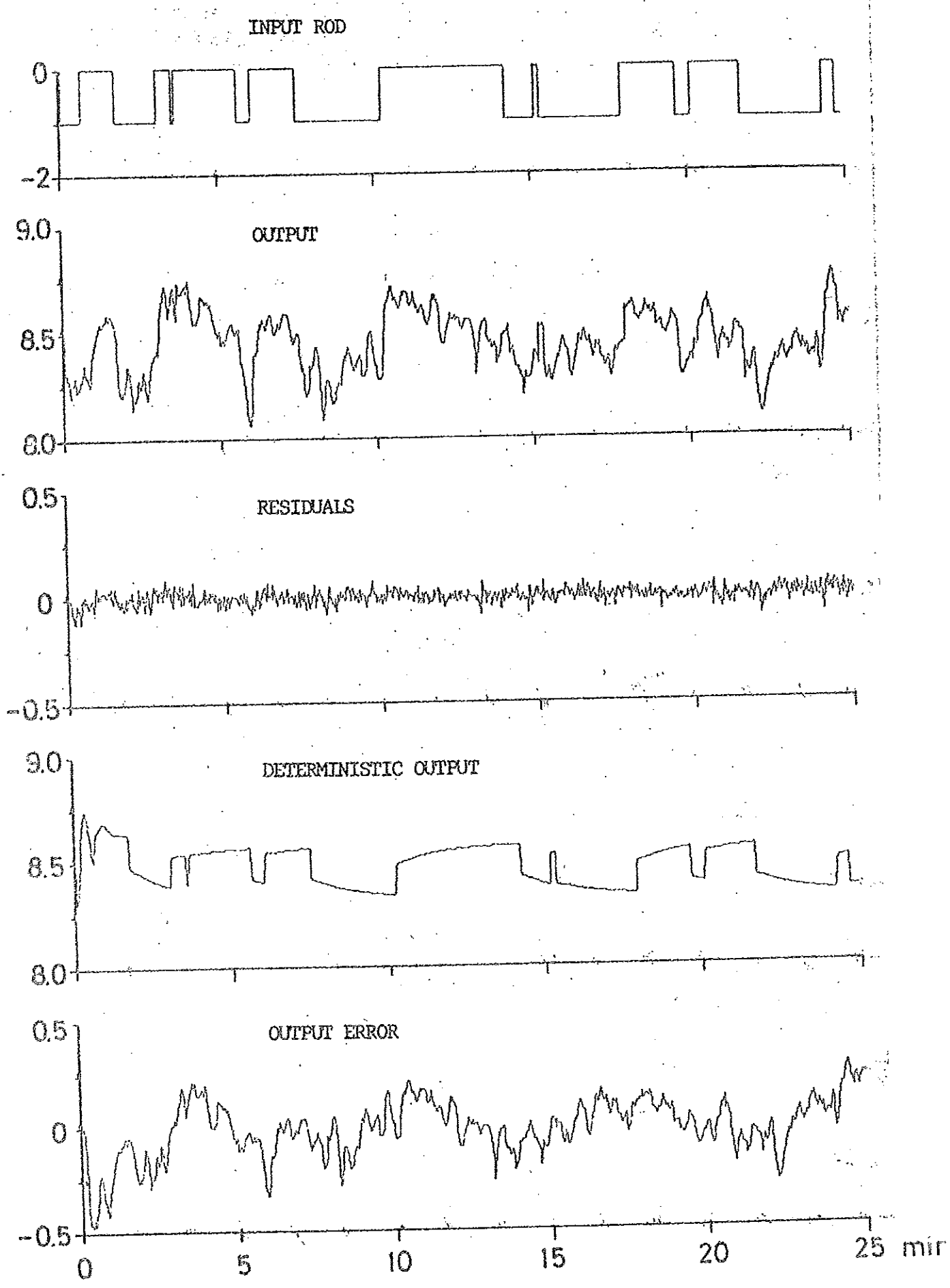

Fig. 6.7 - (See page 42)
Reactivity input, nuclear power output. Experimental output from EP-708, run 84. Simulated output from the 3rd order model from EP-710, run 5 (not prefiltered).

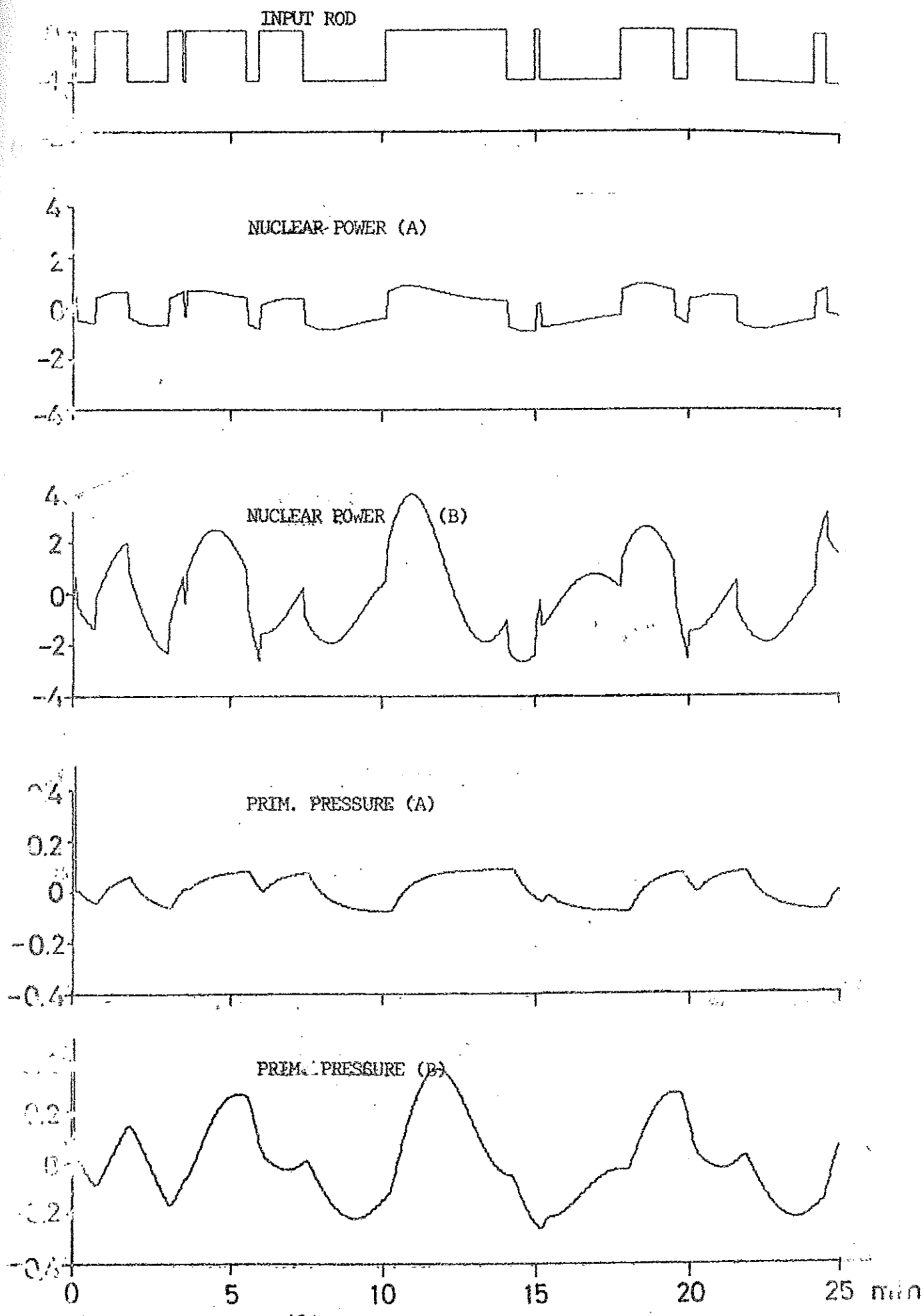

Fig. 6.8 - (See page 42)
Deterministic simulation of the theoretical state model. Reactivity input from EP-708, run 84. Output nuclear power and primary pressure, conditions a and b.

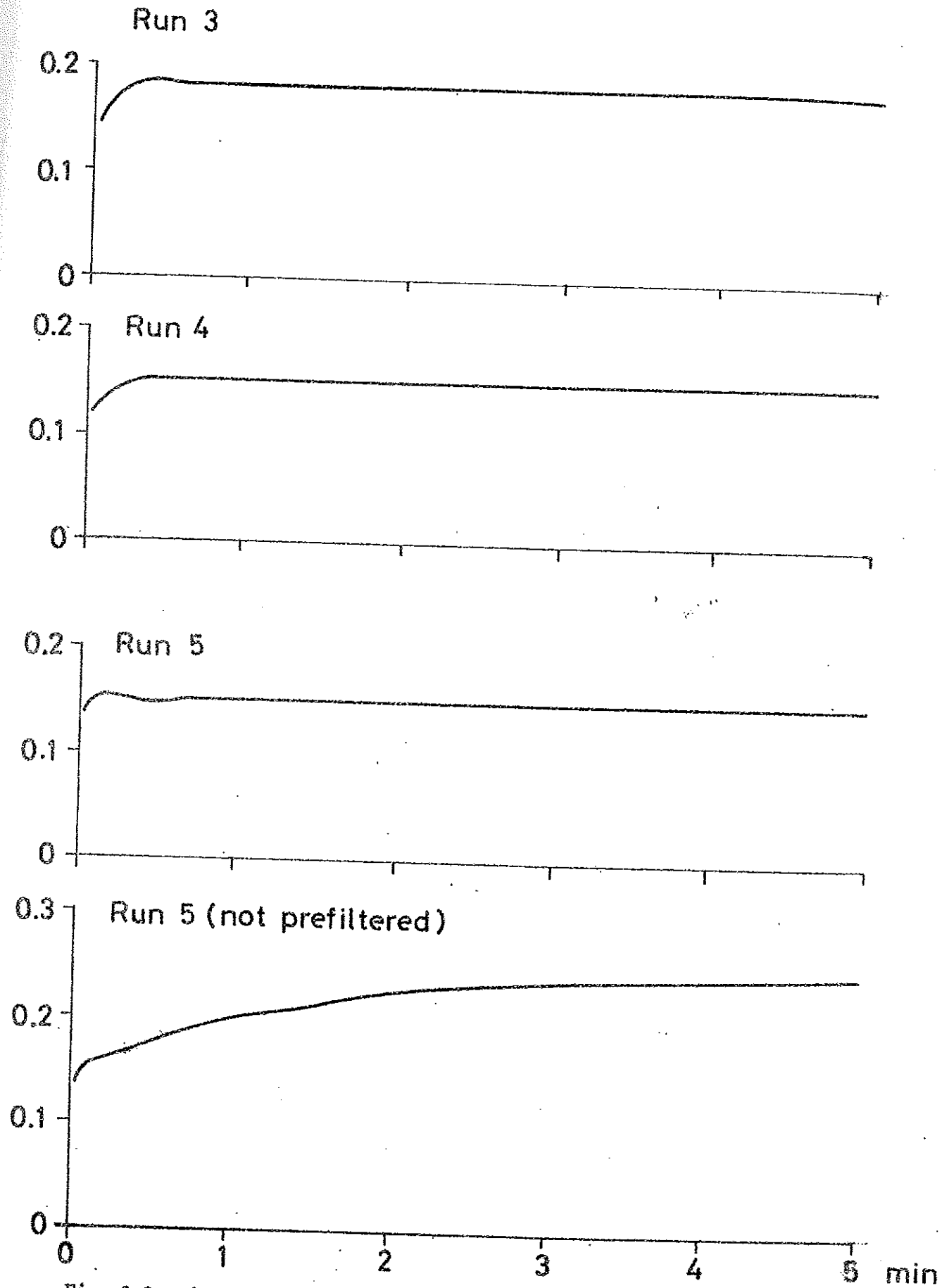

Fig. 6.9 - (See page 42)
Nuclear power responses on reactivity steps of the deterministic models from EP-710(in MW).

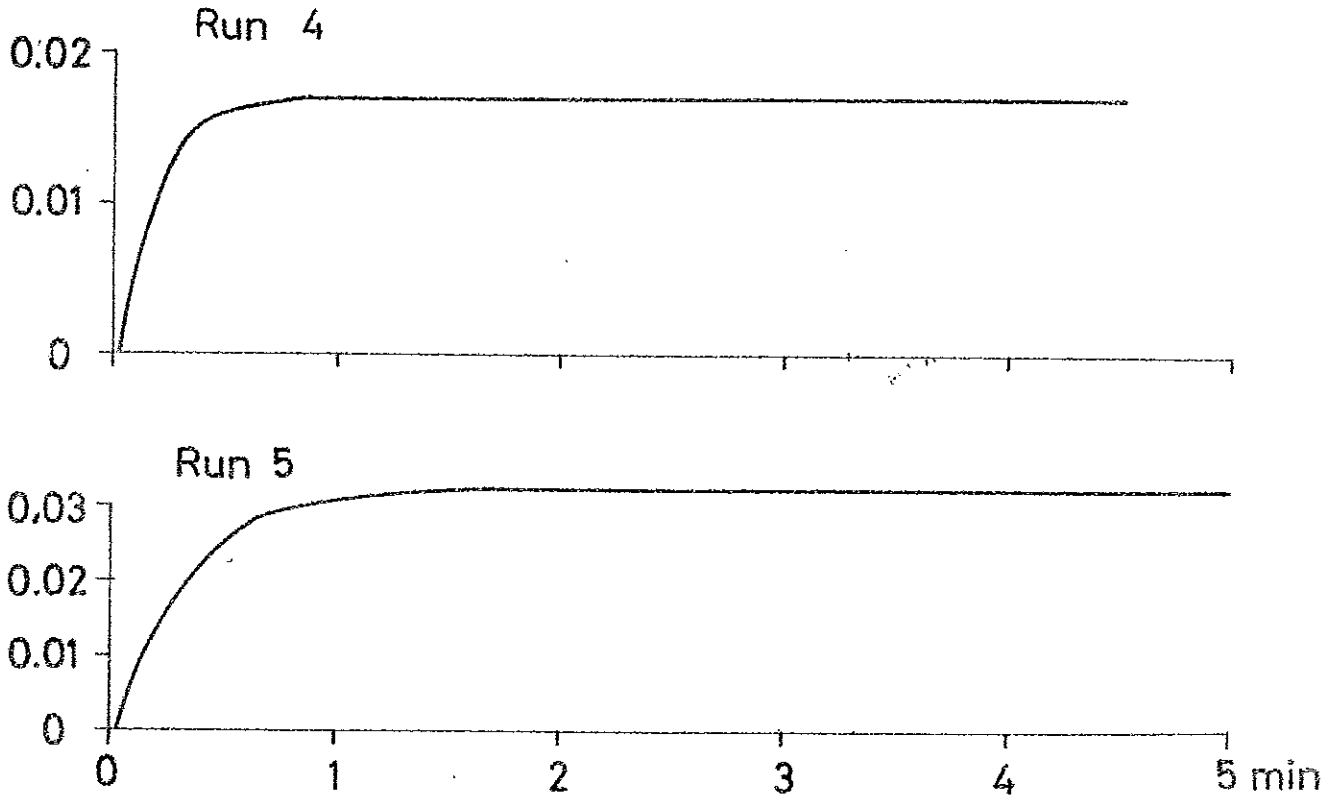

Fig. 6.10 - (See page 43)
Primary pressure responses on reactivity steps of the deterministic models from EP-710 (in bar).

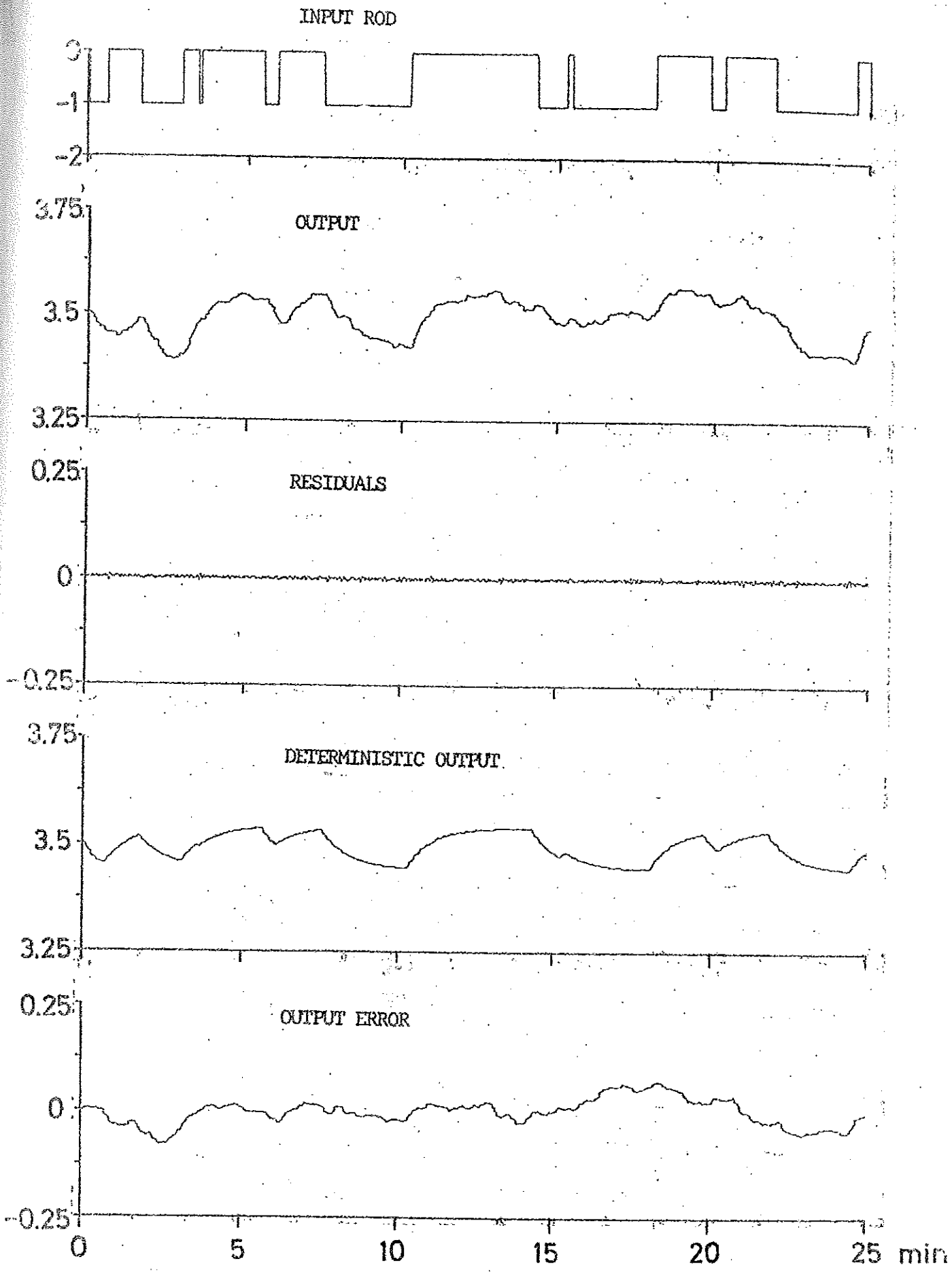

Fig. 6.11 - (See page 43)
Experiment EP-708, run 84. Reactivity input, primary pressure output. Experimental and simulated outputs of a 2nd order model (from |19|).